ANALYSIS OF THE MOLECULAR COMPONENTS AND DIFFERENT STEPS OF AUTOPHAGY-RELATED PATHWAYS IN *SACCHAROMYCES CEREVISIAE*

by

Yang Cao

A dissertation submitted in partial fulfillment
of the requirements for the degree of
Doctor of Philosophy
(Molecular, Cellular and Developmental Biology)
in The University of Michigan
2009

Doctoral Committee:

Professor Daniel J. Klionsky, Chair
Professor Lois Weisman
Associate Professor Laura Olsen
Assistant Professor Yanzhuang Wang

DEDICATION

This dissertation is dedicated to my parents, for their endless and unconditional love and support; and to my husband, for his love and care, encouragement and criticism.

ACKNOWLEDGEMENTS

I would like to thank everyone who has given me this opportunity to start and finish my doctoral studies. First, I want to thank my graduate mentor, Dr. Daniel J. Klionsky for his training and support. He is the best mentor I could have ever imagined of. I would also like to thank my committee members, Dr. Lois Weisman, Dr. Laura Olsen, and Dr. Yanzhuang Wang for being always helpful and supportive.

Special thanks are due to all the members of the Klionsky lab for their generous help in the past four years, especially Dr. Usha Nair, with whom I share bench space, ideas and passion. Two of our collaborative projects are presented in Chapter 4 and Chapter 5. I also want to thank Dr. Zhiping Xie for his inputs on our Atg18 and Atg21 project; Dr. Heesun Cheong, Dr. Kyoko Yasumura-Yorimitsu and Hui Song for their involvement in my multiple knockout papers. I also enjoyed collaborating with Congcong He, Wei-Lien Yen, Dr. Tomotaka Kanki and Dr. Takahiro Shintani.

Final thanks are due to my friends and families who have accompanied me on my journey in science and in life.

The first 7 pages of Chapter 1 are reprinted from *Cell Research*, Volume 17, Yang Cao and Daniel J. Klionsky. Physiological functions of Atg6/Beclin 1, a unique autophagy-related protein, pg.839-49, Copyright (2007), with minor modifications.

Chapter 2 is reprinted from the *Journal of Cell Biology*, Volume 182, Yang Cao, Heesun Cheong, Hui Song, and Daniel J. Klionsky. In vivo reconstitution of autophagy in

Saccharomyces cerevisiae, pg.703-13, Copyright (2008), with minor modifications. My work contributed figures 2.1, 2.2, 2.4 and 2.5. Dr. Heesun Cheong contributed Fig. 2.3.

Chapter 3 is a manuscript that has been submitted to *Autophagy*. I contributed figures 3.1, 3.2A and 3.3. Experiments in Figure 3.2B were performed by Dr. Usha Nair.

Chapter 4 is a co-first authorship manuscript that has been submitted to *Molecular Biology of the Cell*. My work contributed figures 4.1B, 4.3, 4.4, 4.S2 and 4.S4. Dr. Usha Nair made all of the plasmids and I constructed all of the strains, and we designed all the experiments together and equally contributed Fig. 4.5. Dr. Usha Nair contributed figures 4.1A, 4.2 and 4.S1, and wrote most of the manuscript. Experiments in Figure 4.S3 were performed by Dr. Zhiping Xie.

Chapter 5 is reprinted from *Autophagy*, Volume 3, Yang Cao and Daniel J. Klionsky. Atg26 is not involved in autophagy-related pathways in *Saccharomyces cerevisiae*, pg.17-20, Copyright (2007). My work contributed figures 5.1-5.3.

Appendix A is reprinted from *Molecular Biology of the Cell*, Volume 19, Congcong He, Misuzu Baba, Yang Cao, and Daniel J. Klionsky. Self-interaction is critical for Atg9 transport and function at the phagophore assembly site during autophagy, pg.5506-16, Copyright (2008). This paper was written by Congcong He. She contributed figures A.1-A.5, A.7 –A.8 and A.S1-A.S3. Dr. Misuzu Baba performed experiments in Fig. A.6. I provided a multiple knockout strain for fluorescence, immunoprecipitation and native gel analyses. My work contributed Table A.2.

TABLE OF CONTENTS

LIST OF TABLES

Table

LIST OF FIGURES

Figure

CHAPTER 1

Introduction

There are various processes that fall under the general name of autophagy, which can be defined simply as any process involving the degradative delivery of a portion of the cytoplasm to the lysosome (or its yeast analogue, the vacuole) that does not involve direct transport through the endocytic or vacuolar protein sorting (Vps) pathways (Klionsky, Cuervo et al. 2007). The best characterized of these processes is macroautophagy, which we refer to hereafter as autophagy. Autophagy is highly conserved in eukaryotic cells, ranging from yeast to mammals (Klionsky 2005). It is the major intracellular pathway for degradation and recycling of long-lived proteins and organelles, whereas the ubiquitin/proteasome system degrades primarily short-lived proteins.

One of the most distinctive features of autophagy is its relatively unlimited capacity for degradation, which reflects the unique mechanism of cargo sequestration. During autophagy, a membrane of unknown origin forms a nucleation site that generates a unique organelle, the phagophore (Fig. 1.1). The phagophore expands, probably through vesicular addition, to form a large double-membrane cytosolic vesicle that is termed an autophagosome. Unlike transient transport vesicles such as those that shuttle

proteins between the organelles of the secretory pathway, the autophagosome forms *de novo*; it does not bud off intact from a pre-existing organelle, although the membrane that adds to the growing phagophore likely includes vesicles that originate within the secretory pathway. This expansion mechanism allows the autophagosome to sequester entire organelles or large protein aggregates, and even invading pathogens. Following completion of the autophagosome, it fuses with the lysosome, or the yeast vacuole. In mammalian cells, autophagy also converges with endocytosis, a form of heterophagy, and the autophagosome may fuse with an endosome to generate an amphisome, which also will ultimately fuse with a lysosome; it is not known if this process occurs in yeast because the endosome is poorly defined and difficult to detect. In either case, the final fusion event provides access to the diverse hydrolases that reside in the lysosome and yeast vacuole, allowing them to break down the inner membrane of the autophagosome along with its cargo. The resulting macromolecules are then released back into the cytosol for reuse.

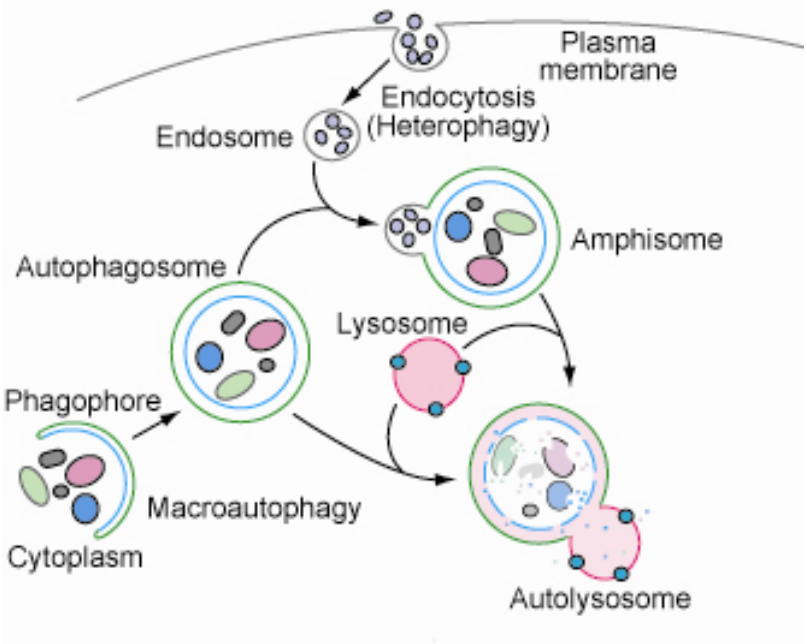

Figure 1.1. A schematic model of macroautophagy in mammalian cells. Autophagy occurs at a low, constitutive basal level, but can be induced by environmental signals including stress (e.g., nutrient depletion) and hormones (e.g., glucagon). The process begins with the formation of a sequestering membrane termed a phagophore. During nonspecific autophagy, bulk cytoplasm (including entire organelles) can be sequestered, whereas specific types of autophagy can target selective cargos. The phagophore expands to form a double-membrane autophagosome. The autophagosome may fuse with an endosome; convergence of endocytosis, a form of heterophagy, and autophagy in the form of a fusion event generates an amphisome. The amphisome or autophagosome acquires hydrolytic enzymes by fusing with a lysosome. The resulting autolysosome breaks down the inner membrane of the autophagosome and its cargo. The macromolecular breakdown products are released back into the cytosol through permeases for reuse.

Why does the cell maintain a process for eating parts of itself? For proper physiology the cell must maintain a balance between anabolism and catabolism. Autophagy is a catabolic process that has homeostatic functions, acting in the turnover of various worn out or damaged macromolecules and organelles (Levine and Klionsky 2004). Autophagy also has cytoprotective roles during stress conditions, such as nutrient starvation, growth factor depletion (Li, Capan et al. 2006) and pathogen invasion (Levine 2005) that might otherwise lead to apoptosis, or type I programmed cell death (PCD). For example, damaged mitochondria pose a threat to cell stability due to the generation of

excess reactive oxygen species that can cause nuclear DNA damage (Mathew, Kongara et al. 2007; Zhang, Qi et al. 2007). The compromised organelle may release cytochrome c into the cytosol, which can trigger apoptosis as a barrier against oncogenesis. If the cell can remove the damaged organelle in a timely manner, however, it may avoid the need for apoptosis. Thus, although we are not aware of evidence demonstrating a direct connection between the removal of damaged organelles and the prevention of apoptosis, it seems likely that autophagy can protect the cell against apoptotic death through its action as an organelle quality control mechanism.

On the other hand, autophagy presents us with a challenging conundrum because it sometimes acts as a killer of cells by promoting autophagic, or type II, programmed cell death with the hallmark of accumulated autophagosomes in dying cells (Gozuacik and Kimchi 2004). In this case, extensive autophagy may participate along with, or instead of, apoptosis to ensure the death and removal of cells that cannot be rescued; it is not difficult to imagine that an excessive level of self-digestion would be deleterious. The dual role of autophagy, in cytoprotection and cell death, is one of the most fascinating features of this process, and one that needs to be better understood if we ever hope to harness autophagy for therapeutic use. Indeed, there are many possibilities for modulating autophagy for purposes of human health: Autophagy has been implicated in various human diseases, including cancer, cardiomyopathy and the prevention of certain neurodegenerative disorders (Shintani and Klionsky 2004; Rubinsztein, Difiglia et al. 2005; Rubinsztein, Gestwicki et al. 2007).

In the last decade, with the identification of approximately 30 AuTophaGy-related (*ATG*) genes in *Saccharomyces cerevisiae* and other fungi (Klionsky, Cregg et al. 2003),

the molecular mechanisms of autophagy have gradually been elucidated (Klionsky 2005). As mentioned above, autophagy is conserved across all eukaryotes, and homologues of many yeast *ATG* genes have recently been identified in various eukaryotic systems; the underlying molecular mechanisms of autophagy are also conserved. In general, autophagy is considered to be nonspecific, but there are also specific types of autophagy. For example, excess peroxisomes can be selectively degraded through a specific autophagy-like process termed pexophagy (Dunn, Cregg et al. 2005). One well-characterized selective type of autophagy is the cytoplasm to vacuole targeting (Cvt) pathway that is used for the delivery of two vacuolar hydrolases, aminopeptidase I (Ape1) and α-mannosidase (Reggiori, Shintani et al. 2005). The protein machinery of nonspecific autophagy overlaps extensively with the Cvt pathway (Harding, Hefner-Gravink et al. 1996; Scott, Hefner-Gravink et al. 1996); however, there are some proteins that are specific for each pathway. A brief summary of the functions of the Atg proteins is presented in Table 1.1.

Table 1.1. Proteins required for specific and nonspecific autophagy in yeast.

Protein	Function
Atg1	A serine/threonine kinase that participates in the induction step and also in the cycling of the Atg9 complex. Atg1 interacts with Atg11, Atg13-Atg17 and Atg29.
Atg2	Required for retrograde transport of Atg9 from the PAS to peripheral sites that may mark the membrane donor for sequestering vesicle formation.
Atg3	A ubiqutin-conjugating enzyme analogue involved in the attachment of phosphatidylethanolamine (PE) to Atg8.
Atg4	A cysteine protease that processes the C terminus of Atg8 to expose a glycine residue prior to

	PE lipidation.
Atg5	A protein with two ubiquitin-like domains that is modified by conjugation to Atg12, through an isopeptide bond at an internal lysine of Atg5.
Atg6	A component of two PtdIns 3-kinase complexes involved in autophagy and vacuolar protein sorting.
Atg7	A ubiquitin-activating enzyme homologue required for conjugation of Atg8 to PE and Atg12 to Atg5.
Atg8	A ubiquitin-like protein that modifies PE via attachment at the C-terminal glycine. Atg8 is the only protein required for nonspecific autophagy that clearly remains associated with the completed autophagosome.
Atg9	A transmembrane protein that is localized at the PAS and at peripheral sites in the cell that may correspond to the donor site(s) that provides membrane for expansion of the phagophore. This protein interacts with Atg2, Atg11, Atg18, Atg23 and Atg27.
Atg10	A ubiqutin-conjugating enzyme analogue involved in the attachment of Atg12 to Atg5.
Atg11	This protein serves as an adaptor or scaffold during specific types of autophagy including the Cvt pathway and pexophagy (selective degradation of peroxisomes). It interacts with Atg1, Atg9, itself, Atg17, Atg19 and Atg20.
Atg12	A ubiquitin-like protein that modifies Atg5 through attachment at a C-terminal glycine.
Atg13	An Atg1-interacting protein that modulates the kinase activity of Atg1. Atg13 undergoes nutrient-dependent changes in phosphorylation.
Atg14	A component of PtdIns 3-kinase complex I that is involved in autophagy; it determines the localization of the complex at the PAS.
Atg15	A vacuolar lipase that is needed for the lysis of the inner membrane of the autophagosome after fusion with the vacuole, which releases the inner membrane into the organelle lumen.
Atg16	This protein forms a complex with Atg5 that has been conjugated with Atg12. Atg16 self-interacts to form a tetrameric complex.
Atg17	An Atg13-interacting protein that is part of the Atg1 complex and modulates the kinase activity of Atg1. This protein is not needed for specific types of autophagy and is not essential

	for nonspecific autophagy; however, in its absence there are fewer and smaller autophagosomes.
Atg18	Interacts with Atg9 and required for retrograde transport of Atg9 from the PAS to peripheral sites. This protein binds PtdIns(3)phosphate and its localization is dependent on the PtdIns 3-kinase complex.
Atg19	A receptor for the substrates of the Cvt pathway that interacts with Atg11; this protein is not needed for nonspecific autophagy.
Atg20	A PX domain-containing protein that binds PtdIns(3)P and is required for the Cvt pathway, but not nonspecific autophagy. This protein binds Atg11, Atg17 and Atg24, and is therefore part of a putative Atg1 complex.
Atg21	A homologue of Atg18 that also binds PtdIns(3)P; this protein is only essential for the Cvt pathway.
Atg22	A vacuolar permease that functions in the final step of autophagy, the release of macromolecules (amino acids) generated by vacuolar degradation back into the cytosol.
Atg23	A cytosolic protein that displays a localization pattern and cycles similar to, and interacts with, Atg9. This protein is needed for the Cvt pathway and for efficient nonspecific autophagy; an *atg23*Δ mutant forms a reduced number of autophagosomes.
Atg24	A PX domain-containing protein that binds PtdIns(3)P and is required for the Cvt pathway, but not nonspecific autophagy. This protein binds Atg17 and Atg20, and is therefore part of a putative Atg1 complex.
Atg25	This protein is not found in *S. cerevisiae*, but it is required for specific peroxisome degradation in *Hansenula polymorpha*.
Atg26	A GRAM domain-containing protein that binds PtdIns(4)P; this protein is required for specific peroxisome degradation in *Pichia pastoris*, but not in *S. cerevisiae*.
Atg27	A transmembrane protein that displays a localization pattern and cycles similar to, and interacts with, Atg9. This protein is needed for the Cvt pathway and for efficient nonspecific autophagy; an *atg27*Δ mutant forms a reduced number of autophagosomes.
Atg28	A coiled-coil domain protein required for specific peroxisome degradation in *P. pastoris*.

Atg29	Interacts with Atg1 and Atg17, and is therefore a component of a putative Atg1 complex; involved in nonspecific autophagy, but not the Cvt pathway.
Atg30	A protein required for specific peroxisome degradation in *P. pastoris*.
Atg31	A protein similar to Atg29 is only involved in nonspecific autophagy. Interacts with Atg1 and Atg17.

The autophagic pathway can be dissected into several discrete steps: induction, cargo recognition and packaging, vesicle nucleation, expansion and completion, Atg protein retrieval, vesicle fusion with the lysome/vacuole, degradation, and recycling (Klionsky 2005). Of the 27 *ATG* genes identified in *S. cerevisiae,* 18 of them are required for nonspecific autophagy, 7 for specific autophagy (the Cvt pathway), and 2 for degradation and recycling. A majority of the Atg proteins function in the general vesicle formation process, i.e., vesicle nucleation, expansion and completion. Depending on their function and the interactions among them, the Atg and additional proteins can be roughly organized into different functional groups: the Atg1 protein kinase complex (Atg1, Atg11, Atg13, Atg17, Atg20, Atg24, Atg29 and Atg31), the cargo complex (precursor Ape1 [prApe1], Atg11 and Atg19), the Atg12 conjugation system (Atg5, Atg7, Atg10, Atg12 and Atg16), the Atg8 conjugation system (Atg3, Atg4, Atg7 and Atg8), the PtdIns 3-kinase complex I (Atg6, Atg14, Vps15 and Vps34), the Atg9 targeting complex (Atg9, Atg11, Atg23 and Atg27), and the Atg18 complex (Atg2, Atg18 and Atg21). Some of these complexes contain common factors, probably serving the function of connecting different steps of autophagy. Also note that those complexes may contain subcomplexes, and function at more than one step in autophagy and the Cvt pathway. In the remaining

section, I will introduce each of the functional groups mentioned above, following a brief introduction about the presumed nucleation site for autophagosome formation—the phagophore assembly site (PAS).

The PAS

In yeast, most of the Atg proteins at least transiently localize to the PAS, or a membrane sac, in both autophagy and the Cvt pathway, shown as a perivacuolar punctate structure if tagged with a fluorophore. The PAS could be defined as a hybrid of Atg proteins and the forming vesicle (phagophore). Thus, knowing how Atg proteins are recruited to, and act at the PAS to expand the phagophore may help us understand the vesicle formation process. Early studies suggest that the cargo complex (prApe1, Atg11 and Atg19) in the Cvt pathway is the scaffold for PAS assembly in vegetative conditions (Shintani, Huang et al. 2002), whereas in starvation conditions, a recent study indicates that Atg17 is the key protein and the initial factor for PAS assembly (Suzuki, Kubota et al. 2007). Single deletions of different Atg proteins were constructed in yeast strains expressing individual Atg-GFP proteins, and fluorescence intensities of these proteins at the PAS during starvation were determined by fluorescence microscopy. In the absence of Atg17, most Atg proteins required for nonspecific autophagy lose their PAS localization, but when Atg8 is absent, most Atg proteins are still recruited to the PAS, indicating that the latter is the last component recruited. Atg9, Atg13, Atg6 and Atg14 are some of the initial factors recruited to the PAS dependent on Atg17. This extensive epistatic analysis provides a hierarchy diagram of Atg proteins at the PAS during starvation. However, when cells are shifted from vegetative conditions to starvation

conditions, there is a transition from the constitutive Cvt pathway to induced nonspecific autophagy, and the Cvt specific PAS, well-established in growing conditions, may facilitate the formation of a starvation-specific PAS, obscuring the effects of a single Atg protein deletion in starvation. For example, when Atg11, a Cvt-specific factor is additionally deleted, Atg1 and Atg13 are as important as Atg17 in organizing the PAS during starvation (Cheong, Nair et al. 2008; Kawamata, Kamada et al. 2008). And it is possible that PAS assembly is not a linear event: different complexes may form in the cytosol and depend on each other to localize to the PAS. Some proteins may even act together, or can substitute for one another, to establish the PAS. To avoid these complications, the order of assembly of Atg proteins at the PAS may be best studied in the complete absence of the other Atg proteins.

In mammalian systems, there are multiple sites of colocalization of Atg proteins within one cell, possibly corresponding to multiple PAS. Atg proteins may still arrive in an ordered manner, but instead of asking why all Atg proteins go to a particular site, the question becomes why and how Atg proteins are dispatched to different sites.

The Atg1 protein kinase complex

Atg1 is the only serine/threonine protein kinase identified among Atg proteins, and functions downstream of the protein kinase target of rapamycin (Tor) (Noda and Ohsumi 1998). It is part of a complex that includes additional Atg proteins, such as Atg11, Atg13, Atg17, Atg20, Atg24, Atg29 and Atg31. Atg13 is a regulatory subunit of the Atg1 complex: in response to starvation, it is rapidly dephosphorylated, and may interact with a higher affinity with Atg1, activating Atg1 kinase activity (Kamada,

Funakoshi et al. 2000). Other factors of the Atg1 complex are usually required for a subtype of autophagy: Atg17, Atg29 and Atg31 are only needed for nonspecific autophagy (Cheong, Yorimitsu et al. 2005; Kabeya, Kamada et al. 2005; Kawamata, Kamada et al. 2005; Kabeya, Kawamata et al. 2007), whereas Atg11, Atg20 and Atg24 are Cvt-specific proteins (Kim, Kamada et al. 2001; Nice, Sato et al. 2002). This finding that certain proteins act only in one or the other pathway raises the possibility that Atg1 subcomplexes exist and function in different types of autophagy.

Atg1 functions at multiple steps of autophagy. Similar to Atg17, it has a role in initial PAS assembly during nonspecific autophagy (Cheong, Nair et al. 2008; Kawamata, Kamada et al. 2008). It also regulates the recycling of Atg9 between the PAS and a peripheral pool (Reggiori, Tucker et al. 2004). Atg1 kinase activity is required for autophagosome formation based on electron microscopy analysis (Cheong, Nair et al. 2008). However, the kinase activity is not required for PAS assembly. Rather, it plays a role in disassembly of the PAS or the dissociation kinetics of Atg proteins upon autophagosome completion.

Homologues of Atg1 have been identified in many species, and mammals have at least two Atg1 homologues (Hara, Takamura et al. 2008), Unc-51-like kinase 1 (ULK1) and ULK2. Recently, a human homologue of Atg13 (Chan, Longatti et al. 2009) and a putative human counterpart of yeast Atg17 (FIP200) have been identified (Hara, Takamura et al. 2008). Human Atg13 was identified through repetitive rounds of PSI-BLAST, whereas human Atg17 was identified based on its ability to bind ULK1. Human counterparts of other Atg proteins in the Atg1 protein kinase complex have not been identified in metazoan, but it will be no surprise if they exist.

The cargo complex

The Cvt pathway shares most of the components needed for autophagy, but utilizes additional proteins in cargo recognition and packaging. After synthesis in the cytosol, the precursor form of Ape1 forms a large oligomer, and its propeptide binds the receptor Atg19 (Shintani, Huang et al. 2002). Then, an adaptor protein, Atg11, binds to Atg19 and targets the complex to the PAS (Yorimitsu and Klionsky 2005). The PAS is not formed in the absence of prApe1, Atg19 or Atg11 under nutrient-rich conditions, indicating that proteins in the cargo complex play an important role in PAS assembly.

Atg11 may act as a scaffold for protein assembly and/or as a bridge between different steps of autophagy and the Cvt pathway, for it interacts with many Atg proteins (Yorimitsu and Klionsky 2005). Atg11 is required for both the Cvt pathway and pexophagy (selective peroxisome degradation). And recent data from our lab suggest that it is also essential for selective mitochondria degradation (mitophagy) (Kanki and Klionsky 2008). Atg11 acts as an adaptor to target the cargo-receptor complex to the PAS: prApe1-Atg19 in the Cvt pathway, and peroxisome-Atg30 in pexophagy (Farre, Manjithaya et al. 2008). It is possible that through an unidentified receptor protein, Atg11 targets unwanted mitochondria for degradation. The Cvt pathway including Atg11 has not been found outside of fungi, but a similar recognition mechanism may exist in mammalian examples of selective autophagy.

The Atg8 conjugation system

Atg8 is a ubiquitin-like protein conjugated to phosphatidylethanolamine (PE) through the serial action of Atg4, Atg7 and Atg3 (Ichimura, Kirisako et al. 2000). The C-

terminal arginine residue of Atg8 is first removed by a cysteine protease, Atg4, to expose a glycine residue that is now accessible to the E1-like activating enzyme Atg7. The activated Atg8 is then transferred to the E2-like conjugating enzyme Atg3 and finally conjugated to PE through an amide bond. Atg8 can be deconjugated from Atg8–PE through a second cleavage by Atg4. However, the mechanism that triggers and regulates Atg4 mediated Atg8–PE cleavage is not known. In mammalian cells, multiple Atg8 homologues, such as LC3, GATE-16 and GABARAP, exist and undergo a modification process similar to the yeast Atg8 (Kabeya, Mizushima et al. 2000; Kabeya, Mizushima et al. 2004). Among them, LC3 has been best characterized and commonly employed as a marker for autophagosome formation.

Atg8–PE may be the last component recruited to the PAS (Suzuki, Kubota et al. 2007). It localizes to both sides of the expanding phagophore, and a significant population remains in the completed autophagosome and is degraded along with cargos trapped in the autophagosome (Mizushima, Yamamoto et al. 2001). Despite our understanding of the conjugation reaction for Atg8 and its role in autophagosme formation, the exact function of Atg8 and its lipidation is not very clear. Recent studies suggest that the amount of Atg8 determines the size of autophagosomes (Xie, Nair et al. 2008), and Atg8–PE has membrane tethering and hemifusion activity *in vitro* (Nakatogawa, Ichimura et al. 2007).

The Atg12 conjugation system

Atg12 is another ubiquitin-like Atg protein involved in autophagy. It shares the E1-like enzyme Atg7 with the Atg8 conjugation system. The C-terminal glycine residue

of Atg12 is first activated by Atg7 via a thioester bond. The activated Atg12 is then transferred to an E2-like enzyme Atg10, which catalyzes the conjugation with Atg5 through an isopeptide bond (Mizushima, Noda et al. 1998). In contrast to ubiquitin, there is no E3-like enzyme involved in Atg12–Atg5 conjugation; Atg5 seems to be the only target of Atg12; and the reaction is irreversible. Atg5 interacts with a small coiled-coil protein Atg16, whose oligomerization leads to a tetrameric complex of Atg12–Atg5-Atg16 (Mizushima, Noda et al. 1999; Kuma, Mizushima et al. 2002). The Atg12–Atg5-Atg16 complex mainly localizes to the outer face of the expanding phagophore, and dissociates from the membrane upon completion of autophagosome formation (Mizushima, Yamamoto et al. 2001). The absence of Atg12, Atg5 or Atg16 affects Atg8 conjugation, and a recent study suggests that the Atg12–Atg5 conjugate may act as an E3-like enzyme in the Atg8–PE conjugation system (Suzuki, Kirisako et al. 2001; Hanada, Noda et al. 2007). This complex also specifies the site of Atg8 conjugation in mammalian cells (Fujita, Itoh et al. 2008).

The PtdIns 3-kinase complex I

Vps34, the sole PtdIns 3-kinase in yeast is essential for autophagy. It forms two PtdIns 3-kinase complexes (Kihara, Noda et al. 2001). The two complexes contain three common subunits: the PtdIns 3-kinase Vps34, the regulatory protein Vps15 and Atg6/Vps30. In addition, each complex has a specific factor, Atg14 for complex I and Vps38 for complex II. These specific factors regulate localization of the two complexes. Atg14 directs complex I to the PAS, whereas Vps38 is responsible for the endosomal localization of complex II (Obara, Sekito et al. 2006). The PtdIns 3-kinase complex I

presumably functions in autophagy through its production of PtdIns(3)P and recruitment of PtdIns(3)P-binding proteins, such as Atg18, Atg20, Atg21 and Atg24. These effectors may in turn act as a scaffold in membrane formation. This hypothesis is supported by studies showing that PtdIns(3)P is enriched on autophagosome and autophagic body membranes in yeast (Obara, Noda et al. 2008), and that during autophagosome biogenesis PtdIns(3)P-enriched membrane compartments emerge upon amino acid starvation in HEK 293 cells (Axe, Walker et al. 2008). However, it is still not clear how PtdIn3(P) enrichment is involved in autophagy and how PtdIn3(P)-binding proteins function in autophagy.

Atg9

Atg9 is the only transmembrane protein that is required for autophagosome formation across species (Noda, Kim et al. 2000), and is a proposed membrane carrier for this process. Different from the majority of Atg proteins, Atg9 localizes to multiple punctate structures in addition to the PAS (Reggiori, Shintani et al. 2005). In yeast, Atg9 cycles between the PAS and mitochondria. The forward movement of Atg9 from mitochondria to the PAS requires Atg11, Atg23 and Atg27 in nutrient-rich conditions (He, Song et al. 2006; Yen, Legakis et al. 2006), and the retrieval of Atg9 from the PAS requires the Atg1 kinase complex, the PtdIns 3-kinase complex I, Atg2 and Atg18 (Reggiori, Tucker et al. 2004). These results suggest that Atg9 may supply the forming vesicle with lipid through its cycling. But direct evidence for involvement of Atg9 in membrane expansion is lacking. Human Atg9 undergoes a similar redistribution from nutrient-rich to starvation conditions. The translocation of Atg9L1 from the Golgi

apparatus to the endosome is prevented by blocking the function of ULK1 (an Atg1 homologue) (Young, Chan et al. 2006).

The Atg18 complex

Atg18 forms a complex with Atg2 (Suzuki, Kubota et al. 2007), but no interaction has been reported between Atg18 and Atg21, or between Atg2 and Atg21. For simplicity, Atg18, Atg2 and Atg21 are included in the Atg18 complex, as Atg18 and Atg21 are homologous proteins. Both Atg18 and Atg21 are predicted to be multi-WD-40 repeat proteins, and are able to bind PtdIns(3)P and PtdIns(3,5)P_2 (Dove, Piper et al. 2004). Repeated WD-40 motifs fold into β-propeller structures and act as sites for protein-protein interaction. Both Atg18 and Atg21 bind phosphoinositides through conserved Phe-Arg-Arg-Gly (FRRG) motifs within the proposed β-propellers (Dove, Piper et al. 2004; Stromhaug, Reggiori et al. 2004).

Atg18 functions in autophagy, the Cvt pathway, and retrograde trafficking from the vacuole to the Golgi (Barth, Meiling-Wesse et al. 2001; Guan, Stromhaug et al. 2001; Efe, Botelho et al. 2007). The deletion of Fab1, the sole PtdIns(3)P 5-kinase in yeast, has no effect on either autophagy or the Cvt pathway, suggesting that PtdIns(3,5)P_2 is not required for either pathway (Dove, Piper et al. 2004; Obara, Noda et al. 2008). In contrast, retrograde trafficking from the vacuole depends on the PtdIns(3,5)P_2-binding ability of Atg18 (Efe, Botelho et al. 2007). Mutational analyses of the FRRG motif suggest that phosphoinositide binding or more specifically PtdIns(3)P binding, is critical for Atg18 PAS localization and for the function of this protein in the Cvt pathway, but is not absolutely required for autophagy (Obara, Noda et al. 2008). The lipid binding FRRG

motif is also conserved in the human Atg18 homologue WIPI-1. WIPI-1 binds PtdIns(3)P in several cell lines, and deletion of the FRRG motif in WIPI-1 results in reduced PtdIns(3)P binding and loss of WIPI-1 puncta formation (Proikas-Cezanne, Ruckerbauer et al. 2007).

Atg18 interacts with Atg2, and they depend on each other for their PAS localization (Suzuki, Kubota et al. 2007). The interaction is independent of the PtdIns(3)P-binding ability of Atg18, but the PAS localization of the Atg18-Atg2 complex requires its PtdIns(3)P-binding ability (Obara, Noda et al. 2008). Both Atg18 and Atg2 interact with Atg9, and are required for retrieval of Atg9 from the PAS (Reggiori, Tucker et al. 2004).

Atg21 is only required for the Cvt pathway (Stromhaug, Reggiori et al. 2004). Its FRRG motif is essential for the Cvt pathway, but the role of its PtdIns(3,5)P_2 binding function is unknown (Stromhaug, Reggiori et al. 2004).

Before going into details about the following chapters, I will briefly describe the work I have done in the past four years. I started my doctoral research by characterizing the *S. cerevisiae* Atg26 protein (ScAtg26), and I found it is not required for nonspecific or specific autophagy in *S. cerevisiae*. This piece of negative data was published in the journal *Autophagy* and is reprinted in Chapter 5. Then I quickly moved to my major project: reconstituting autophagy *in vivo*. I constructed a multiple knockout (MKO) strain deleted for 24 *ATG* genes, and by introducing a subset of *ATG* genes back into the MKO strain, I was able to reconstitute different aspects of autophagy and gain new information

about PAS assembly, Atg12 conjugation, and Atg8 conjugation. This work was published in the *Journal of Cell Biology*, and is reprinted in Chapter 2. Based on the existing MKO strain, I made a MKO yeast two-hybrid (Y2H) strain by integrating three different reporters. Furthermore, I assessed the reporters via known and unknown interactions, and identified a new interaction between Atg29 and Atg31. The work on the MKO Y2H strain is in Chapter 3 and has been submitted as a toolbox paper to the journal *Autophagy*. During my third year, I developed an interest in, and wrote a review on Atg6, a component of the PtdIns 3-kinase complex I, for *Cell Research*. But instead of working directly on Atg6, I initiated a collaboration with Dr. Usha Nair to study the downstream PtdIns(3)P-binding proteins Atg18 and Atg21. The outlook for the paper had been good until most of our data were published by another group. Then it was a quest for more data and mechanistic insights. We managed to finish the project and submitted our manuscript to *Molecular Biology of the Cell*, and the preprint is in Chapter 4. Interestingly, our work on Atg18 and Atg21 partially answered a question about Atg8 conjugation raised in my first MKO paper. The MKO strain has also been used as a tool by Congcong He to test if Atg9 interacts with itself in the absence of other Atg proteins, and I constructed point mutants losing Atg9 self-interaction and studied their phenotypes. The work on Atg9 gave me a third authorship on a paper published in *Molecular Biology of the Cell*, and the paper is reprinted in Appendix A.

References

Axe, E. L., S. A. Walker, et al. (2008). "Autophagosome formation from membrane compartments enriched in phosphatidylinositol 3-phosphate and dynamically connected to the endoplasmic reticulum." J Cell Biol **182**(4): 685-701.

Barth, H., K. Meiling-Wesse, et al. (2001). "Autophagy and the cytoplasm to vacuole targeting pathway both require Aut10p." FEBS Lett **508**(1): 23-8.

Chan, E. Y., A. Longatti, et al. (2009). "Kinase-inactivated ULK proteins inhibit autophagy via their conserved C-terminal domains using an Atg13-independent mechanism." Mol Cell Biol **29**(1): 157-71.

Cheong, H., U. Nair, et al. (2008). "The Atg1 kinase complex is involved in the regulation of protein recruitment to initiate sequestering vesicle formation for nonspecific autophagy in *Saccharomyces cerevisiae*." Mol Biol Cell **19**(2): 668-81.

Cheong, H., T. Yorimitsu, et al. (2005). "Atg17 regulates the magnitude of the autophagic response." Mol Biol Cell **16**(7): 3438-53.

Dove, S. K., R. C. Piper, et al. (2004). "Svp1p defines a family of phosphatidylinositol 3,5-bisphosphate effectors." EMBO J **23**(9): 1922-33.

Dunn, W. A. Jr., J. M. Cregg, et al. (2005). "Pexophagy: the selective autophagy of peroxisomes." Autophagy **1**(2): 75-83.

Efe, J. A., R. J. Botelho, et al. (2007). "Atg18 regulates organelle morphology and Fab1 kinase activity independent of its membrane recruitment by phosphatidylinositol 3,5-bisphosphate." Mol Biol Cell **18**(11): 4232-44.

Farre, J. C., R. Manjithaya, et al. (2008). "PpAtg30 tags peroxisomes for turnover by selective autophagy." Dev Cell **14**(3): 365-76.

Fujita, N., T. Itoh, et al. (2008). "The Atg16L complex specifies the site of LC3 lipidation for membrane biogenesis in autophagy." Mol Biol Cell **19**(5): 2092-100.

Gozuacik, D. and A. Kimchi (2004). "Autophagy as a cell death and tumor suppressor mechanism." Oncogene **23**(16): 2891-906.

Guan, J., P. E. Stromhaug, et al. (2001). "Cvt18/Gsa12 is required for cytoplasm-to-vacuole transport, pexophagy, and autophagy in *Saccharomyces cerevisiae* and *Pichia pastoris*." Mol Biol Cell **12**(12): 3821-38.

Hanada, T., N. N. Noda, et al. (2007). "The Atg12-Atg5 conjugate has a novel E3-like activity for protein lipidation in autophagy." J Biol Chem **282**(52): 37298-302.

Hara, T., A. Takamura, et al. (2008). "FIP200, a ULK-interacting protein, is required for autophagosome formation in mammalian cells." J Cell Biol **181**(3): 497-510.

Harding, T. M., A. Hefner-Gravink, et al. (1996). "Genetic and phenotypic overlap between autophagy and the cytoplasm to vacuole protein targeting pathway." J Biol Chem **271**(30): 17621-4.

He, C., H. Song, et al. (2006). "Recruitment of Atg9 to the preautophagosomal structure by Atg11 is essential for selective autophagy in budding yeast." J Cell Biol **175**(6): 925-35.

Ichimura, Y., T. Kirisako, et al. (2000). "A ubiquitin-like system mediates protein lipidation." Nature **408**(6811): 488-92.

Kabeya, Y., Y. Kamada, et al. (2005). "Atg17 functions in cooperation with Atg1 and Atg13 in yeast autophagy." Mol Biol Cell **16**(5): 2544-53.
Kabeya, Y., T. Kawamata, et al. (2007). "Cis1/Atg31 is required for autophagosome formation in *Saccharomyces cerevisiae*." Biochem Biophys Res Commun **356**(2): 405-10.
Kabeya, Y., N. Mizushima, et al. (2000). "LC3, a mammalian homologue of yeast Apg8p, is localized in autophagosome membranes after processing." EMBO J **19**(21): 5720-8.
Kabeya, Y., N. Mizushima, et al. (2004). "LC3, GABARAP and GATE16 localize to autophagosomal membrane depending on form-II formation." J Cell Sci **117**(13): 2805-12.
Kamada, Y., T. Funakoshi, et al. (2000). "Tor-mediated induction of autophagy via an Apg1 protein kinase complex." J Cell Biol **150**(6): 1507-13.
Kanki, T. and D. J. Klionsky (2008). "Mitophagy in yeast occurs through a selective mechanism." J Biol Chem **283**(47): 32386-93.
Kawamata, T., Y. Kamada, et al. (2008). "Organization of the pre-autophagosomal structure responsible for autophagosome formation." Mol Biol Cell **19**(5): 2039-50
Kawamata, T., Y. Kamada, et al. (2005). "Characterization of a novel autophagy-specific gene, *ATG29*." Biochem Biophys Res Commun **338**(4): 1884-9.
Kihara, A., T. Noda, et al. (2001). "Two distinct Vps34 phosphatidylinositol 3-kinase complexes function in autophagy and carboxypeptidase Y sorting in *Saccharomyces cerevisiae*." J Cell Biol **152**(3): 519-30.
Kim, J., Y. Kamada, et al. (2001). "Cvt9/Gsa9 functions in sequestering selective cytosolic cargo destined for the vacuole." J Cell Biol **153**(2): 381-96.
Klionsky, D. J. (2005). "The molecular machinery of autophagy: unanswered questions." J Cell Sci **118**(1): 7-18.
Klionsky, D. J., J. M. Cregg, et al. (2003). "A unified nomenclature for yeast autophagy-related genes." Dev Cell **5**(4): 539-45.
Klionsky, D. J., A. M. Cuervo, et al. (2007). "How shall I eat thee?" Autophagy **3**: 413-416.
Kuma, A., N. Mizushima, et al. (2002). "Formation of the approximately 350-kDa Apg12-Apg5·Apg16 multimeric complex, mediated by Apg16 oligomerization, is essential for autophagy in yeast." J Biol Chem **277**(21): 18619-25.
Levine, B. (2005). "Eating oneself and uninvited guests: autophagy-related pathways in cellular defense." Cell **120**(2): 159-62.
Levine, B. and D. J. Klionsky (2004). "Development by self-digestion: molecular mechanisms and biological functions of autophagy." Dev Cell **6**(4): 463-77.
Li, C., E. Capan, et al. (2006). "Autophagy is induced in $CD4^+$ T cells and important for the growth factor-withdrawal cell death." J Immunol **177**(8): 5163-8.
Mathew, R., S. Kongara, et al. (2007). "Autophagy suppresses tumor progression by limiting chromosomal instability." Genes Dev **21**(11): 1367-81.
Mizushima, N., T. Noda, et al. (1999). "Apg16p is required for the function of the Apg12p-Apg5p conjugate in the yeast autophagy pathway." EMBO J **18**(14): 3888-96.

Mizushima, N., T. Noda, et al. (1998). "A protein conjugation system essential for autophagy." Nature **395**(6700): 395-8.
Mizushima, N., A. Yamamoto, et al. (2001). "Dissection of autophagosome formation using Apg5-deficient mouse embryonic stem cells." J Cell Biol **152**(4): 657-68.
Nakatogawa, H., Y. Ichimura, et al. (2007). "Atg8, a ubiquitin-like protein required for autophagosome formation, mediates membrane tethering and hemifusion." Cell **130**(1): 165-78.
Nice, D. C., T. K. Sato, et al. (2002). "Cooperative binding of the cytoplasm to vacuole targeting pathway proteins, Cvt13 and Cvt20, to phosphatidylinositol 3-phosphate at the pre-autophagosomal structure is required for selective autophagy." J Biol Chem **277**(33): 30198-207.
Noda, T., J. Kim, et al. (2000). "Apg9p/Cvt7p is an integral membrane protein required for transport vesicle formation in the Cvt and autophagy pathways." J Cell Biol **148**(3): 465-80.
Noda, T. and Y. Ohsumi (1998). "Tor, a phosphatidylinositol kinase homologue, controls autophagy in yeast." J Biol Chem **273**(7): 3963-6.
Obara, K., T. Noda, et al. (2008). "Transport of phosphatidylinositol 3-phosphate into the vacuole via autophagic membranes in *Saccharomyces cerevisiae*." Genes Cells **13**(6): 537-47.
Obara, K., T. Sekito, et al. (2006). "Assortment of phosphatidylinositol 3-kinase complexes--Atg14p directs association of complex I to the pre-autophagosomal structure in *Saccharomyces cerevisiae*." Mol Biol Cell **17**(4): 1527-39.
Proikas-Cezanne, T., S. Ruckerbauer, et al. (2007). "Human WIPI-1 puncta-formation: a novel assay to assess mammalian autophagy." FEBS Lett **581**(18): 3396-404.
Reggiori, F., T. Shintani, et al. (2005). "Atg9 cycles between mitochondria and the pre-autophagosomal structure in yeasts." Autophagy **1**(2): 101-9.
Reggiori, F., K. A. Tucker, et al. (2004). "The Atg1-Atg13 complex regulates Atg9 and Atg23 retrieval transport from the pre-autophagosomal structure." Dev Cell **6**(1): 79-90.
Rubinsztein, D. C., M. Difiglia, et al. (2005). "Autophagy and its possible roles in nervous system diseases, damage and repair." Autophagy **1**(1): 11-22.
Rubinsztein, D. C., J. E. Gestwicki, et al. (2007). "Potential therapeutic applications of autophagy." Nat Rev Drug Discov **6**(4): 304-12.
Scott, S. V., A. Hefner-Gravink, et al. (1996). "Cytoplasm-to-vacuole targeting and autophagy employ the same machinery to deliver proteins to the yeast vacuole." Proc Natl Acad Sci U S A **93**(22): 12304-8.
Shintani, T., W.-P. Huang, et al. (2002). "Mechanism of cargo selection in the cytoplasm to vacuole targeting pathway." Dev Cell **3**(6): 825-37.
Shintani, T. and D. J. Klionsky (2004). "Autophagy in health and disease: a double-edged sword." Science **306**(5698): 990-5.
Stromhaug, P. E., F. Reggiori, et al. (2004). "Atg21 is a phosphoinositide binding protein required for efficient lipidation and localization of Atg8 during uptake of aminopeptidase I by selective autophagy." Mol Biol Cell **15**(8): 3553-66.
Suzuki, K., T. Kirisako, et al. (2001). "The pre-autophagosomal structure organized by concerted functions of *APG* genes is essential for autophagosome formation." EMBO J **20**(21): 5971-81.

Suzuki, K., Y. Kubota, et al. (2007). "Hierarchy of Atg proteins in pre-autophagosomal structure organization." Genes Cells **12**(2): 209-18.
Xie, Z., U. Nair, et al. (2008). "Atg8 controls phagophore expansion during autophagosome formation." Mol Biol Cell **19**(8): 3290-8.
Yen, W.-L., J. E. Legakis, et al. (2006). "Atg27 is required for autophagy-dependent cycling of Atg9." Mol Biol Cell **18**(2): 581-93.
Yorimitsu, T. and D. J. Klionsky (2005). "Atg11 links cargo to the vesicle-forming machinery in the cytoplasm to vacuole targeting pathway." Mol Biol Cell **16**(4): 1593-605.
Young, A. R.J., E. Y.W. Chan, et al. (2006). "Starvation and ULK1-dependent cycling of mammalian Atg9 between the TGN and endosomes." J Cell Sci **119**(18): 3888-900.
Zhang, Y., H. Qi, et al. (2007). "The role of autophagy in mitochondria maintenance: characterization of mitochondrial functions in autophagy-deficient *S. cerevisiae* strains." Autophagy **3**(4): 337-46.

CHAPTER 2

In vivo reconstitution of autophagy in *Saccharomyces cerevisiae*

Abstract

Autophagy is a major intracellular degradative pathway, which is involved in various human diseases. The role of autophagy, however, is complex; although the process is generally considered to be cytoprotective, it can also contribute to cellular dysfunction and disease progression. Much progress has been made in our understanding of autophagy, aided in large part by the identification of the *AuTophaGy*-related (*ATG*) genes. Nonetheless, our understanding of the molecular mechanism remains limited. In this study we generated a *Saccharomyces cerevisiae* multiple-knockout strain with twenty-four *ATG* genes deleted, and we used it to carry out an *in vivo* reconstitution of the autophagy pathway. We determined minimum requirements for different aspects of autophagy, and studied the initial protein assembly steps at the phagophore assembly site. *In vivo* reconstitution enables the study of autophagy within the context of the complex regulatory networks that control this process, an analysis that is not possible with an *in vitro* system.

Introduction

Macroautophagy (hereafter autophagy) is a conserved degradative pathway in eukaryotic cells that also plays an essential role in development and differentiation, and is implicated in many human diseases (Levine and Klionsky 2004; Mizushima 2007). Autophagy involves *de novo* formation of a double-membrane vesicle (the autophagosome) in the cytosol, fusion of this vesicle with the lysosome/vacuole, and the subsequent breakdown and recycling of the cargo. With the identification of *AuTophaGy*-related (*ATG*) genes in yeast, autophagy research has shifted from morphological analyses to the understanding of molecular mechanisms (Klionsky 2007). 31 *ATG* genes have been identified in baker's and methylotrophic yeasts, and many of them have homologues in higher eukaryotes (Rubinsztein, Gestwicki et al. 2007).

Autophagy is generally considered to be non-selective, but there are also selective types of autophagy. The cytoplasm to vacuole targeting (Cvt) pathway is an example of selective autophagy wherein the precursor form of the resident vacuolar hydrolase aminopeptidase I (prApe1) is selectively transported from the cytoplasm into the vacuole under vegetative conditions (Klionsky 2005). The Cvt pathway shares most of the components needed for autophagy but utilizes additional proteins in cargo recognition and packaging. After synthesis in the cytosol, prApe1 forms an oligomer, which is targeted through a receptor, Atg19, and an adaptor, Atg11 (Kim, Scott et al. 1997; Scott, Guan et al. 2001; Shintani, Huang et al. 2002; Shintani and Klionsky 2004; Yorimitsu and Klionsky 2005). There is no evidence that the Cvt pathway exists outside of fungi.

However, a similar recognition mechanism might be utilized in mammalian examples of selective autophagy (Iwata, Ezaki et al. 2006).

Most of the Atg proteins at least transiently colocalize at the phagophore assembly site (PAS, the presumed nucleating site of the autophagosome) in both the Cvt pathway and nonselective autophagy; however, this site is poorly defined and characterized. Knowing how Atg proteins are targeted to the PAS will help us dissect the vesicle formation process and understand how these proteins interact and function. The cargo complex including Atg11 is the initial component for PAS assembly in vegetative conditions (Shintani, Huang et al. 2002), whereas Atg17 has been shown to be an initial factor for PAS assembly in starvation (Suzuki, Kubota et al. 2007). Components in the Atg17 complex, such as Atg1 and Atg13 are also involved in organizing the PAS during starvation (Cheong, Nair et al. 2008; Kawamata, Kamada et al. 2008). However, many questions regarding the temporal order of protein assembly at the PAS still remain.

Among the conserved genes, eight participate in two separate but related conjugation systems, involving two ubiquitin-like proteins, Atg8 and Atg12. Atg8 is conjugated to phosphatidylethanolamine (PE) through the serial action of Atg4, Atg7 and Atg3 (Ichimura, Kirisako et al. 2000). The C-terminal arginine residue of Atg8 is first removed by the cysteine protease Atg4, exposing a glycine residue that is now accessible to the E1-like activating enzyme Atg7. The activated Atg8 is then transferred to the E2-like conjugating enzyme Atg3 and finally conjugated to PE. Atg8 can be deconjugated from Atg8–PE through a second cleavage by Atg4, although the mechanism that regulates the timing of Atg4 cleavage is not known. The second ubiquitin-like protein, Atg12, is covalently linked to Atg5 through the action of the E1-like Atg7 and an E2-like

enzyme, Atg10 (Mizushima, Noda et al. 1998). The Atg12–Atg5 conjugate also binds another protein, Atg16, whose oligomerization leads to a tetrameric complex of Atg12–Atg5-Atg16 (Mizushima, Noda et al. 1999; Kuma, Mizushima et al. 2002). The Atg8–PE level is reduced in the absence of Atg12, Atg5 or Atg16, and the Atg12–Atg5 conjugate may act as an E3-like enzyme in the Atg8–PE conjugation system (Suzuki, Kirisako et al. 2001; Hanada, Noda et al. 2007). On the other hand, the efficiency of Atg12–Atg5 conjugation is apparently not affected by the Atg8–PE system (Kuma, Mizushima et al. 2002). Although *in vitro* reconstitution of both Atg8–PE and Atg12–Atg5 conjugation has been reported (Ichimura, Imamura et al. 2004; Fujioka, Noda et al. 2007; Hanada, Noda et al. 2007; Shao, Gao et al. 2007), *in vivo* reconstitution of the two reactions in eukaryotic cells is not available. Thus, the physiological significance of some of the *in vitro* observations has not been verified.

Many steps of autophagy have been analyzed *in vivo* using standard molecular genetics in single- and double-deletion mutant strains, and a smaller subset of the reactions have been reconstituted *in vitro*. It is unlikely that the entire process will be reconstituted *in vitro* in the near term due to the complexity of the system and the lack of knowledge regarding basic issues such as the origin of the sequestering membrane. In addition, *in vitro* studies inherently lack many critical elements such as the cytoskeleton, and the regulatory controls that play important roles *in vivo*. To provide a physiological reconstitution system we deleted 24 *ATG* genes directly required for autophagy and/or the Cvt pathway using a multiple knockout (MKO) strategy. We used this MKO strain to determine the minimum requirements for cargo packaging, initial assembly of the starvation-specific PAS, and conjugation of the ubiquitin-like Atg proteins. Our results

with the MKO strain verify the role of particular Atg proteins in cargo packaging, and extend previous studies on PAS assembly and protein conjugation that were based on work with individual or double-deletion strains and/or *in vitro* studies. With this work, we present a new method to tackle complex cellular pathways, and particularly those with extensive regulatory networks such as autophagy that cannot be easily replicated *in vitro*.

Results

Construction of a MKO strain to study autophagy

We were able to construct the MKO strain because all the *ATG* genes directly required for autophagy and the Cvt pathway are nonessential and the *loxP/Cre* system allows the use and recycling of markers for multiple knockouts (Fig. 2.1A) (Gueldener, Heinisch et al. 2002). Among the 31 *ATG* genes, 24 of them were deleted in strain YCY123 (Table 2.1). *ATG15*, *ATG22*, *ATG25*, *ATG26*, *ATG28* and *ATG30* were not deleted because the first two function after autophagosomes fuse with the lysosomal/vacuolar membrane, and the rest are either not found in *Saccharomyces cerevisiae* or are only required for peroxisome degradation in other methylotrophic yeasts (Cao and Klionsky 2007). *ATG31* was not deleted because we finished generating the MKO strain and the experiments described in this manuscript before it was published (Kabeya, Kawamata et al. 2007). We refer to strain YCY123 as the MKO strain. Additional deletions, or the presence of *ATG* genes, are indicated in parentheses.

The MKO strain does not have any obvious unexpected defect other than a slight growth delay (Fig. 2.1B). In the MKO strain, we observed one abnormally enlarged vacuole, which is similar to the *atg18*Δ phenotype (Fig. 2.1C) (Dove, Piper et al. 2004). The normal vacuole morphology was restored when we introduced Atg18 back into the MKO strain (Fig. 2.1C). We also tested whether the MKO strain was defective for other vacuolar targeting pathways. Carboxypeptidase Y (Prc1) transits through the endoplasmic reticulum (ER), Golgi complex, and late endosome/multivesicular body (MVB) for delivery to the vacuole. Carboxypeptidase S (Cps1) is a cargo for the MVB pathway and

transits through the early secretory pathway similar to Prc1, but is packaged into lumenal vesicles of the MVB prior to vacuolar delivery. Vacuolar alkaline phosphatase (Pho8) is transported through the ER to the Golgi, but it bypasses the endosome/MVB (Bowers and Stevens 2005). By pulse-chase and immunoprecipitation, we followed Prc1, Cps1 and Pho8 processing in the MKO strain. As *ATG6* is essential for the carboxypeptidase Y pathway, we transformed a plasmid expressing Atg6 into the MKO and the *atg6Δ* strains. As shown in Fig. 2.1D, although there was a kinetic delay in the MKO strain expressing Atg6, most of the precursor Prc1, Cps1 (not depicted) and Pho8 became mature after 45 min in chase medium. Taking the growth delay of the MKO strain into consideration, these data suggest that the MKO strain expressing Atg6 is not defective for the carboxypeptidase Y, MVB and alkaline phosphatase vacuolar protein delivery pathways, which are non-autophagic.

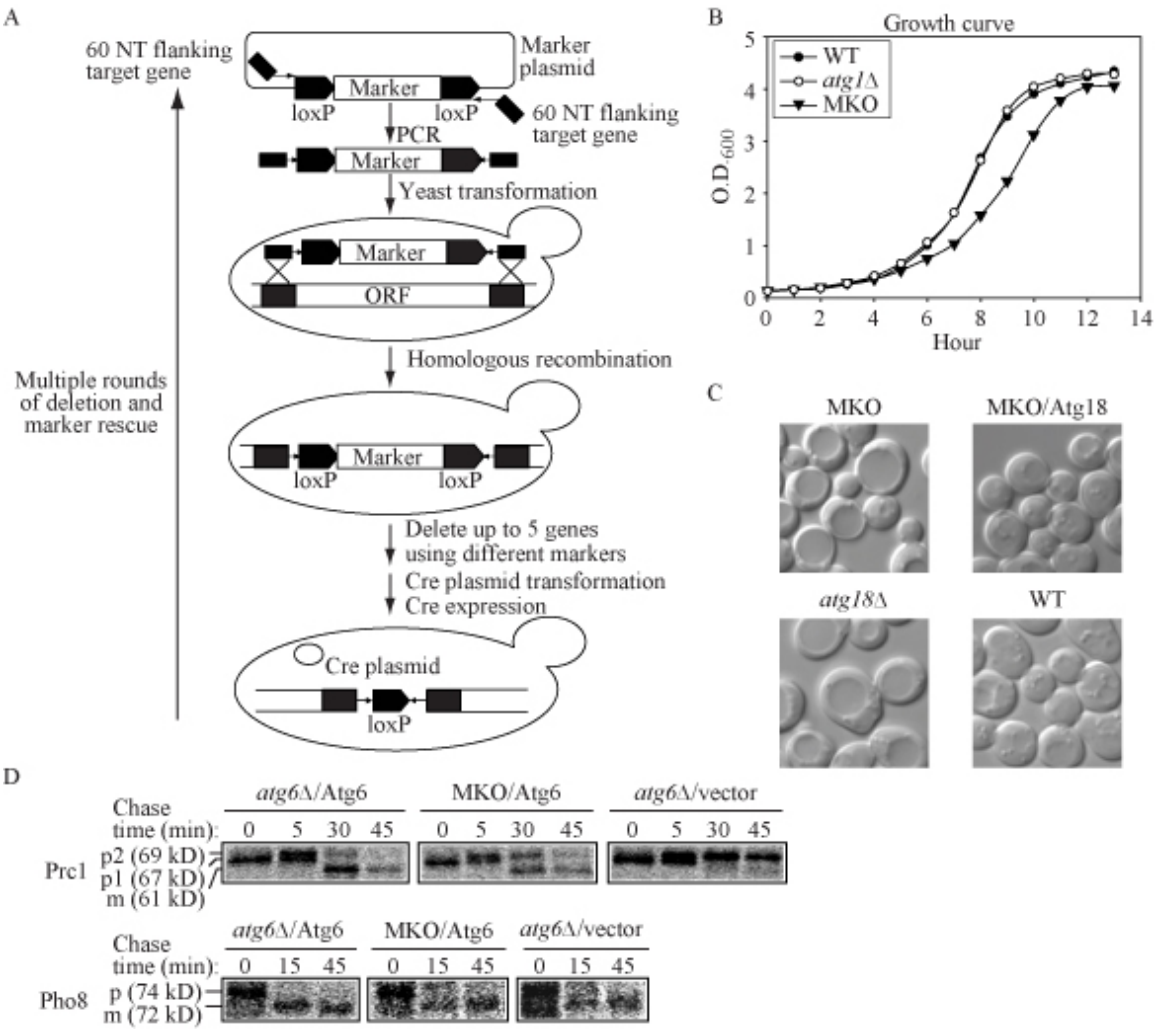

Figure 2.1. Generation and properties of the MKO strain. (A) Schematic representation of the MKO strategy. The *loxP–Cre* system allows disruption of up to five genes using different markers, and efficient removal of markers by Cre expression. Multiple rounds of deletion and marker rescue yielded the MKO strain. See Materials and methods for detailed information. (B) Growth curve of the MKO strain compared with wild-type (WT) and *atg1Δ* strains. WT, *atg1Δ*, and the MKO strains were grown overnight in YPD and diluted to OD_{600} = 0.1. Aliquots were removed for OD_{600} readings every hour for 13 h. (C) Morphology of the MKO strain. WT and *atg18Δ* strains and the MKO strain with or without a plasmid expressing Atg18 (pATG18(415)) were grown in YPD to mid-log phase and observed by microscopy. The MKO strain had an enlarged vacuole similar to the *atg18Δ* strain; once transformed with Atg18, the vacuole size became the same as that in the wild type. Bar, 2 μm. (D) The MKO strain expressing Atg6 is not defective for the carboxypeptidase Y, MVB, or alkaline phosphatase pathways, and was assayed by pulse-chase experiments for Prc1, Cps1 (not depicted), and Pho8 processing. The *atg6Δ* and MKO strains transformed with a plasmid expressing Atg6 (pATG6(414)) or the empty pRS414 vector were subjected to a radioactive label/nonradioactive chase and tripleimmunoprecipitated as described in Materials and methods, then analyzed by 8% SDS-PAGE. Carboxypeptidase Y (Prc1) transits through the ER in a precursor (p1) form, acquires its p2 form in the Golgi complex, and, via the late endosome–MVB pathway, is delivered to the vacuole and converted to its mature (m) form. Vacuolar alkaline phosphatase (Pho8) is transported through the ER to the Golgi in a precursor (p) form but bypasses the endosome and is proteolytically activated to its mature (m) form in the vacuole. Atg6 is not required for the alkaline phosphatase pathway; however, for consistency, cells expressing Atg6 were used throughout the experiment.

Table 2.1. Yeast strains used in this study.

Strain	Descriptive Name	Genotype	Source or reference
CWY241	WT (*ATG17-GFP*)	SEY6210 *ATG17-GFP::HIS3*	(Cheong, Yorimitsu et al. 2005)
HCY107	MKO (*ATG17-GFP*)	YCY123 *ATG17-GFP::HIS3*	This study
HCY113	MKO (*ATG29 ATG17-GFP*)	YCY121 *ATG17-GFP::HIS3*	This study
HCY151	MKO (*ATG11 ATG17-GFP*)	YCY152 *ATG17-GFP::HIS3*	This study
JLY2	*atg12*Δ	SEY6210 *atg12*Δ*::kanMX*	This study
PSY161	*atg6*Δ	SEY6210 *atg6*Δ*::HIS3*	This study
SEY6210	WT	*MAT*α *ura3–52 leu2–3,112 his3-*Δ*200 trp1-*Δ*901 lys2–801 suc2-*Δ*9 GAL*	(Robinson, Klionsky et al. 1988)
TVY1	*pep4*Δ	SEY6210 *pep4*Δ*::LEU2*	(Gerhardt, Kordas et al. 1998)
WHY001	*atg1*Δ	SEY6210 *atg1*Δ*::HIS5*	(Shintani, Huang et al. 2002)
YCY26	*atg18*Δ	SEY6210 *atg18*Δ*::kanMX*	This study
YCY32	*atg8*Δ *atg4*Δ	SEY6210 *atg8*Δ*::HIS5, atg4*Δ*::LEU2*	This study
YCY121	MKO (*ATG29*)	SEY6210 *atg1*Δ*, 2*Δ*, 3*Δ*, 4*Δ*, 5*Δ*, 6*Δ*, 7*Δ*, 8*Δ*, 9*Δ*, 10*Δ*, 11*Δ*, 12*Δ*, 13*Δ*, 14*Δ*, 16*Δ*, 17*Δ*, 18*Δ*, 19*Δ*, 20*Δ*, 21*Δ*, 23*Δ*, 24*Δ*, 27*Δ	This study
YCY123	MKO	SEY6210 *atg1*Δ*, 2*Δ*, 3*Δ*, 4*Δ*, 5*Δ*, 6*Δ*, 7*Δ*, 8*Δ*, 9*Δ*, 10*Δ*, 11*Δ*, 12*Δ*, 13*Δ*, 14*Δ*, 16*Δ*, 17*Δ*, 18*Δ*, 19*Δ*, 20*Δ*, 21*Δ*, 23*Δ*, 24*Δ*, 27*Δ*, 29*Δ	This study
YCY124	MKO (*atg15*Δ)	YCY123 *atg15*Δ*::kanMX*	This study
YCY125	MKO (*atg15*Δ *ape1*Δ)	YCY123 *atg15*Δ*::kanMX, ape1*Δ*::HIS3*	This study
YCY126	MKO (*atg15*Δ *RFP-APE1*)	YCY123 *atg15*Δ*::kanMX, RFP-APE1::LEU2*	This study
YCY137	MKO (*ATG3*)	SEY6210 *atg1*Δ*, 2*Δ*, 4*Δ*, 5*Δ*, 6*Δ*, 7*Δ*, 8*Δ*, 9*Δ*, 10*Δ*, 11*Δ*, 12*Δ*, 13*Δ*, 14*Δ*, 16*Δ*, 17*Δ*, 18*Δ*, 19*Δ*, 20*Δ*, 21*Δ*, 23*Δ*, 24*Δ*, 27*Δ*, 29*Δ	This study
YCY152	MKO (*ATG11*)	YCY123 *ATG11::LYS2*	This study

Components necessary and sufficient for cargo packaging in the Cvt pathway

We next wanted to determine if the MKO strain faithfully reproduced different steps of autophagy when expressing the appropriate autophagy genes. Previous studies with standard deletion strains have only been able to demonstrate the requirement, but not the sufficiency, for various proteins involved in different steps of autophagy. In the next set of experiments, we reconstituted the cargo packaging step of the Cvt pathway. At the beginning of the cargo packaging process, prApe1 forms a large oligomer and a bright single punctate structure representing the oligomer can be observed by fluorescence microscopy if the protein is tagged with a fluorophore (Kim, Scott et al. 1997; Shintani, Huang et al. 2002). The same pattern was also detected in the MKO (*atg15*Δ *RFP-APE1*) strain expressing prApe1 tagged with RFP (Fig. 2.2A, left panel). Additional knockout of *ATG15* in the MKO strain slightly reduced its growth rate, but did not affect Cvt vesicle/autophagosome formation (not depicted). In *ape1*Δ cells, both the Atg19 receptor and the Atg11 adaptor are dispersed in the cytosol (Yorimitsu and Klionsky 2005). To determine whether the MKO strain reproduced these phenotypes, we constructed a version lacking *APE1* and transformed it with a plasmid expressing either YFP-Atg19 or GFP-Atg11. In the absence of prApe1 (the cargo), YFP-Atg19 was cytosolic (Fig. 2.2A, middle panel), but GFP-Atg11 formed a punctate structure (Fig. 2.2A, right panel). Atg11 is able to interact with itself and several other Atg proteins, and the coiled-coil domains through which Atg11 self-interacts overlap with the interaction sites used by Atg1, Atg17 and Atg20 (Yorimitsu and Klionsky 2005). Therefore, it is possible that without competition from the other Atg proteins, Atg11 can form a large oligomer by self-

interaction in the MKO strain. Analysis of the Atg11 protein by gradient fractionation suggests that it indeed forms a large complex in the MKO strain (unpublished data).

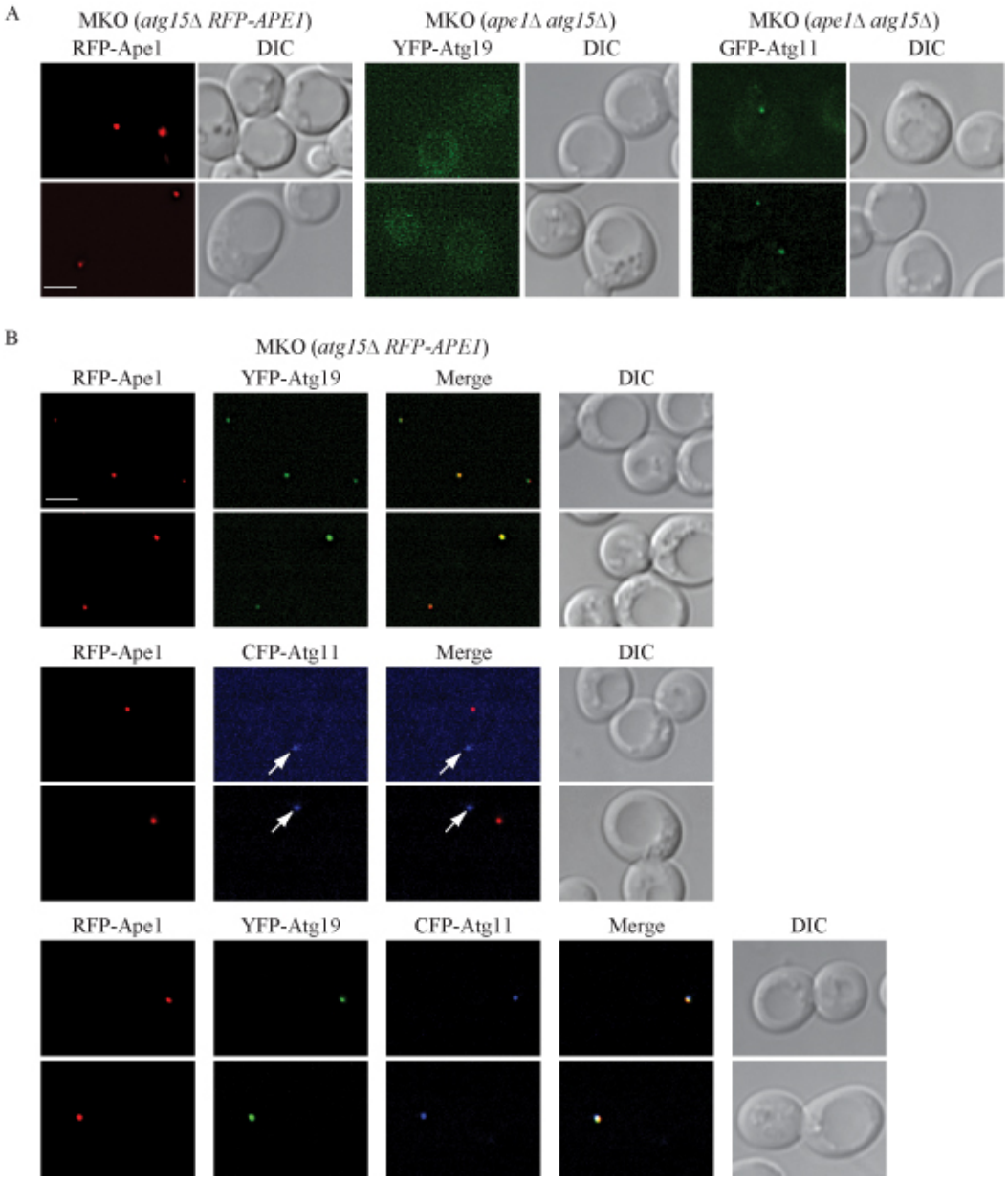

Figure 2.2. Reconstitution of the cargo recognition and packaging step of the Cvt pathway. (A) Localization of the cargo prApe1 in the MKO (*atg15Δ RFP-APE1*) strain, and localization of the receptor Atg19 and the adaptor Atg11 in the MKO (*ape1Δ atg15Δ*) strain. The MKO (*atg15Δ RFP-APE1*) strain and the MKO (*ape1Δ atg15Δ*) strain transformed with a plasmid expressing YFP-Atg19 (pYFPATG19(416)) or HA-tagged CFP-Atg11 (pCuHACFPATG11(414)) were grown in selective SMD medium to mid-log phase and observed by fluorescence microscopy. DIC, differential interference contrast. (B) Colocalization of prApe1, Atg19, and Atg11. The MKO (*atg15Δ RFP-APE1*) strain was transformed with a plasmid expressing YFP-Atg19, HA-tagged CFP-Atg11, or both, grown to mid-log phase and observed by fluorescence microscopy. When Atg19 was coexpressed with prApe1 in the MKO (*atg15Δ RFP-APE1*) strain, the cargo prApe1 colocalized with the receptor Atg19 (top). When Atg19 was absent, the adaptor Atg11 (arrows) did not colocalize with the cargo (middle). When prApe1, Atg19, and Atg11 were all present, the three proteins colocalized to the same structure (bottom). Bars, 2.5 μm.

In wild-type cells, Atg19 binds the propeptide of, and colocalizes with, prApe1. Atg11 interacts with Atg19, and targets the complex to the PAS (Scott, Guan et al. 2001; Shintani, Huang et al. 2002; Yorimitsu and Klionsky 2005). Thus, there is a temporal order of protein interaction, whereby Atg11 cannot bind the prApe1 complex in the absence of Atg19. To test whether this temporal organization is faithfully retained in the MKO strain, we transformed the MKO (*atg15*Δ *RFP-APE1*) strain with plasmids expressing YFP-Atg19, CFP-Atg11, or both. In agreement with the previous model, RFP-Ape1 and YFP-Atg19 colocalized with each other in the absence of other Atg proteins (Fig. 2.2B, upper panel). In contrast, without Atg19, RFP-Ape1 did not colocalize with CFP-Atg11 (Fig. 2.2B, middle panel). The three proteins colocalized in a single punctum when all of them were co-expressed (Fig. 2.2B, lower panel). These data suggest that prApe1, Atg19 and Atg11 are necessary and sufficient for cargo packaging in the Cvt pathway. We note, however, that only approximately 50% of the puncta representing the cargo complex (comprised of prApe1, Atg19 and Atg11) were at the PAS (i.e., perivacuolar), which suggests that an additional Atg protein(s) is required to facilitate the targeting of the cargo complex to this site.

Assembly of the initial starvation-specific PAS

The analysis of cargo packaging verified that the MKO strain faithfully replicated the temporal order of Atg protein interactions that have been deduced from previous studies. Next, we decided to use the MKO strain to address a question that would otherwise be extremely difficult to approach. In particular, we wanted to determine the order of assembly of Atg proteins at the PAS. In theory, it might be possible to order the

proteins through an extensive analysis of multiple deletion strains, generating a series of epistatic relationships. However, a definitive study is best performed in the complete absence of the other (i.e., those not being examined) Atg proteins. Recent reports suggest that Atg11 and Atg17 are the two initial factors that establish the assembly sequence for Atg proteins at the PAS (Shintani, Huang et al. 2002; Suzuki, Kubota et al. 2007). In particular, Atg11 is critical for PAS assembly during vegetative growth, whereas Atg17 is proposed to act as a scaffold for recruiting other Atg proteins during starvation-specific PAS formation.

To test whether Atg17 itself is sufficient to assemble the initial PAS, we observed the localization of Atg17 tagged with GFP in the MKO strain by fluorescence microscopy. In wild-type cells, Atg17-GFP displayed a clear PAS punctum as well as a diffuse cytosolic signal in both vegetative and starvation conditions; in some cells we could detect more than one punctum, particularly under starvation conditions (Fig. 2.3A). In contrast, Atg17-GFP was largely cytosolic in the MKO (*ATG17-GFP*) strain (Fig. 2.3A, vector), suggesting that Atg17 is not sufficient for the initial PAS assembly even during starvation. Therefore, we decided to determine what additional factors were needed to allow correct localization of Atg17 during autophagy.

Recently, it was reported that Atg1 and Atg13 are required along with Atg17 in assembly of the starvation-specific PAS (Cheong, Nair et al. 2008). Accordingly, we hypothesized that Atg1, Atg13 and Atg17 are all required for the initial PAS assembly during non-specific autophagy. To examine this, we transformed plasmids expressing Atg1, Atg13 or both into the MKO (*ATG17-GFP*) strain and observed localization of Atg17-GFP by fluorescence microscopy. Atg17-GFP showed clear punctate structures

under starvation conditions only when Atg1 and Atg13 were expressed together (Fig. 2.3A, Atg1 + Atg13). In contrast, expression of either Atg1 or Atg13 alone or in combination with Atg11 did not facilitate Atg17-GFP puncta formation (Fig. 2.3A). The same localization pattern was detected with GFP-Atg1; this protein was cytosolic when expressed by itself, and formed punctate structures in starvation conditions only when Atg13 and Atg17 were both present (unpublished data). Furthermore, approximately 75% of Atg17-GFP or GFP-Atg1 puncta were peri-vacuolar (detected with the lipophilic dye FM 4-64), indicating that Atg1, Atg13 and Atg17 are sufficient for the initial PAS assembly during starvation (Fig. 2.3B). All together, these data suggest that Atg17 is not sufficient for starvation-specific PAS formation; rather, Atg1, Atg13 and Atg17 all appear to have an initial role in PAS assembly during starvation.

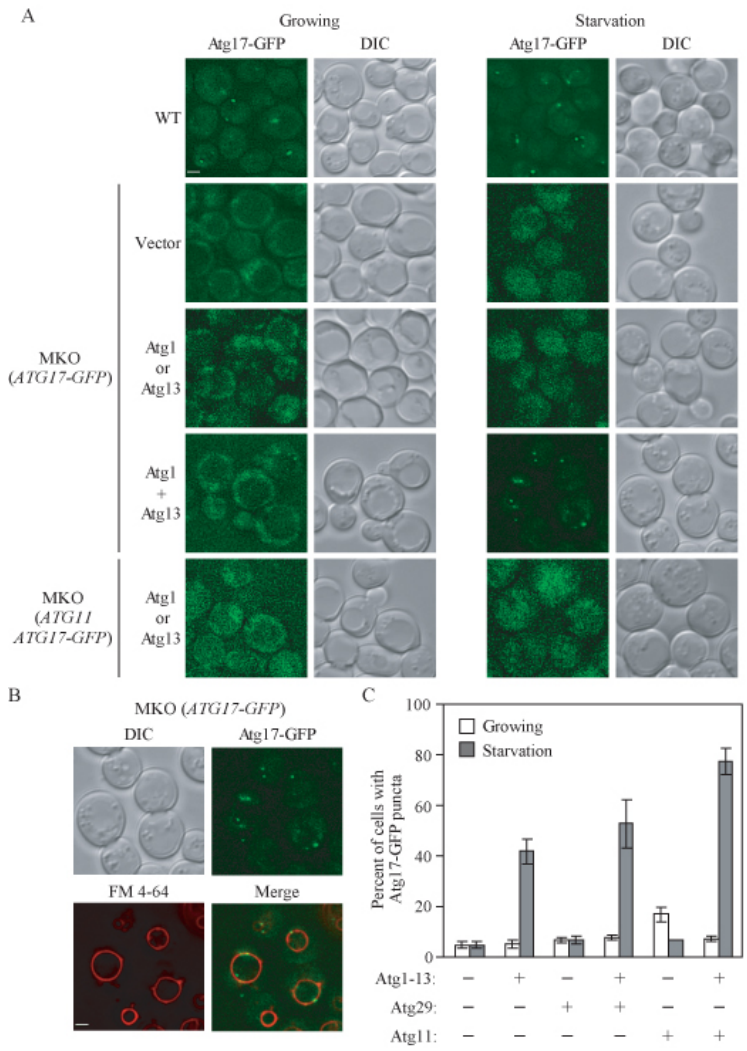

Figure 2.3. Reconstitution of the initial step of starvation-specific PAS assembly. (A) Localization of Atg17-GFP in the wild-type (WT) and MKO (*ATG17-GFP*) strains. The WT (*ATG17-GFP*) strain; the MKO (*ATG17-GFP*) strain transformed with vector (pRS415), a plasmid expressing Atg1 (pATG1(415)), Atg13 (pATG13(415)), or both Atg1 and Atg13 (pATG1-ATG13(415)); and the MKO (*ATG11 ATG17-GFP*) strain transformed with a plasmid expressing Atg1 or Atg13 were grown in selective SMD medium to mid-log phase and shifted to SD-N for 2 h for starvation. Samples were taken from both growing (mid-log phase) and starvation conditions for fluorescence microscopy analyses. Atg17-GFP displayed a punctate structure in WT cells in both growing and starvation conditions; some cells had more than one punctum in starvation conditions. In the MKO (*ATG17-GFP*) strain, Atg17 was cytosolic in both conditions; its localization pattern changed to punctate structures in starvation only when Atg1 and Atg13 were coexpressed. Coexpression of Atg1 and Atg11 or Atg13 and Atg11 could not redistribute Atg17 from the cytosol to punctate structures. Representative images are shown. DIC, differential interference contrast. (B) Perivacuolar localization of Atg17-GFP in the MKO (*ATG17-GFP*) strain. The MKO (*ATG17-GFP*) strain transformed with a plasmid expressing both Atg1 and Atg13 (pATG1-ATG13(415)) was grown to mid-log phase, stained with the vacuolar dye FM 4-64 as described in Materials and methods, and shifted to SD-N for 2 h before imaging. When both Atg1 and Atg13 were expressed, Atg17-GFP puncta localized at perivacuolar sites under starvation conditions. Bars, 2.5 μm. (C) The number of cells that contained Atg17-GFP PAS puncta in MKO strains (HCY107, HCY113, and HCY151) with coexpression of various combinations of Atg proteins was quantified under vegetative (open bars) and starvation (closed bars) conditions. Approximately 100-250 cells for each strain were analyzed for scoring the percentage of cells with fluorescent PAS puncta.

Finally, we quantified the percentage of cells containing Atg17-GFP puncta in the MKO strain expressing different Atg proteins. Approximately 40% of the cells co-expressing Atg1 and Atg13 showed Atg17-GFP puncta under starvation conditions, whereas less than 5% of the cells displayed any punctate structure when Atg17-GFP was expressed by itself (Fig. 2.3C). Additional expression of other components in the Atg17 complex further increased the percentage of cells displaying Atg17-GFP puncta. For example, Atg29 by itself did not significantly affect Atg17-GFP puncta formation, but expression of Atg29 in the presence of Atg1 and Atg13 increased the percentage of cells with puncta to approximately 53% during starvation. Atg11, when expressed together with Atg1 and Atg13, resulted in an even greater increase to approximately 80% (Fig. 2.3C). Taken together, these results indicate that starvation-specific PAS formation initially requires a minimal set of Atg proteins consisting of Atg1, Atg13 and Atg17; other components in the Atg1 complex, such as Atg29 and Atg11, further enhance assembly.

The Atg8 conjugation system affects formation of the Atg12–Atg5 conjugate

Having established that the MKO strain reproduces the temporal order of action of components involved in cargo packaging in growing conditions, and determined the initial factors for PAS assembly during starvation, we decided to extend our analysis of the utility of this system. In particular, we chose to examine the Atg12–Atg5 conjugation system because this part of the autophagy process has been reconstituted *in vitro*. Therefore, components have been identified that are both necessary and sufficient for the reaction. The question we posed was whether the information gained from these previous

experiments accurately reflected the complete *in vivo* situation. Previous data show that Atg5, Atg7, Atg10 and Atg12 are essential for the conjugation (Mizushima, Noda et al. 1998), and Atg16 is required for the efficiency of this reaction (Mizushima, Noda et al. 1999), but Atg3, Atg4 and Atg8 from the Atg8–PE system are not involved in Atg12–Atg5 conjugation (Kuma, Mizushima et al. 2002). Accordingly, we expressed various combinations of these proteins in the MKO strain. We used 3xHA-tagged Atg12 to allow detection of the Atg12–Atg5 conjugate. When expressed in an *atg12*Δ strain we detected both free HA-Atg12 and HA-Atg12 conjugated to Atg5 (Fig. 2.4, lane 2). As expected, when only Atg5 and HA-Atg12 were expressed in the MKO strain we did not detect the conjugated species (Fig. 2.4, lane 4). In contrast, if Atg7 and Atg10 were also present, we detected a faint band corresponding to the HA-Atg12–Atg5 conjugate; however, the majority of the HA-Atg12 was in the free form (Fig. 2.4, lane 5). When we added Atg16 we found that a substantially greater amount of conjugate was formed (Fig. 2.4, lane 6).

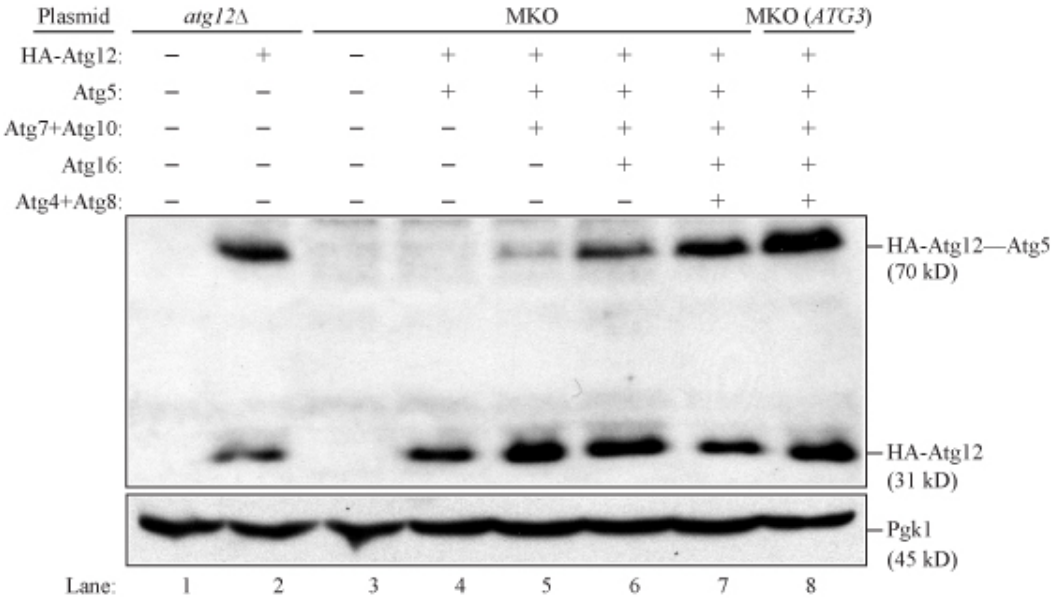

Figure 2.4. Reconstitution of the Atg12–Atg5 conjugation system. MKO, MKO (*ATG3*), and *atg12Δ* cells transformed with various plasmids were grown in selective SMD medium, collected at mid-log phase, and subjected to Western blot analysis using an anti-HA antibody. 0.2 OD_{600} units of cells were loaded in each lane. Pgk1 was used as a loading control. Plasmids expressing HA-tagged Atg12 (pHA-ATG12(416)); Atg7 and Atg10 (pATG7-ATG10(414)); Atg5 and HA-tagged Atg12 (pATG5-HA-ATG12(416)); Atg5, HA-Atg12, and Atg16 (pATG5-HA-ATG12-ATG16(416)); and Atg8, Atg4, Atg7, and Atg10 (pATG8-ATG4-ATG7-ATG10(414)) were used as indicated. With Atg5, Atg12, Atg7, and Atg10 expressed in the MKO strain, a small amount of Atg12–Atg5 conjugate formed (lane 5). Additional expression of Atg16 improved the conjugation efficiency (lane 6). The presence of Atg8, Atg4, and Atg3 from the Atg8 conjugation system further facilitated the formation and/or enhanced the stability of Atg12–Atg5 (lanes 7 and 8).

Next, we examined possible contributions from the Atg8 conjugation system. When we expressed Atg4 and Atg8 together with Atg5, Atg7, Atg10, Atg12 and Atg16, the Atg12–Atg5 conjugation efficiency was further enhanced (Fig. 2.4, lane 7). Atg8–PE was not generated in this strain due to the absence of Atg3 (not depicted). Thus, it seems that even without the formation of Atg8–PE, the presence of some protein(s) in the Atg8–PE system can facilitate the conjugation of Atg12 to Atg5. Furthermore, the level of the Atg12–Atg5 conjugate was even greater when Atg3 was added (Fig. 2.4, lane 8). Thus, our data suggest that Atg5, Atg7, Atg10 and Atg12 are minimum requirements for

Atg12–Atg5 conjugate formation, and Atg16 facilitates the conjugation, in agreement with published data. We further found, however, that components in the Atg8–PE system also enhance the conjugation reaction. The same conclusions were reached in either vegetative (Fig. 2.4) or starvation (not depicted) conditions.

Atg8–PE formation and Atg4 cleavage

We extended our analysis with the MKO strain to the reconstitution of Atg8–PE conjugation. Although there have been extensive studies on the *in vitro* reconstitution of Atg8–PE, *in vivo* reconstitution has only been reported in *E. coli* where autophagy does not occur (Ichimura, Imamura et al. 2004). The C-terminal arginine of nascent Atg8 is normally removed by Atg4, which can also release Atg8 from PE. When the C-terminal arginine is removed, as in Atg8ΔR, the initial processing step is bypassed. Previous experiments using purified Atg8ΔR, Atg3, Atg7 and PE-containing liposomes suggest that Atg8–PE formation is at its peak when the PE content reaches 70% of the total membrane, but with a concentration close to that of yeast organelle membranes the efficiency is very low (Ichimura, Imamura et al. 2004). However, the efficiency of conjugation is boosted by the presence of the Atg12–Atg5 conjugate, and further addition of Atg16 only slightly increases Atg8–PE formation (Hanada, Noda et al. 2007). Our data support this current view of Atg8 lipidation. Moreover, they provided additional insights into both the conjugation and deconjugation reactions.

We first tested if Atg8, Atg4, Atg7 and Atg3 are sufficient for Atg8–PE formation. When we transformed a plasmid expressing these proteins into the MKO (*ATG3*) strain, Atg8–PE was essentially not detected in both growing and starvation conditions (Fig.

2.5A, lane 3); even when we expressed all the components for the Atg12–Atg5 conjugation system, we were still not able to detect a signal for Atg8–PE (Fig. 2.5A, lane 4). These data do not agree with the *in vitro* reconstitution data. One of the differences between these previous studies and our experiments is that the previous analyses used the modified Atg8ΔR to bypass the need for the initial Atg4 cleavage, and omitted Atg4 from the subsequent reactions. However, the absence of Atg4 also blocks the deconjugation of Atg8–PE and thus favors the accumulation of the conjugated species. Considering the role of Atg4 in determining the balance between Atg8 and Atg8–PE, we introduced a plasmid expressing Atg8ΔR, Atg7 and Atg10, into the MKO (*ATG3*) strain; in this case a significant amount of Atg8–PE was detected (Fig. 2.5A, lane 5). When we additionally expressed Atg5, HA-Atg12 and Atg16, almost all of the Atg8 was in its conjugated form (Fig. 2.5A, lane 6). Thus, when Atg4 is present, as is the case *in vivo*, Atg8–PE levels are extremely low in the MKO strain, even in the presence of the Atg12–Atg5 conjugation system. These results suggest that the *in vitro* system does not faithfully reflect the contribution of other factors that are required to control the activity of Atg4.

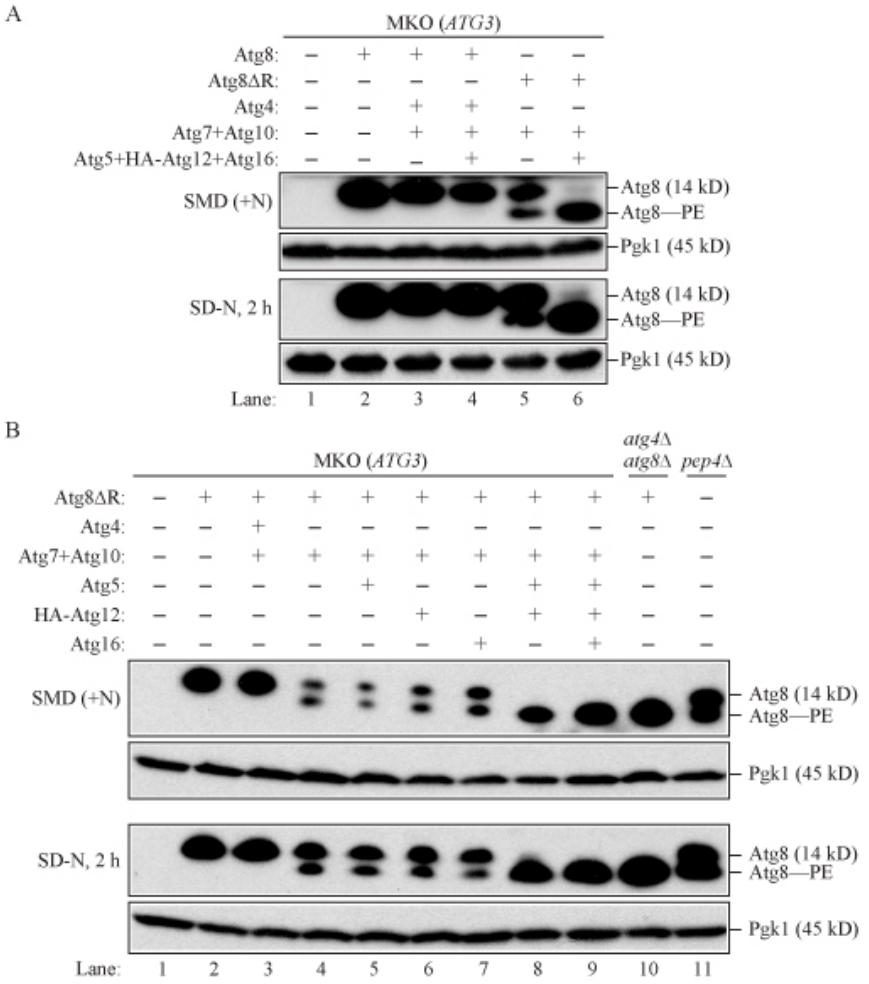

Figure 2.5. Reconstitution of the Atg8–PE conjugation system. (A) The role of Atg4 and the Atg12–Atg5 conjugation system in Atg8–PE formation. MKO (*ATG3*) cells transformed with different combinations of plasmids were grown in selective SMD medium, collected at mid-log phase or 2 h after starvation, and then subjected to Western blot analysis using anti-Atg8 antiserum. 0.2 OD_{600} units of cells were loaded in each lane. Pgk1 was used as a loading control. Plasmids expressing Atg8 (pATG8(414)); Atg8, Atg4, Atg7, and Atg10 (pATG8-ATG4-ATG7-ATG10(414)); Atg5, HA-Atg12, and Atg16 (pATG5-HA-ATG12-ATG16(416)); and Atg8ΔR, Atg7, and Atg10 (pATG8ΔR-ATG7-ATG10(414)) were used as indicated. Atg8–PE was hardly detected in both growing and starvation conditions even when all the known components from the Atg8–PE and Atg12–Atg5 conjugation systems were expressed (lane 4). However, when Atg8ΔR was expressed and Atg4 was absent, a significant amount of Atg8–PE was observed (lane 5), and the amount was further increased when all the components from the Atg12–Atg5 conjugation system were also expressed (lane 6). Note that Atg8–PE migrates aberrantly during SDS-PAGE and runs lower than Atg8. (B) The role of the Atg12–Atg5 conjugation system on Atg8–PE formation. The experimental procedures were the same as in A. Plasmids expressing Atg8ΔR (pATG8ΔR(414)); Atg8ΔR, Atg4, Atg7, and Atg10 (pATG8ΔR-ATG4-ATG7-ATG10(414)); Atg8ΔR, Atg7, and Atg10; Atg5 (pATG5(416)); HA-tagged Atg12 (pHA-ATG12(416)); Atg16 (pATG16(416)); Atg5 and HA-Atg12 (pATG5-HA-ATG12(416)); and Atg5, HA-Atg12, and Atg16 were used as indicated. The *atg4Δ atg8Δ* strain transformed with the plasmid expressing Atg8ΔR (pATG8ΔR(414)) and the *pep4Δ* strain were used as controls (lanes 10 and 11). When Atg4 was present, an Atg8–PE band was not detected (compare lanes 3 and 4). Expression of Atg5, Atg12, or Atg16 alone did not improve Atg8–PE formation (compare lanes 5-7 to lane 4). When the Atg12–Atg5 conjugate was formed through the expression of Atg7, Atg10, Atg12, and Atg5, the efficiency of Atg8–PE formation was greatly enhanced (lane 8). Atg16 further facilitated Atg8–PE conjugation and/or enhanced the stability of the conjugate (lane 9).

Finally, we attempted to further define the reason for the low level of Atg8–PE in this system. In wild-type cells, a population of Atg8 is constantly degraded inside the vacuole, so the total amount of Atg8 is lower than that in the MKO strain. Therefore, we used a *pep4*Δ strain, which blocks Atg8 degradation, as a control (Fig. 2.5B, lane 11). When deconjugation occurs, an Atg8–PE band was not detected (Fig. 2.5B, lane 3), whereas expression of Atg8ΔR in an *atg4*Δ *atg8*Δ strain defective in deconjugation causes all of the protein to accumulate in the lipidated form (Fig. 2.5B, lane 10). When we expressed Atg8ΔR, Atg7 and Atg10 along with Atg5, Atg12 or Atg16 separately, Atg8–PE conjugation was not increased (Fig. 2.5B, lane 4-7). On the other hand, the presence of the Atg12–Atg5 conjugate facilitated Atg8–PE formation (Fig. 2.5B, lane 8; and not depicted). In this *in vivo* system, Atg16 also facilitated the formation and/or enhanced the stability of Atg8–PE (Fig. 2.5B, lane 9), which could be indirect through its action on the Atg12–Atg5 conjugate (Fig. 2.4, lane 6).

Discussion

In this study, we created and validated a multiple knockout strain in which 24 *ATG* genes directly required for autophagy and the Cvt pathway were deleted (Fig. 2.1). Using this *in vivo* system, we determined minimum requirements for cargo packaging (Fig. 2.2), initial starvation-specific PAS assembly (Fig. 2.3), Atg12–Atg5 conjugation (Fig. 2.4) and Atg8–PE formation (Fig. 2.5). Although single- and double-deletion analyses and *in vitro* reconstitution have provided us with important insights into mechanisms, in general the minimum requirements for, and regulation of, these steps have not been explored extensively. The MKO strain serves as a valuable and powerful tool for these purposes. Moreover, it also has an obvious advantage over an *in vitro* reconstitution system, more accurately recapitulating what occurs *in vivo* and making studies of complex steps/aspects of autophagy possible and more efficient.

Our *in vivo* reconstitution of the Atg12–Atg5 and Atg8–PE conjugation systems demonstrated the usefulness of the MKO strain as it provided us with information missing from the *in vitro* studies. For example, our data suggest that components in the Atg8–PE system contribute to the efficiency of Atg12–Atg5 conjugation (Fig. 2.4). With regard to the Atg8–PE conjugation system, the results are even more intriguing. We find that when Atg4 is present to cleave the C-terminal arginine of Atg8 and to deconjugate Atg8 from PE, a situation that is more physiologically relevant than the conditions employed for the *in vitro* reconstitution studies, even all the proteins in the two conjugation systems cannot sustain a detectable amount of Atg8–PE (Fig. 2.5A) in contrast to wild-type cells. This means either deconjugation occurs too quickly or

conjugation efficiency is still somehow compromised in the MKO strain, or both. One possibility is that the plasmid-based Atg4 in the MKO strain results in overexpression and elevated Atg4 activity that favors deconjugation of Atg8–PE. Because we do not have antibodies against the Atg4 protein, we cannot directly determine the Atg4 levels. To address this possibility, however, we examined the functionality of our Atg4-expressing plasmid in an *atg4*Δ strain. We found that expression of Atg4 in the *atg4*Δ strain complemented prApe1 maturation, and this strain did not accumulate unconjugated Atg8 (unpublished data), which suggests that our plasmid expressing Atg4 is functional, and that additional factors are needed for Atg4 to exert its protease activity or deconjugation function in the MKO strain. Regulation of Atg4 is an important topic for autophagy. For example, why is Atg8 synthesized with a residue(s) following the C-terminal glycine when this residue(s) is/are immediately removed by Atg4? Also, how is Atg4 regulated to prevent premature deconjugation of Atg8–PE? One recent study suggests that Atg4 activity is subject to redox regulation (Scherz-Shouval, Shvets et al. 2007), although the actual mechanism through which this might occur *in vivo* is not known. Follow-up analyses will yield more insights into the regulation of deconjugation and conjugation.

With the MKO strain, we can study the order of protein assembly at the PAS more directly and efficiently compared to analyses with single- or double-deletion strains. Previous studies suggest that Atg11 and Atg17 are the initial factors for PAS assembly in vegetative and starvation conditions, respectively (Shintani, Huang et al. 2002; Suzuki, Kubota et al. 2007). However, it is possible that some proteins in the autophagy pathway may act together, or can substitute for one another, to target Atg11 and Atg17 to the PAS.

Our data suggest that in vegetative conditions Atg11 is not sufficient to localize itself and the cargo complex to the PAS even though the cargo complex forms, which means that an additional protein(s) is/are needed for efficient assembly of the Cvt-specific PAS. We also provided direct evidence that not only Atg17, but also Atg1 and Atg13 are important for the initial starvation-specific PAS assembly (Fig. 2.3A). Approximately 75% of the Atg17-GFP puncta observed in the presence of Atg1 and Atg13 were peri-vacuolar (Fig. 2.3B), suggesting that these three proteins are sufficient for this process. We also noted that MKO cells expressing Atg1, Atg13 and Atg17-GFP tend to have more punctate structures than the wild-type cells. Some of the puncta might be precursor or intermediate structures of the initial PAS. In addition to Atg1, Atg13 and Atg17, other proteins such as Atg29 and Atg11 also contribute to the efficiency of the assembly process (Fig. 2.3C). During the course of our studies a paper was published verifying a role for Atg29 in the assembly of the starvation-specific PAS (Kawamata, Kamada et al. 2008). However, there are some discrepancies between the two sets of studies. For example, Kawamata *et al*., (2008) find that Atg29 is essential for assembly of the starvation-specific PAS, whereas our present studies indicate that this protein enhances PAS assembly but is not essential. Further analyses will be needed to resolve this and other questions pertaining to this topic. Although Atg11 is a Cvt-specific factor, it contributed to PAS assembly along with Atg1, Atg13 and Atg17 during starvation conditions (Fig. 2.3C). Generation of the Cvt-specific PAS that is dependent upon Atg11 during vegetative growth may help to recruit components in the Atg17 complex, resulting in enhanced PAS assembly when cells are subsequently shifted to starvation conditions (Cheong *et al.*, 2008).

In vitro systems can be extremely useful and powerful tools for dissecting molecular mechanisms, and the present study does not suggest otherwise. Rather, we demonstrate that *in vivo* reconstitution can complement and extend *in vitro* analyses. Generation of a strain with 24 *ATG* genes knocked out is a unique and novel approach for studying complex pathways such as autophagy, and the strain will be a very useful tool for autophagy research. We can foresee potential uses of the strain in determining the temporal order of protein arrival at the PAS, in Atg protein retrieval after autophagosome formation and many other aspects of autophagy. These experiments will reward us with new findings and open up areas for potential research.

Materials and methods

Yeast strains, media, reagents and antisera

The yeast *Saccharomyces cerevisiae* strains used in this study are listed in Table 2.1. Knockout strains were constructed using the *loxP/Cre* system (Gueldener, Heinisch et al. 2002). GFP tagging of Atg17 at the corresponding chromosomal locus was performed by a PCR-based procedure (Longtine, McKenzie et al. 1998). Yeast media including YPD (1% yeast extract, 2% peptone and 2% dextrose) or synthetic minimal medium with casamino acids (SMD+CA) and SD-N for nitrogen starvation have been described previously (Shintani, Huang et al. 2002). FM 4-64 and antibodies to alkaline phosphatase (Pho8) and carboxypeptidase Y (Prc1) were from Molecular Probes/Invitrogen. Antisera against Ape1 (Klionsky, Cueva et al. 1992) and Atg8 (Huang, Scott et al. 2000) were described previously. Antibody to the hemagglutinin epitope was from Santa Cruz Biotechnology. Antisera against carboxypeptidase S (Cps1) and phosphoglycerate kinase (Pgk1) were gifts from Drs. Scott Emr (Cornell University) and Jeremy Thorner (University of California at Berkeley), respectively.

Construction of the MKO strain

The MKO strains were derived from wild-type haploid strain SEY6210 (Robinson, Klionsky et al. 1988), and the *loxP/Cre* system (Gueldener, Heinisch et al. 2002) was modified for multiple gene knockouts (Fig. 2.1A). The gene disruption cassette consisting of a selection marker flanked by two *loxP* sequences was amplified by PCR using primers containing 60 nucleotide stretches that are homologous to sequences upstream of

the start codon or downstream of the stop codon of the target gene, followed by 19 or 22 nucleotides complementary to sequences flanking the *loxP* sites in the marker plasmid. The PCR products were transformed into yeast cells and transformants were selected on plates lacking a particular amino acid or containing a specific antibiotic. Selected transformants were checked for correct integration by colony PCR using two sets of primers. *ATG* genes were deleted one at a time using markers including *kanMX*, *ble*^{r}, *HIS5*, *URA3* and *LEU2*. A maximum of five *ATG* genes were deleted before Cre recombinase was expressed to loop out the marker gene. Replica plating was used to identify colonies that had lost all of the markers. The markers can thus be reused to delete other *ATG* genes. After several rounds of deletion and marker rescue, 24 *ATG* genes were deleted. The strain was named YCY123 (MKO).

Plasmid construction

For pATG4(414), pATG7(414), pATG10(414), pATG5(416) and pATG16(416), the individual gene with its endogenous promoter and terminator region, was amplified from wild-type genomic DNA, digested with SacI, XmaI, KpnI, BamHI and NotI, respectively, and cloned into the corresponding site of pRS414 or pRS416 (Sikorski and Hieter 1989). SacI and BamHI sites were used to clone pATG6(414), NotI and NcoI for pATG8(414), SacI and PstI for pATG1(415), and XbaI and XmaI for pATG13(415). For pHA-ATG12(416), the insert was amplified from 3xHA-APG12 (Mizushima, Noda et al. 1998) and cloned into pRS416. The functionality of these plasmids was tested in the corresponding knockout strains by examining prApe1 maturation.

The promoter, open reading frame and terminator inserts were subsequently removed by restriction digestion and cloned in various combinations to generate the multi-gene plasmids pATG1-ATG13(415), pATG7-ATG10(414), pATG5-HA-ATG12(416), pATG5-HA-ATG12-ATG16(416) and pATG8-ATG4-ATG7-ATG10(414). The key in the design was that the site(s) for cloning each subsequent gene was not present within the existing plasmid. A one-step site-directed mutagenesis protocol (Zheng, Baumann et al. 2004) was used to remove the last arginine from the *ATG8* open reading frame to generate pATG8ΔR(414). The NotI- and NcoI-digested Atg8ΔR fragment was exchanged with the Atg8 fragment to generate pATG8ΔR-ATG4-ATG7-ATG10(414), from which Atg4 was removed by BglII and SacII digestion followed by blunt-ending and religation to form pATG8ΔR-ATG7-ATG10(414). Plasmids pRFPAPE1(305) (Stromhaug, Reggiori et al. 2004), pGFPATG11(416) (pGFPCVT9(416); (Kim, Kamada et al. 2001), pYFPATG19(416) (pYFP-Cvt19; (Shintani, Huang et al. 2002), pCuHACFPATG11(414) (Yorimitsu and Klionsky 2005) and pATG18(415) (pCVT18(415); (Guan, Stromhaug et al. 2001) have been described previously.

Pulse-chase analysis and immunoprecipitation

Cells (5 ml) in mid-log phase grown in SMD+CA medium were collected and labeled in 500 µl SMD with 20 µCi ^{35}S for 5 min at 30°C. Chase medium (5 ml YPD containing 2 mM cysteine and 1 mM methionine) was added, and at each time point 1 ml cells were collected, precipitated with TCA, washed with acetone, dried and resuspended in 100 µl MURB (50 mM sodium phosphate, 25 mM MES, pH 7.0, 1% SDS, 3 M urea, 0.5% β-mercaptoethanol). Glass beads were added to break the cells, and then each

sample was boiled and diluted in 800 µl TWIP (0.5% Tween-20, 50 mM Tris hydrochloride pH 7.5, 150 mM NaC1, 0.1 mM EDTA). The supernatant fraction was subjected to triple immunoprecipitation: The first precipitation was carried out with 3 µl Prc1 antiserum, and the supernatant after removal of the antibody-antigen complex with protein A-sepharose was immunoprecipitated with 1 µl Cps1 antiserum, and then with 6 µl Pho8 antiserum; the second and third immunoprecipitations were carried out twice each to eliminate carryover of the previous antisera.

Protein extraction and western blotting

Yeast cells were grown at 30°C to mid-log phase in the appropriate medium, harvested, resuspended with 10% trichloroacetic acid (TCA) and held for 30 min on ice. Cell pellets were washed with 100% acetone, air-dried, and resuspended in MURB buffer. Cells were further broken by vortexing with glass beads, and were heated at 75°C for 10 min. For each sample, 0.2 OD_{600} units of cells were resolved by SDS-PAGE, transferred to PVDF membrane and probed with appropriate antisera or antibodies.

Fluorescence microscopy

Yeast cells were grown to mid-log phase in selective SMD medium. To label the vacuolar membrane, cells were stained with 0.8 mM FM 4-64 for 15 min, washed and incubated in the same medium for 30 min. For starvation, cells were shifted to SD-N medium for 2 h. Cells (1 ml) were pelleted and resuspended in 30 µl of the same medium before imaging. Microscopy was performed at room temperature on an Olympus IX71 microscope with a 100X Olympus Universal Plan Apochromat objective lens and a

CoolSnap HQ camera (Photometrics, Tucson, AZ). The microscope was controlled by a DeltaVision Spectris workstation (Applied Precision, Issaquah, WA). Images were acquired and deconvolved with DeltaVision softWoRx® software (Applied Precision).

References

Bowers, K. and T. H. Stevens (2005). "Protein transport from the late Golgi to the vacuole in the yeast *Saccharomyces cerevisiae*." Biochim Biophys Acta **1744**(3): 438-54.

Cao, Y. and D. J. Klionsky (2007). "Physiological functions of Atg6/Beclin 1: a unique autophagy-related protein." Cell Res **17**(10): 839-49.

Cheong, H., U. Nair, et al. (2008). "The Atg1 kinase complex is involved in the regulation of protein recruitment to initiate sequestering vesicle formation for nonspecific autophagy in *Saccharomyces cerevisiae*." Mol Biol Cell **19**(2): 668-81.

Cheong, H., T. Yorimitsu, et al. (2005). "Atg17 regulates the magnitude of the autophagic response." Mol Biol Cell **16**(7): 3438-53.

Dove, S. K., R. C. Piper, et al. (2004). "Svp1p defines a family of phosphatidylinositol 3,5-bisphosphate effectors." EMBO J **23**(9): 1922-33.

Fujioka, Y., N. N. Noda, et al. (2008). "*In vitro* reconstitution of plant Atg8 and Atg12 conjugation systems essential for autophagy." J Biol Chem **283**(4): 1921-8.

Gerhardt, B., T. J. Kordas, et al. (1998). "The vesicle transport protein Vps33p is an ATP-binding protein that localizes to the cytosol in an energy-dependent manner." J Biol Chem **273**(25): 15818-29.

Guan, J., P. E. Stromhaug, et al. (2001). "Cvt18/Gsa12 is required for cytoplasm-to-vacuole transport, pexophagy, and autophagy in *Saccharomyces cerevisiae* and *Pichia pastoris*." Mol Biol Cell **12**(12): 3821-38.

Gueldener, U., J. Heinisch, et al. (2002). "A second set of loxP marker cassettes for Cre-mediated multiple gene knockouts in budding yeast." Nucleic Acids Res **30**(6): e23.

Hanada, T., N. N. Noda, et al. (2007). "The Atg12-Atg5 conjugate has a novel E3-like activity for protein lipidation in autophagy." J Biol Chem. **282**(52): 37298-302.

Huang, W.-P., S. V. Scott, et al. (2000). "The itinerary of a vesicle component, Aut7p/Cvt5p, terminates in the yeast vacuole via the autophagy/Cvt pathways." J Biol Chem **275**(8): 5845-51.

Ichimura, Y., Y. Imamura, et al. (2004). "*In vivo* and *in vitro* reconstitution of Atg8 conjugation essential for autophagy." J Biol Chem **279**(39): 40584-92.

Ichimura, Y., T. Kirisako, et al. (2000). "A ubiquitin-like system mediates protein lipidation." Nature **408**(6811): 488-92.

Iwata, J., J. Ezaki, et al. (2006). "Excess peroxisomes are degraded by autophagic machinery in mammals." J Biol Chem **281**(7): 4035-41.

Kabeya, Y., T. Kawamata, et al. (2007). "Cis1/Atg31 is required for autophagosome formation in *Saccharomyces cerevisiae*." Biochem Biophys Res Commun **356**(2): 405-10.

Kawamata, T., Y. Kamada, et al. (2008). "Organization of the pre-autophagosomal structure responsible for autophagosome formation." Mol Biol Cell **19**(5): 2039-50

Kim, J., Y. Kamada, et al. (2001). "Cvt9/Gsa9 functions in sequestering selective cytosolic cargo destined for the vacuole." J Cell Biol **153**(2): 381-96.
Kim, J., S. V. Scott, et al. (1997). "Transport of a large oligomeric protein by the cytoplasm to vacuole protein targeting pathway." J Cell Biol **137**(3): 609-18.
Klionsky, D. J. (2005). "The molecular machinery of autophagy: unanswered questions." J Cell Sci **118**(1): 7-18.
Klionsky, D. J. (2007). "Autophagy: from phenomenology to molecular understanding in less than a decade." Nat Rev Mol Cell Biol **8**(11): 931-7.
Klionsky, D. J., R. Cueva, et al. (1992). "Aminopeptidase I of *Saccharomyces cerevisiae* is localized to the vacuole independent of the secretory pathway." J Cell Biol **119**(2): 287-99.
Kuma, A., N. Mizushima, et al. (2002). "Formation of the approximately 350-kDa Apg12-Apg5·Apg16 multimeric complex, mediated by Apg16 oligomerization, is essential for autophagy in yeast." J Biol Chem **277**(21): 18619-25.
Levine, B. and D. J. Klionsky (2004). "Development by self-digestion: molecular mechanisms and biological functions of autophagy." Dev Cell **6**(4): 463-77.
Longtine, M. S., A. McKenzie III, et al. (1998). "Additional modules for versatile and economical PCR-based gene deletion and modification in *Saccharomyces cerevisiae*." Yeast **14**(10): 953-61.
Mizushima, N. (2007). "Autophagy: process and function." Genes Dev **21**(22): 2861-73.
Mizushima, N., T. Noda, et al. (1999). "Apg16p is required for the function of the Apg12p-Apg5p conjugate in the yeast autophagy pathway." EMBO J **18**(14): 3888-96.
Mizushima, N., T. Noda, et al. (1998). "A protein conjugation system essential for autophagy." Nature **395**(6700): 395-8.
Robinson, J. S., D. J. Klionsky, et al. (1988). "Protein sorting in Saccharomyces cerevisiae: isolation of mutants defective in the delivery and processing of multiple vacuolar hydrolases." Mol Cell Biol **8**(11): 4936-48.
Rubinsztein, D. C., J. E. Gestwicki, et al. (2007). "Potential therapeutic applications of autophagy." Nat Rev Drug Discov **6**(4): 304-12.
Scherz-Shouval, R., E. Shvets, et al. (2007). "Reactive oxygen species are essential for autophagy and specifically regulate the activity of Atg4." EMBO J **26**(7): 1749-60.
Scott, S. V., J. Guan, et al. (2001). "Cvt19 is a receptor for the cytoplasm-to-vacuole targeting pathway." Mol Cell **7**(6): 1131-41.
Shao, Y., Z. Gao, et al. (2007). "Stimulation of ATG12-ATG5 conjugation by ribonucleic acid." Autophagy **3**(1): 10-6.
Shintani, T., W.-P. Huang, et al. (2002). "Mechanism of cargo selection in the cytoplasm to vacuole targeting pathway." Dev Cell **3**(6): 825-37.
Shintani, T. and D. J. Klionsky (2004). "Cargo proteins facilitate the formation of transport vesicles in the cytoplasm to vacuole targeting pathway." J Biol Chem **279**(29): 29889-94.
Sikorski, R. S. and P. Hieter (1989). "A system of shuttle vectors and yeast host strains designed for efficient manipulation of DNA in *Saccharomyces cerevisiae*." Genetics **122**(1): 19-27.

Stromhaug, P. E., F. Reggiori, et al. (2004). "Atg21 is a phosphoinositide binding protein required for efficient lipidation and localization of Atg8 during uptake of aminopeptidase I by selective autophagy." Mol Biol Cell **15**(8): 3553-66.

Suzuki, K., T. Kirisako, et al. (2001). "The pre-autophagosomal structure organized by concerted functions of *APG* genes is essential for autophagosome formation." EMBO J **20**(21): 5971-81.

Suzuki, K., Y. Kubota, et al. (2007). "Hierarchy of Atg proteins in pre-autophagosomal structure organization." Genes Cells **12**(2): 209-18.

Yorimitsu, T. and D. J. Klionsky (2005). "Atg11 links cargo to the vesicle-forming machinery in the cytoplasm to vacuole targeting pathway." Mol Biol Cell **16**(4): 1593-605.

Zheng, L., U. Baumann, et al. (2004). "An efficient one-step site-directed and site-saturation mutagenesis protocol." Nucleic Acids Res **32**(14): e115.

CHAPTER 3

A multiple *ATG* gene knockout strain for yeast two-hybrid analysis

Abstract

Autophagy is a major intracellular degradative pathway that is involved in many human diseases. The molecular mechanism of autophagy has been elucidated largely through studies on autophagy-related (Atg) proteins. One difficulty in understanding the mechanism of autophagy has been the lack of functional motifs in most of the Atg proteins. In the absence of this information, studies that have focused on the interactions between Atg proteins have shed light on their functions. However, in most studies, it is difficult to determine whether an interaction is direct or occurs through other Atg proteins. Here, we took advantage of a new reagent, a multiple knockout (MKO) strain lacking 24 *ATG* genes, and converted the strain into a yeast two-hybrid (Y2H) host strain. We introduced three reporter genes into the existing MKO strain, and analyzed known interactions in the new MKO Y2H strain background to verify its utility. We also probed a new interaction using the MKO Y2H strain, and our results suggest that Atg29 and Atg31 interact independently of other known Atg proteins.

Introduction

Macroautophagy (hereafter autophagy) is a complex intracellular degradative pathway that utilizes approximately 30 autophagy-related (Atg) proteins. Our understanding of autophagy has been greatly improved through research on these Atg proteins, and in particular many insights have come from studies concerning the interactions among them. For example, Atg16 was identified through a yeast two-hybrid (Y2H) screen using Atg12 as bait (Mizushima, Noda et al. 1999), and the interaction between Atg19 and precursor aminopeptidase I, together with that between Atg19 and Atg11 made it possible for us to understand the temporal order of the cargo packaging event in the cytoplasm to vacuole targeting pathway (Shintani, Huang et al. 2002). Thus, different protein complexes held together by protein-protein interactions have helped us dissect and connect different steps of autophagy. However, most of the previous studies did not address a question very important to understand complex formation—whether or not a particular interaction is direct. Two proteins may show a positive interaction by coimmunoprecipitation and Y2H analyses, but still may interact indirectly through other proteins in the complex.

Recently, we published a new reagent useful for determining *in vivo* whether an interaction is direct, or more precisely, whether the interaction is independent of other known Atg proteins. We created a yeast multiple knockout (MKO) strain lacking 24 *ATG* genes that are involved in the induction and vesicle formation steps in *Saccharomyces cerevisiae* (Cao, Cheong et al. 2008). With regard to protein-protein interactions, the MKO strain (YCY123) has been useful for studying Atg9 self-interaction (He, Baba et al.

2008). To supplement the existing MKO strain and make protein-protein interaction analyses faster and more efficient, in this study we converted the MKO strain into a Y2H host strain. We integrated three reporter genes (*GAL1-HIS3*, *GAL2-ADE2* and *GAL7-lacZ* (James, Halladay et al. 1996)) into the MKO strain and tested those reporter genes with known interactions, such as some of those that occur within the Atg1 complex(Klionsky 2005; Cheong, Nair et al. 2008). After having validated the utility of this strain, we then extended our research to a previously unknown interaction. Using our MKO Y2H strain, we found that Atg29 (Kawamata, Kamada et al. 2005) and Atg31 (Kabeya, Kawamata et al. 2007) interact independently of other Atg proteins, an interaction that was further verified by coimmunoprecipitation.

Results

Construction of the MKO Y2H strain

In this study we created a MKO Y2H strain to provide a new tool for autophagy research. The MKO strain YCY123 (Cao, Cheong et al. 2008) was chosen as the starting strain. *GAL4*, *GAL80* and *ADE2* open reading frames (ORFs) were knocked out in YCY123. Three reporter genes were then introduced into the genome by sequential gene replacement as described previously (James, Halladay et al. 1996). The *HIS3* gene under the control of the *GAL1* promoter (*GAL1-HIS3*) was inserted downstream of the *LYS2* gene. The *ade2*Δ*::KanMX* locus was replaced by the *ADE2* gene under the control of the *GAL2* promoter (*GAL2-ADE2*). Finally, the *lacZ* gene under the control of the *GAL7* promoter (*GAL7-lacZ*) was inserted into the *MET2* gene locus. The resulting strain, YCY148, is His^+, Ade^+ and $lacZ^+$ in the presence of Gal4 activity.

Table 3.1. Yeast strains used in this study.

Strain	Genotype	Source or reference
HCY111	SEY6210 *atg31Δ::HIS3*	This study
KYY003	YCY123 *gal4*Δ *ga80*Δ *ade2*Δ*::KanMX*	This study
PJ69-4A	*MATa trpl-901 leu2-3,112 ura3-52 his3-200 ga14Δ ga180Δ LYS2::GALl-HIS GAL2-ADE2 met2::GAL7-lacZ*	(James, Halladay et al. 1996)
SEY6210	*MATα ura3–52 leu2–3,112 his3-Δ200 trp1-Δ901 lys2–801 suc2-Δ9 GAL*	(Robinson, Klionsky et al. 1988)
YCY77	HCY111 *ATG31-3GFP::URA3*	This study

YCY123	SEY6210 *atg1*Δ, *2*Δ, *3*Δ, *4*Δ, *5*Δ, *6*Δ, *7*Δ, *8*Δ, *9*Δ, *10*Δ, *11*Δ, *12*Δ, *13*Δ, *14*Δ, *16*Δ, *17*Δ, *18*Δ, *19*Δ, *20*Δ, *21*Δ, *23*Δ, *24*Δ, *27*Δ, *29*Δ	(Cao, Cheong et al. 2008)
YCY132	YCY123 *atg31*Δ*:: HIS3*	(Cao and Klionsky 2008)
YCY147	YCY123 *gal4*Δ *ga80*Δ *GAL1-HIS3 GAL2-ADE2*	This study
YCY148	YCY147 *met2::GAL7-lacZ*	This study
YCY149	YCY148 *atg31*Δ*:: KanMX*	This study
YCY154	YCY132 *ATG31-3GFP::URA3*	This study

Assessment of known interactions using the MKO Y2H strain

We tested the utility of the MKO Y2H strain and its three reporter genes by examining known interactions. First, we tested the *GAL1-HIS3* reporter gene by checking the Atg9 self-interaction. Atg9 self-interacts in the absence of other Atg proteins in the MKO strain as assessed by coimmunoprecipitation (He, Baba et al. 2008). The same conclusion could be reached using Y2H analysis (Fig. 3.1). The Y2H strain PJ69-4A (James, Halladay et al. 1996) (a "wild-type" strain that expresses all of the *ATG* genes) expressing activation domain (AD)-fused Atg9 and binding domain (BD)-fused Atg9 was used as a positive control. Cells expressing AD-Atg9 or BD-Atg9 alone (along with the appropriate empty vector) were used as negative controls. After 3 days on plates lacking histidine, cells that expressed AD-Atg9 and the empty BD vector showed only background levels of growth. Cells expressing BD-Atg9 and the empty AD vector also showed minimal growth, although the background level was higher. In contrast, both YCY148 and PJ69-4A cells expressing AD-Atg9 and BD-Atg9 were His^+, indicating that Atg9 interacts with itself independently of other Atg proteins by the Y2H approach.

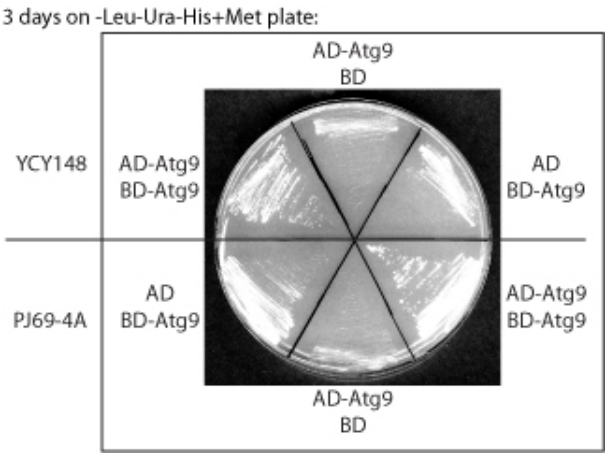

Figure 3.1. Validation of the MKO Y2H strain and assessment of the *HIS3* reporter gene. The *GAL1-HIS3* reporter gene was tested through Atg9 self-interaction. The MKO Y2H strain YCY148 and the original Y2H strain PJ69-4A were transformed with plasmids expressing AD-Atg9, BD-Atg9, or both. Interactions were assessed by cell growth on plates lacking leucine, uracil and histidine for 3 days.

Second, we tested the *GAL2-ADE2* reporter gene by checking interactions between Atg1 and its known binding partners Atg11 (Kim, Kamada et al. 2001), Atg13 (Kamada, Funakoshi et al. 2000) and Atg17 (Cheong, Yorimitsu et al. 2005). Because the full-length Atg1 Y2H chimera autoactivates, in our experiments we used a Y2H plasmid expressing a truncated version of Atg1 lacking its N-terminal kinase domain (Atg1ΔK) (Yorimitsu and Klionsky 2005). Cell growth on plates lacking adenine was compared between YCY148 and PJ69-4A cells expressing AD-Atg11 and BD-Atg1ΔK, AD-Atg13 and BD-Atg1ΔK, or AD-Atg17 and BD-Atg1ΔK (Fig. 3.2A). After 3 days, both YCY148 and PJ69-4A cells expressing the above-mentioned plasmid combinations were positive on plates lacking adenine, whereas cells expressing AD-Atg11, AD-Atg13, AD-Atg17 or BD-Atg1ΔK alone were negative. In general, we found that growth of the cells was slower with the MKO Y2H strain; however, we note that, because cell growth of the MKO strain itself is slower than the corresponding wild-type strain (Cao, Cheong et al.

2008), we cannot conclude that the strength of those interactions in the MKO Y2H strain is weaker than that in the PJ69-4A strain.

Finally, to quantitatively compare the strength of the interactions among the Atg1 complex, we measured β-galactosidase activity of YCY148 and PJ69-4A cells expressing AD-Atg11 and BD-Atg1ΔK, AD-Atg13 and BD-Atg1ΔK, or AD-Atg17 and BD-Atg1ΔK (Fig. 3.2B). Cells expressing empty AD and BD vectors were used as negative controls. All three combinations of Atg proteins showed interactions based on the measurement of β-galactosidase activity, with the Atg13-Atg1ΔK interaction being the strongest. By this assay the Atg11-Atg1, and Atg17-Atg1 interactions in YCY148 seemed to be stronger compared to the same interactions in PJ69-4A. In this case, the background level of β-galactosidase activity in YCY148 was higher than that in PJ69-4A.

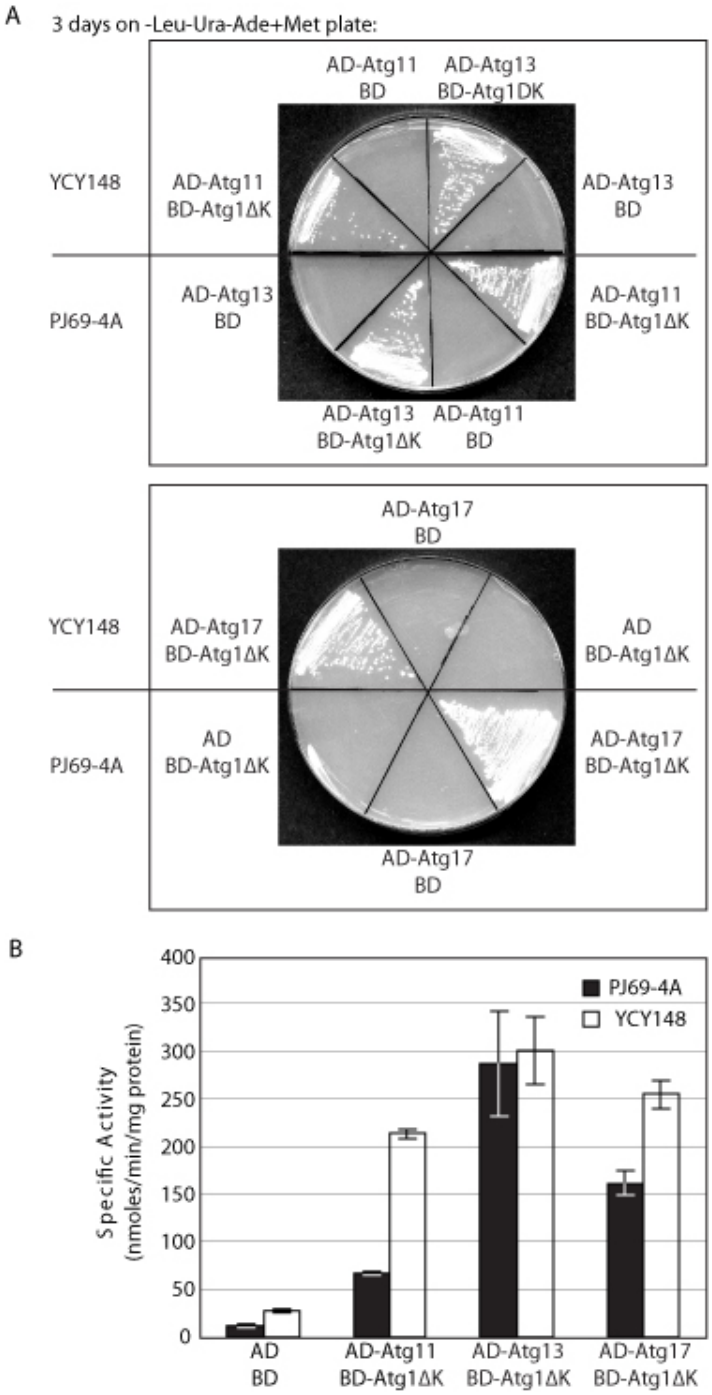

Figure 3.2. Assessment of two reporter genes in the MKO Y2H strain. (A) The *GAL2-ADE2* reporter gene was tested via interactions between Atg1 lacking the N-terminal kinase domain (Atg1ΔK) and its known interaction partners Atg11, Atg13 and Atg17. The Y2H strains YCY148 and PJ69-4A were transformed with different plasmid combinations and cell growth was monitored after 3 days on plates lacking leucine, uracil and adenine. (B) The *GAL7-lacZ* reporter gene was assessed via interactions between Atg1ΔK and its known interaction partners. The strains with plasmid combinations used in (A) were grown in minimal medium to maintain plasmid selection. The strength of the interaction for each set of proteins was quantified by measuring β-galactosidase activity from three independent experiments. The error bars represent the standard deviation.

A new interaction identified using the MKO Y2H strain

Next, we used the MKO Y2H strain to explore a previously unknown interaction. Atg17, Atg29 and Atg31 are not required for the cytoplasm to vacuole targeting pathway, but they have partial or severe defects in nonselective autophagy, and in selective pexophagy and/or mitophagy (Cheong, Yorimitsu et al. 2005; Kawamata, Kamada et al. 2005; Kabeya, Kawamata et al. 2007; Kanki and Klionsky 2008). Atg17 interacts with both Atg29 (Kawamata, Kamada et al. 2008) and Atg31 (Kabeya, Kawamata et al. 2007), which makes it likely that the three of them form a ternary complex. We wanted to know whether Atg29 and Atg31 interact with each other, and if so, whether this interaction is independent of other Atg proteins, such as Atg17.

With our MKO Y2H strain, we found that a direct interaction between Atg29 and Atg31 exists (Fig. 3.3A). Control cells expressing AD-Atg31 and the empty BD vector, or BD-Atg29 and the empty AD vector showed minimal growth on plates lacking histidine, and essentially no growth on plates lacking adenine. In contrast, cells expressing AD-Atg31 and BD-Atg29 together were able to grow in either PJ69-4A or the MKO Y2H strain YCY149 (YCY148 deleted for *ATG31*), suggesting that there is an interaction between Atg29 and Atg31, and the interaction exists in the absence of other Atg proteins. To verify the results from the Y2H analysis, we performed a coimmunoprecipitation experiment in the MKO strain YCY132 (YCY123 *atg31*Δ). Endogenous promoter-driven Atg31-3GFP was coexpressed with endogenous promoter-driven Atg29 fused to protein A (PA) in both an *ATG31* single-knockout strain (HCY111) and a MKO strain (YCY132). Protein extracts were generated under native conditions and subject to affinity isolation using IgG-sepharose. We found that Atg29-PA

coprecipitated Atg31-3GFP in both strains (Fig. 3.3B). As controls, we examined cells expressing Atg29-PA without Atg31-3GFP, or cells expressing Atg31-3GFP but not Atg29-PA, and we did not observe any coprecipitating Atg31-3GFP bands. Taken together, these results indicate that Atg29 interacts with Atg31 independently of other Atg proteins.

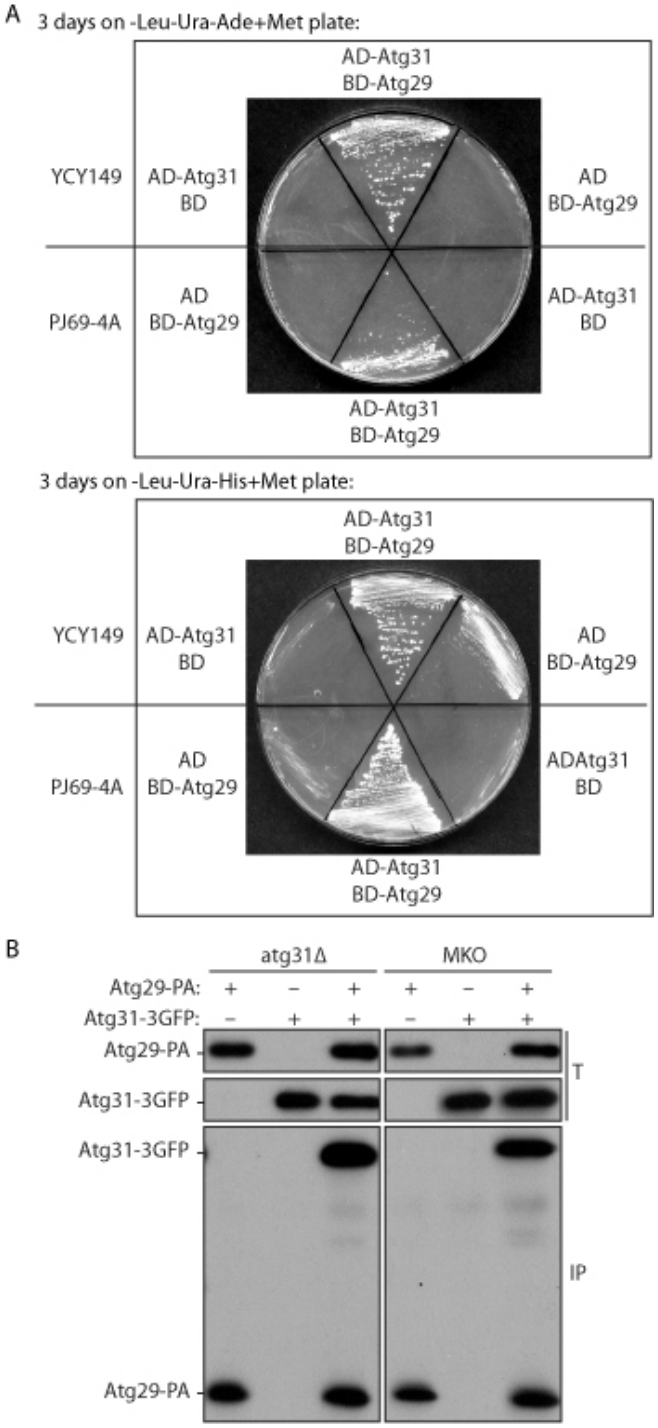

Figure 3.3. Atg31 interacts directly with Atg29 in the absence of other Atg proteins. (A) YCY149 and PJ69-4A cells were transformed with plasmids expressing AD-Atg31 and the empty BD vector, or AD-Atg31 and BD-Atg29, or the empty AD vector and BD-Atg29. The cells were grown on plates lacking leucine, uracil, and adenine or histidine for 3 days. (B) An *atg31*Δ strain (HCY111) or the MKO *atg31*Δ strain (YCY132) expressing endogenous promoter-driven Atg29-PA, Atg31-3GFP or both, were grown to mid-log phase and subjected to coimmunoprecipitation analysis. Note that *ATG31-3GFP* was integrated into the genome of HCY111 and YCY132, and we listed the derivatives of those two strains as YCY77 and YCY154 in Table 3.1. T, total lysates; IP, immunoprecipitates.

Discussion

In this study, we created a Y2H version of the multiple *ATG* gene knockout strain, and used the strain to study known and unknown protein-protein interactions. This MKO Y2H strain is very useful and informative regarding questions about direct or indirect interactions. It can be used along with the wild-type Y2H strain PJ69-4A, providing information about the possible nature of an interaction. We found that consistent with published data, Atg9 self-interacts in the absence of other Atg proteins by the Y2H approach (Fig. 3.1). Using this strain, we also found that Atg1 interacts with Atg11, Atg13 and Atg17 similar to previous reports (Fig. 3.2A and B). Finally, we also found a new "direct" (i.e., not involving other known Atg proteins) interaction between Atg29 and Atg31 using our MKO Y2H strain (Fig. 3.3).

Even though interactions indicated by cell growth sometimes seemed poorer in the MKO Y2H strain than in the wild-type Y2H strain, this was not necessarily reflective of a reduced interaction due to the overall slower growth rate of the MKO strain. Also, in a Y2H system bait and prey proteins are vastly overexpressed and forced into the nucleus to allow interaction, which might result in false positives. For example, an Atg1-Atg17 interaction was not detected in the absence of Atg13 by coimmunoprecipitaion (Kabeya, Kamada et al. 2005), but in our MKO Y2H strain these proteins showed a very strong interaction (Fig. 3.2A and B). Thus, it is worth noting that even though the MKO Y2H system shows a positive interaction, the same interaction may not be detected in the MKO strain by coimmunoprecipitation, similar to the case with wild-type strains. Therefore, data from the MKO Y2H strain need to be verified by other experiments.

However, the MKO Y2H strain still has the merit of any yeast two-hybrid system for quick and effective *in vivo* analysis and screening.

Materials and methods

Yeast strains and media

The yeast *Saccharomyces cerevisiae* strains used in this study are listed in Table 3.1. Knockout strains were constructed using the *loxP/Cre* system (Gueldener, Heinisch et al. 2002). For integration of the Atg31-3GFP fusion, the plasmid pATG31-3GFP(306) was linearized with SalI and integrated into the promoter region of the *ATG31* gene locus. Yeast cells were grown in rich medium (YPD; 1% yeast extract, 2% peptone, 2% glucose) or synthetic minimal medium lacking appropriate amino acids.

Plasmids

Plasmids used for construction of the MKO Y2H strains—pGH1, pGAL2-ADE2, and pGAL7-lacZ—have been described previously (James, Halladay et al. 1996). Y2H plasmids pAD-ATG9 (He, Baba et al. 2008), pBD-ATG9 (He, Baba et al. 2008), pGBD-ATG1ΔK (Kim, Kamada et al. 2001), pAD-ATG11 (He, Baba et al. 2008), pAD-ATG13 (Cheong, Yorimitsu et al. 2005) and pAD-ATG17 (Cheong, Yorimitsu et al. 2005) have been described previously. To clone pGAL4(414), the *GAL4* ORF with its 1 kb promoter and 0.5 kb terminator was amplified from yeast genomic DNA and cloned into XmaI and SacI sites of pRS414. pGAD-ATG31-C1 and pGBDU-ATG29-C1 were cloned as follows: The *ATG29* ORF was amplified from genomic DNA using primers 5' Y2H EcoRI-Atg29 (5'-GCGCGGGAATTCATGATTATGAATAGTACAAA CACAGT-3') and 3' Y2H PstI-Atg29 (5'-GCGCGGCTGCAGTCAGAATTGCAATCTGTCCATTAGC-3'). The PCR product

was then digested with EcoRI and PstI, and cloned into the pGBDU-C1 (James, Halladay et al. 1996) vector linearized with EcoRI and PstI. Similarly, the *ATG31* ORF was cloned into pGAD-C1 (James, Halladay et al. 1996) with EcoRI and PstI, using primers 5' Y2H EcoRI-Atg31 (5'-GCGCGGGAATTCATGAATGTTACAGTTACTGTTTATGA-3') and 3' Y2H PstI-Atg31 (5'-GCGCGGCTGCAGTCATACGGAATTGGAGAGCATTTGTA-3'). For cloning pATG31-3GFP(306), the *ATG31* ORF with its native promoter was cloned into the integration vector pPG5-3xGFP (Boyd, Hughes et al. 2004) using primers 5' XhoI-Atg31 (5'-CGCCGGGCTCGAGCGAATCTTGTTTTGACCCAATCTTTGT-3') and 3' ClaI-Atg31 (5'-CGCCGGGATCGATGATACGGAATTGGAGAGCATTTGTAATT-3'). For constructing pAtg29–PA(314), the full-length *ATG29* ORF with its endogenous promoter was PCR-amplified and ligated into the XhoI and XmaI sites of pNopPA(314) (He, Song et al. 2006).

Construction of the MKO Y2H strains

The MKO Y2H strains were created using multiple rounds of gene knockout, plasmid integration and 5-FOA selected excision. The MKO strain YCY123 (Cao, Cheong et al. 2008) was used as the starting strain, in which *GAL4* and *GAL80* were knocked out and the markers for knockout were recovered using the *loxP/Cre* system (Gueldener, Heinisch et al. 2002). *ADE2* was further deleted with a *KanMX* marker, yielding strain KYY003. The three reporter genes *GAL1-HIS3, GAL2-ADE2* and *GAL7-lacZ* were integrated as described before (James, Halladay et al. 1996), but with slight modifications. In brief, for integration of *GAL1-HIS3*, the strain KYY003 was

transformed with the plasmid pGH1 linearized with PvuII, and spread on plates lacking uracil and histidine. Ura^+ and His^+ colonies were grown and plated on 5-FOA plates to select for excision of the vector sequences. Ura^- and His^- colonies were then transformed with pGAL4(414). A Trp^+ and His^+ transformant was selected and transformed with a 2.6 kb SmaI/HaeII fragment of pGAL2-ADE2. Trp^+ and Ade^+ transformants were selected. A colony that was Ade^- without pGAL4(414) was selected and named YCY147. The YCY147 strain in the presence of pGAL4(414) was transformed with the plasmid pGAL7-lacZ linearized with PacI, resulting in integration of the plasmid at the *MET2* locus. Ura^+, Trp^+ and $lacZ^+$ transformants were plated on 5-FOA plates to select for excision of the vector sequences. Ura^-, Trp^+ and $lacZ^+$ colonies were selected, among which a colony that was $lacZ^-$ without pGAL4(414) was selected and named YCY148. *ATG31* was knocked out with a *KanMX* marker in strain YCY148 using the *loxP/Cre* system, to generate strain YCY149.

Protein A affinity isolation

Cells were grown in 50 ml of SMD lacking the appropriate auxotrophic amino acids to mid-log phase. The cells (40 OD_{600} units) were collected, washed with water, and frozen at -80°C if desired. Cells were thawed on ice, resuspended in 4 ml lysis buffer (1×PBS, 200 mM Sorbitol, 1 mM $MgCl_2$, 1% Tween 20, 2 mM PMSF and protease inhibitor cocktail), and broken by mixing with a vortex 6 times for 30 seconds each time, with 2 ml glass beads. Cell debris was removed by centrifugation and cell extracts were brought up to 4 ml. An aliquot (200 µl) of the cell extracts were saved as total lysate, with the rest being incubated with 100 µl IgG-sepharose beads for 1 h at 4°C. The beads

were then washed with lysis buffer 6 times and the eluates were resolved by SDS-PAGE, transferred to PVDF membrane and probed with anti-PA (DAKO) or anti-YFP (Clontech) antibody.

Enzyme assays

To select lacZ^+ colonies after integration of the *GAL7-lacZ* reporter into the *MET2* locus, a colony-lift filter assay was performed following a protocol from Clontech. β-galactosidase assays were performed as described previously (Cheong, Nair et al. 2008).

References

Boyd, C., T. Hughes, et al. (2004). "Vesicles carry most exocyst subunits to exocytic sites marked by the remaining two subunits, Sec3p and Exo70p." J Cell Biol **167**(5): 889-901.

Cao, Y., H. Cheong, et al. (2008). "In vivo reconstitution of autophagy in *Saccharomyces cerevisiae*." J Cell Biol **182**(4): 703-13.

Cao, Y. and D. J. Klionsky (2008). "New insights into autophagy using a multiple knockout strain." Autophagy **4**(8): 1073-5.

Cheong, H., U. Nair, et al. (2008). "The Atg1 kinase complex is involved in the regulation of protein recruitment to initiate sequestering vesicle formation for nonspecific autophagy in *Saccharomyces cerevisiae*." Mol Biol Cell **19**(2): 668-81.

Cheong, H., T. Yorimitsu, et al. (2005). "Atg17 regulates the magnitude of the autophagic response." Mol Biol Cell **16**(7): 3438-53.

Gueldener, U., J. Heinisch, et al. (2002). "A second set of loxP marker cassettes for Cre-mediated multiple gene knockouts in budding yeast." Nucleic Acids Res **30**(6): e23.

He, C., M. Baba, et al. (2008). "Self-interaction is critical for Atg9 transport and function at the phagophore assembly site during autophagy." Mol Biol Cell **19**(12): 5506-16.

He, C., H. Song, et al. (2006). "Recruitment of Atg9 to the preautophagosomal structure by Atg11 is essential for selective autophagy in budding yeast." J Cell Biol **175**(6): 925-35.

James, P., J. Halladay, et al. (1996). "Genomic libraries and a host strain designed for highly efficient two-hybrid selection in yeast." Genetics **144**(4): 1425-36.

Kabeya, Y., Y. Kamada, et al. (2005). "Atg17 functions in cooperation with Atg1 and Atg13 in yeast autophagy." Mol Biol Cell **16**(5): 2544-53.

Kabeya, Y., T. Kawamata, et al. (2007). "Cis1/Atg31 is required for autophagosome formation in *Saccharomyces cerevisiae*." Biochem Biophys Res Commun **356**(2): 405-10.

Kamada, Y., T. Funakoshi, et al. (2000). "Tor-mediated induction of autophagy via an Apg1 protein kinase complex." J Cell Biol **150**(6): 1507-13.

Kanki, T. and D. J. Klionsky (2008). "Mitophagy in yeast occurs through a selective mechanism." J Biol Chem **283**(47): 32386-93.

Kawamata, T., Y. Kamada, et al. (2008). "Organization of the pre-autophagosomal structure responsible for autophagosome formation." Mol Biol Cell **19**(5): 2039-50

Kawamata, T., Y. Kamada, et al. (2005). "Characterization of a novel autophagy-specific gene, *ATG29*." Biochem Biophys Res Commun **338**(4): 1884-9.

Kim, J., Y. Kamada, et al. (2001). "Cvt9/Gsa9 functions in sequestering selective cytosolic cargo destined for the vacuole." J Cell Biol **153**(2): 381-96.

Klionsky, D. J. (2005). "The molecular machinery of autophagy: unanswered questions." J Cell Sci **118**(1): 7-18.

Mizushima, N., T. Noda, et al. (1999). "Apg16p is required for the function of the Apg12p-Apg5p conjugate in the yeast autophagy pathway." EMBO J **18**(14): 3888-96.

Robinson, J. S., D. J. Klionsky, et al. (1988). "Protein sorting in *Saccharomyces cerevisiae*: isolation of mutants defective in the delivery and processing of multiple vacuolar hydrolases." Mol Cell Biol **8**(11): 4936-48.

Shintani, T., W.-P. Huang, et al. (2002). "Mechanism of cargo selection in the cytoplasm to vacuole targeting pathway." Dev Cell **3**(6): 825-37.

Yorimitsu, T. and D. J. Klionsky (2005). "Atg11 links cargo to the vesicle-forming machinery in the cytoplasm to vacuole targeting pathway." Mol Biol Cell **16**(4): 1593-605.

CHAPTER 4

Compensatory roles for the lipid-binding motifs of Atg18 and Atg21 in autophagy

Abstract

Atg18 and Atg21 are homologous WD-40 repeat proteins that bind phosphoinositides via a novel conserved Phe-Arg-Arg-Gly (FRRG) motif and function in autophagy-related pathways. Atg18 is required for both the Cvt pathway and autophagy, whereas Atg21 is only required for the former process; however, the functions of both proteins are poorly understood. Here we examined the relationship between the PtdIns(3)P-binding abilities of Atg18 and Atg21 and autophagy, by expressing variants of these proteins that have mutations in their phosphoinositide-binding motifs. We found that these proteins have partially redundant functions that affect the subcellular localization of Atg8 and Atg16, components of two related ubiquitin-like protein conjugation systems. Our results suggest that the PtdIns(3)P-binding motifs of Atg18 and Atg21 can compensate for one another in the recruitment of Atg components that are dependent on PtdIns(3)P for their PAS association. In addition, using a unique multiple knockout strain we found that Atg18 and Atg21 facilitate the recruitment of Atg8–PE to the site of autophagosome formation and protect it from premature cleavage by Atg4, which represents a key aspect of posttranslational autophagy regulation.

Introduction

Macroautophagy (hereafter referred to as autophagy) is an intracellular trafficking pathway wherein a double-membrane vesicle, the autophagosome, engulfs cytoplasmic components including proteins and organelles. The autophagosome then fuses with a lysosome (or the vacuole in fungi and plants) where its cargo is degraded, and the breakdown products are recycled back into the cytosol. Autophagy plays a key role in cellular homeostasis, and functions in diverse cellular processes such as development, programmed cell death, immune response, pathogenesis, tumor suppression, cardiac disorders, diabetes and the prevention of neuronal degeneration (reviewed in (Mizushima, Levine et al. 2008)). Autophagosome formation originates at a site known as the phagophore assembly site (PAS, also called the pre-autophagosomal structure; (Suzuki, Kirisako et al. 2001; Kim, Huang et al. 2002)). So far in yeast, 31 autophagy-related (Atg) proteins have been identified, and most of them localize to the PAS. In yeast, apart from autophagy that is primarily a nonselective, degradative pathway that occurs during starvation conditions, there is another vesicular pathway called the cytoplasm to vacuole targeting (Cvt) pathway, which is a selective, biosynthetic pathway that takes place during vegetative growth (Klionsky, Cueva et al. 1992). The Cvt pathway serves in the vacuolar transport of two hydrolases, α-mannosidase and the precursor form of aminopeptidase I (prApe1). Of the 31 Atg proteins, there are some that are exclusively involved in the Cvt pathway, others that are only needed for autophagy, and a subset of proteins that are required for both processes. For these pathways to function normally, several Atg proteins have to act in a concerted manner.

Atg18 and Atg21 are homologous Atg proteins—Atg18 functions in both autophagy and the Cvt pathway, whereas Atg21 is only required for the latter (Barth, Meiling-Wesse et al. 2001; Guan, Stromhaug et al. 2001; Barth, Meiling-Wesse et al. 2002; Stromhaug, Reggiori et al. 2004). There is a third homologue, Ygr223c, which is involved neither in Cvt nor autophagy ((Krick, Henke et al. 2008) and data not shown). Atg18, Atg21 and Ygr223c are predicted to be multi-WD-40 repeat proteins that fold to form seven bladed β-propellers (Dove, Piper et al. 2004). WD-40 repeat proteins are relatively common in all eukaryotes and are implicated in a wide variety of functions such as signal transduction, cytoskeleton assembly, transcriptional regulation, pre-mRNA processing, cell cycle control and apoptosis (Li and Suprenant 1994; Denisenko and Bomsztyk 1997; Achsel, Ahrens et al. 1998; Hu, Benedict et al. 1998; Kamura, Sato et al. 1998). Repeated WD-40 motifs form β-propeller structures that act as sites for protein-protein interaction, and proteins containing these motifs serve as platforms for the assembly of protein complexes or as mediators of stable or transient interactions among other proteins (Smith, Gaitatzes et al. 1999; Li and Roberts 2001).

In addition to WD-40 motifs, Atg18, Atg21 and Ygr223c are able to bind both phosphatidylinositol 3-phosphate (PtdIns(3)P) and phosphatidylinositol (3,5)-bisphosphate (PtdIns(3,5)P_2) (Dove, Piper et al. 2004; Stromhaug, Reggiori et al. 2004; Krick, Tolstrup et al. 2006). Both Atg18 and Atg21 bind phosphoinositides via conserved Phe-Arg-Arg-Gly (FRRG) motifs that lie within the proposed β-propellers; in the case of Atg18 these residues are $_{284}$FRRG$_{287}$, and for Atg21 they are $_{342}$FRRG$_{345}$. Mutations in the FRRG motif of Atg18 (FRRG to FTTG) results in a complete loss of phosphoinositide binding, whereas similar mutations in Atg21 result in highly reduced

phosphoinositide binding, suggesting that this protein may have other lipid-binding domains (Dove, Piper et al. 2004; Stromhaug, Reggiori et al. 2004; Krick, Tolstrup et al. 2006). The Atg18^{FTTG} mutant shows a substantial block in the Cvt pathway and a partial decrease in autophagy. In contrast, the Atg21^{FTTG} mutant is completely defective in the vacuolar transport of prApe1 via the Cvt pathway, thus underscoring the importance of phosphoinositide-binding for both pathways (Dove, Piper et al. 2004; Krick, Tolstrup et al. 2006). The deletion of Fab1, an enzyme that converts PtdIns(3)P to PtdIns(3,5)P_2 has no effect on either Cvt or autophagy (Dove, Piper et al. 2004; Obara, Sekito et al. 2008), suggesting that these pathways require PtdIns(3)P, but not PtdIns(3,5)P_2. In addition to its roles in Cvt and autophagy, Atg18 mediates retrograde trafficking from the vacuole via the endosome to the Golgi, and this function depends on its ability to bind PtdIns(3,5)P_2 (Efe, Botelho et al. 2007). The role of the PtdIns(3,5)P_2 binding function of Atg21 is currently unknown.

In yeast, PtdIns(3)P is generated by the specific phosphorylation of PtdIns at the D-3 position of the inositol ring by Vps34, the only PtdIns 3-kinase in this organism (Schu, Takegawa et al. 1993). Vps34 plays a role in a number of vesicular membrane trafficking processes such as endocytosis, multi-vesicular body formation, soluble vacuolar protein sorting and autophagy (Schu, Takegawa et al. 1993; Munn and Riezman 1994; Kihara, Noda et al. 2001; Katzmann, Stefan et al. 2003). In growing cells, PtdIns(3)P localizes to endosomal and vacuolar membranes, whereas in starvation conditions it is enriched on autophagosomal membranes and is also transported into the vacuole where it ends up on the membrane of autophagic bodies (Burd and Emr 1998; Gillooly, Morrow et al. 2000; Obara, Noda et al. 2008). Vps34 forms two distinct

complexes: PtdIns 3-kinase complex I, and PtdIns 3-kinase complex II, which function in autophagy and vacuolar protein sorting, respectively (Kihara, Noda et al. 2001). Both of the PtdIns 3-kinase complexes have three common subunits: Vps15, Vps34, and Vps30/Atg6. In addition to these common factors, each complex also contains one specific component—for the PtdIns 3-kinase complex I this unique factor is Atg14, whereas Vps38 is specific to complex II (Kihara, Noda et al. 2001). Atg14 mediates the localization of Vps30 and Vps34 to the PAS, however, Vps15 localizes to the PAS by an unknown mechanism that is independent of Atg14 (Obara, Sekito et al. 2006).

The physiological significance of the presence of PtdIns(3)P on the autophagosome membrane, and the functional relevance of Atg protein-PtdIns(3)P interaction is not well understood. Recent data show that one of the functions of PtdIns(3)P on autophagic membranes is the recruitment of the Atg2-Atg18 complex, via the PtdIns(3)P binding activity of Atg18 (Obara, Sekito et al. 2008). Although the Atg18^{FTTG} mutant is able to interact with Atg2, it is defective in the localization of the Atg2-Atg18^{FTTG} complex to the PAS (Obara, Sekito et al. 2008). It is proposed that the localization of some other Atg components such as the Atg12–Atg5-Atg16 complex, and Atg8 may be regulated by PtdIns(3)P, because in the absence of Atg14, the PAS localization of these proteins is abolished (Suzuki, Kubota et al. 2007). These proteins, however, are not dependent on Atg18 for their PAS localization. Here we show that under nitrogen starvation conditions, the PAS localization of Atg16 and Atg8 do in fact depend on the PtdIns(3)P-binding motifs of Atg18 and Atg21; *atg18*Δ *atg21*Δ cells expressing Atg18^{FKKG} and Atg21^{FKKG} mutants, are defective in the PAS recruitment of Atg16 and Atg8. Furthermore, as a result of the aberrant localization of these proteins,

*atg18*Δ *atg21*Δ cells expressing the Atg18^{FKKG} and Atg21^{FKKG} mutants show a severe block in autophagy, whereas either single mutant displays either no, or a greatly reduced, defect. Thus, our results suggest a model wherein the PtdIns(3)P-binding motifs of Atg18 and Atg21 can substitute for one another in the recruitment of Atg components that are dependent on PtdIns(3)P for their PAS association, and in this manner allow autophagy to proceed.

Finally, using a multiple knockout (MKO) strain in which most of the *ATG* genes are deleted and a subset of Atg proteins could thus be expressed to reconstitute *in vivo* a particular step of autophagy or the Cvt pathway (Cao, Cheong et al. 2008)), we found that Atg18 and Atg21 protect Atg8 from being cleaved by Atg4 at the vacuolar membrane and punctate structures. These data provide the first evidence for an *in vivo* mechanism that regulates the cleavage of Atg8–PE.

Results

Mutations in the PtdIns(3)P binding domains of both Atg18 and Atg21 result in a severe reduction of autophagic activity

Atg18 and Atg21 bind PtdIns(3)P, but they do not contain standard motifs that bind this phosphoinositide, such as PX or FYVE domains. These proteins are also unusual in that they are homologues that both function in autophagy-related pathways, although limited information is available in regard to their roles. To investigate the function of these proteins, we generated mutations within the FRRG motifs of Atg18 and/or Atg21 (FRRG to FKKG) and examined the effects of these mutations on the Cvt pathway and autophagy. Consistent with previous analyses (Stromhaug, Reggiori et al. 2004; Krick, Tolstrup et al. 2006; Obara, Sekito et al. 2008) cells in rich medium expressing Atg18^{FKKG} or Atg21^{FKKG} showed a substantial or a complete block in prApe1 maturation, respectively (Fig. 4.S1A).

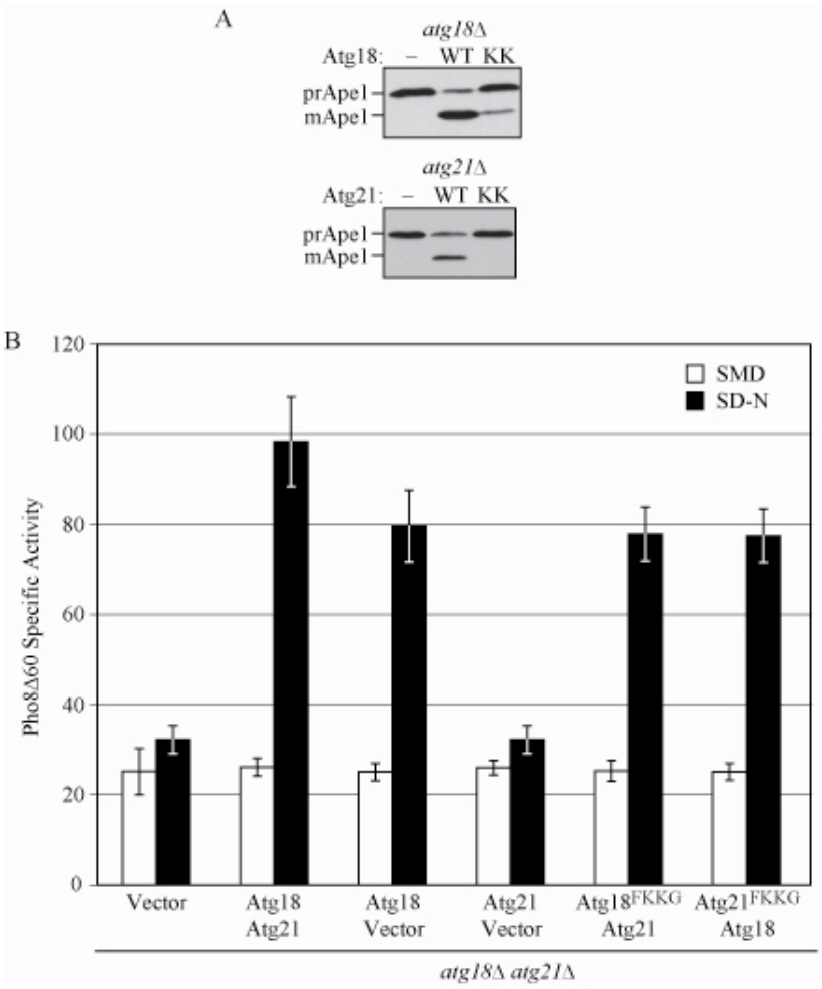

Figure 4.S1. PtdIns(3)P binding of either Atg18 or Atg21 is important for the Cvt pathway and not for nonspecific autophagy activity. (A) SEY6210 *atg18*Δ or *atg21*Δ cells bearing empty vector, or Atg18-PA (WT), Atg18^{FKKG}-PA, Atg21 (WT) or Atg21^{FKKG} centromeric plasmids were grown to mid-log phase, and collected. Protein extracts were separated on 8% SDS-PAGE gels. The precursor and mature forms of Ape1 were examined by immunoblotting with anti-Ape1 antiserum. (B) *atg18*Δ *atg21*Δ cells were transformed with plasmids expressing the indicated combinations of empty vectors, wild-type Atg18-PA, wild-type Atg21, Atg18^{FKKG}-PA or Atg21^{FKKG}. Pho8Δ60 specific activity (nmoles/min/mg) was measured according to Materials and methods from protein extracts prepared from cells grown in SMD or after a 4 h shift to SD-N and the results represent the mean and SD of three independent experiments.

Previous reports indicate that *atg18*Δ cells expressing Atg18^{FKKG} only show a slight reduction in autophagy, and in accordance with Atg21 not having a significant role in autophagy, Atg21^{FKKG} has no effect on this process (Stromhaug, Reggiori et al. 2004); Fig. 4.S1B). Because Atg18 and Atg21 are homologues, however, we considered the

possibility that they were partially redundant. Therefore, we examined nonspecific autophagy in *atg18*Δ *atg21*Δ cells expressing both Atg18^{FKKG}-PA and Atg21^{FKKG} using the Pho8Δ60 assay. In this assay, a truncated form of the vacuolar alkaline phosphatase precursor, Pho8Δ60, is expressed in the cytosol (Noda, Matsuura et al. 1995). In order to be proteolytically activated, precursor Pho8Δ60 must be transported to the vacuole by autophagy. The enzymatic activity of mature Pho8Δ60 can be determined colorimetrically as a function of the cleavage of its substrate p-nitrophenyl phosphate (pNPP). Under nitrogen starvation conditions that induce autophagy, wild-type cells (deletion cells expressing Atg18 and Atg21 from plasmids) showed a clear increase in Pho8Δ60-dependent alkaline phosphatase activity (Fig. 4.1A). In contrast, *atg18*Δ *atg21*Δ cells expressing the double mutants showed Pho8Δ60 activity levels that were almost similar to the background as observed in *atg18*Δ *atg21*Δ cells expressing empty vectors. These results suggest that although Atg18 and Atg21 are not functionally identical, wild-type PtdIns(3)P binding activity of at least one of these proteins is required for, and largely sufficient for, autophagy in the absence of the other; either single PtdIns(3)P-binding mutant displayed autophagy activity that was close to the wild-type level (Fig. 4.S1B) in agreement with previous results (Guan, Stromhaug et al. 2001; Meiling-Wesse, Barth et al. 2004; Stromhaug, Reggiori et al. 2004). The defect in autophagy seen with the double mutants was not due to a decrease in stability resulting from the mutations, as both proteins displayed similar stability as their wild-type counterparts (Fig. 4.S2A). In addition, both of the mutant proteins complemented the respective deletion strain when analyzed for maturation of prApe1 under starvation conditions, further indicating that they were functional.

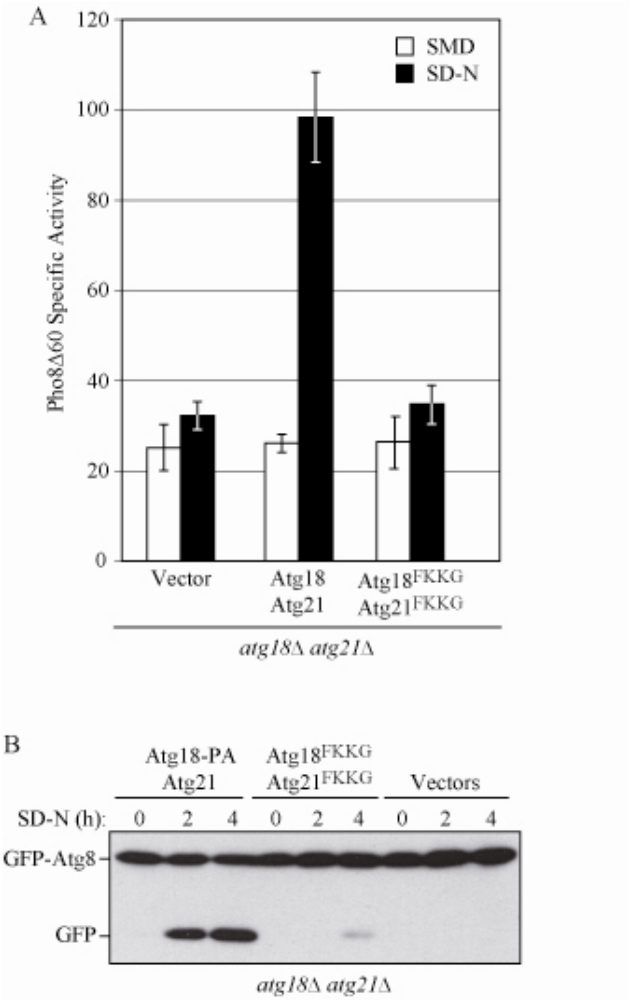

Figure 4.1. Mutations in the PtdIns(3)P binding motifs of both Atg18 and Atg21 result in a drastic reduction of autophagy. (A) Pho8Δ60 activity is severely reduced in Atg18^{FKKG}-PA and Atg21^{FKKG} expressing cells. The TN121 *atg18*Δ *atg21*Δ cells were transformed with the following combinations of constructs: empty vectors, centromeric plasmids expressing wild-type Atg18-PA and Atg21, or two plamids each bearing Atg18 and Atg21 constructs with mutations in their lipid-binding domains (Atg18^{FKKG}-PA and Atg21^{FKKG}). Cells were grown in nutrient-rich medium to mid-log phase and then shifted to starvation conditions for 4 h in SD-N medium. The Pho8Δ60 specific activity (nmoles/min/mg) was measured according to Materials and methods from protein extracts prepared from cells grown in SMD or after a 4 h shift to SD-N and the results represent the mean and SD of three independent experiments. (B) GFP-Atg8 processing is severely affected in *atg18*Δ *atg21*Δ cells expressing Atg18 and Atg21 PtdIns(3)P binding variants. Strain SEY6210 that is deleted for *ATG18* and *ATG21* was transformed with the combination of plasmids as in (A). Cells were grown in nutrient-rich medium until mid-log phase (0 h time point) and then shifted to nitrogen-starvation conditions for 2 or 4 h. Aliquots were collected at the indicated time points and analyzed by immunoblotting using anti-GFP antibody. The positions of full-length GFP-Atg8 and free GFP are indicated.

The block in nonspecific autophagy in *atg18*Δ *atg21*Δ cells expressing Atg18^{FKKG} and Atg21^{FKKG} was not previously examined, so we decided to confirm this result

through another biochemical approach, GFP-Atg8 processing. Atg8 is a ubiquitin-like protein that is conjugated to phosphatidylethanolamine (PE; (Kirisako, Baba et al. 1999; Huang, Scott et al. 2000) and is one of two Atg proteins that remain associated with the completed autophagosome in yeast. Atg8 is degraded after delivery into the vacuole, whereas the GFP moiety is relatively stable (Shintani, Huang et al. 2002); the appearance of free GFP can thus serve as a measure of autophagy. *atg18*Δ *atg21*Δ cells were transformed with a plasmid-based GFP-Atg8, and either Atg18-PA and Atg21, or empty vectors, or Atg18^{FKKG}-PA and Atg21^{FKKG}. The cells were grown in SMD medium until mid-log phase and then shifted to nitrogen starvation conditions. At various time points (0, 2 and 4 h), aliquots were removed, TCA-precipitated and then subjected to western blot using anti-GFP antibody (Fig. 4.1B). In wild-type cells, the amount of free GFP increased over time during starvation, representing a functional autophagy pathway, whereas in autophagy-defective *atg18*Δ *atg21*Δ cells expressing only empty vectors, no free GFP was detected. In the presence of Atg18^{FKKG}-PA and Atg21^{FKKG}, only a very small amount of free GFP could be detected after 4 hours of nitrogen starvation, representing a significant decrease in autophagy. This result is in agreement with the Pho8Δ60 analysis and further confirms the finding that *atg18*Δ *atg21*Δ cells expressing both the Atg18- and Atg21-lipid binding mutants were defective in autophagy.

We also examined whether the subcellular localization of the Atg18^{FKKG} and Atg21^{FKKG} mutants corresponded with their autophagy defects using GFP-tagged chimeras (Fig. 4.S2B and C). Consistent with previous results, we observed that Atg18 and Atg21 localize to several distinct structures in the cell such as the vacuolar membrane, the PAS and endosomes (Barth, Meiling-Wesse et al. 2001; Guan, Stromhaug et al. 2001;

Barth, Meiling-Wesse et al. 2002; Stromhaug, Reggiori et al. 2004; Suzuki, Kubota et al. 2007; Krick, Henke et al. 2008; Obara, Sekito et al. 2008). The Atg18^{FKKG}-GFP and Atg21^{FKKG}-GFP mutants on the other hand, were not localized to membrane structures, but instead were dispersed throughout the cytosol in both growing and starvation conditions (Fig. 4.S2B and C; (Stromhaug, Reggiori et al. 2004; Krick, Tolstrup et al. 2006; Obara, Sekito et al. 2008)). Thus, the localization of Atg18 and Atg21 to the vacuolar membrane and other punctate structures is dependent on their PtdIns(3)P binding domains. We also determined that neither Atg18 nor Atg21 is dependent on the other for its localization, in rich medium or conditions of nitrogen deprivation (Fig. 4.S2D).

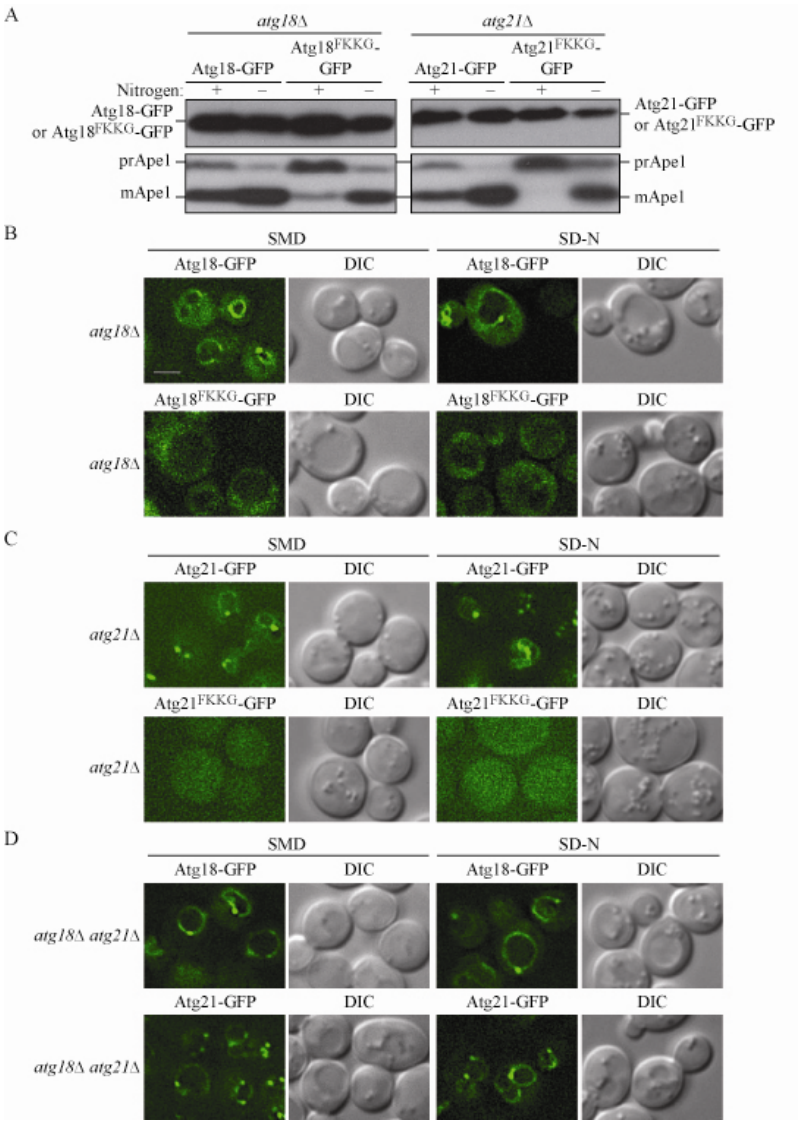

Figure 4.S2. The PAS localization of Atg18 and Atg21 requires their respective PtdIns(3)P binding domains under both growing and starvation conditions but neither protein is dependent on the other for their normal localization pattern. (A) Centromeric plasmids bearing Atg18 or Atg21 and their corresponding PtdIns(3)P-binding mutants were tagged with GFP at their C-termini. SEY6210 *atg18*Δ cells were transformed with plasmids expressing Atg18-GFP or ATG18^{FKKG}-GFP, and *atg21*Δ cells were transformed with plasmids expressing Atg21-GFP or ATG21^{FKKG}-GFP. Protein extracts were collected from cells grown in nutrient-rich or starvation conditions and analyzed by western blot using antisera against GFP (to monitor steady state levels of the chimeric proteins) or Ape1 (monitoring prApe1 maturation to determine functionality of the constructs). (B, C) Atg18^{FKKG}-GFP and Atg21^{FKKG}-GFP were dispersed in the cytosol in both nutrient-rich and starvation conditions. An (B) *atg18*Δ or (C) *atg21*Δ strain was transformed with a plasmid expressing either wild-type Atg18-GFP or Atg18^{FKKG}-GFP, or, either wild-type Atg21-GFP or Atg21^{FKKG}-GFP, respectively. Cells were cultured to mid-log phase, shifted to starvation conditions (SD-N) for 4 h and subjected to fluorescence microscopy. (D) Atg18 and Atg21 do not depend on each other for their localization. SEY6210 *atg18*Δ *atg21*Δ cells were transformed with plasmids expressing Atg18-GFP or Atg21-GFP, grown in nutrient-rich media and shifted to starvation conditions for 4 h and imaged by fluorescence microscopy. DIC, differential interference contrast. Scale bar, 2.5 μm.

Atg9 localization is normal in nitrogen starvation medium in *atg18*Δ *atg21*Δ Cells expressing Atg18 and Atg21 FKKG mutants

Atg9 is an integral membrane protein that partially localizes to the PAS and multiple punctate structures including the mitochondria and endoplasmic reticulum, and is essential for the Cvt pathway and autophagy (Noda, Kim et al. 2000; Kim, Kamada et al. 2001; Suzuki, Kirisako et al. 2001). Atg9 cycles between the PAS and the peripheral structures, and is thought to provide lipids to the forming Cvt vesicles or autophagosomes. The anterograde movement of Atg9 from the peripheral sites to the PAS depends on Atg11, Atg23, Atg27 and actin (He, Song et al. 2006; Legakis, Yen et al. 2007; Monastyrska, He et al. 2008). The retrograde movement of Atg9 from the PAS requires Atg1, Atg13, Atg2, Atg18, and components of the PtdIns 3-kinase complex I—Atg6 and Atg14 (Reggiori, Tucker et al. 2004). Because Atg18 has a role in the retrieval of Atg9 from the PAS, and because of the shared homology between Atg18 and Atg21, we hypothesized that Atg21 might have a similar role. Further, we wanted to determine whether the PtdIns(3)P-binding motifs of these proteins are required for the retrograde movement of Atg9, which might account for the autophagy defect seen with the double FKKG mutants.

In order to determine whether deletion of *ATG21* and/or the PtdIns(3)P-binding mutants of Atg18 and Atg21 affect the localization of Atg9, we chromosomally tagged various strains with Atg9-3xGFP and examined them by fluorescence microscopy. As previously observed, in the wild-type strain Atg9-3xGFP was seen in multiple dots in both nutrient rich and starvation conditions, and some of these dots were peri-vacuolar (Fig. 4.2). In agreement with the role of Atg1 in the retrograde movement of Atg9 from the PAS, in an *atg1*Δ strain, Atg9-3xGFP was seen as one strong peri-vacuolar dot, under

both nutrient conditions. In an *atg18*Δ strain, Atg9-3xGFP fluorescence collapsed into primarily into a single large punctum, although additional smaller dots could also be detected. Thus, Atg18 does not appear to have as important a role as Atg1 in controlling the retrograde cycling of Atg9. We also determined that the Atg18 PtdIns(3)P-binding site is not required for Atg9 localization in nutrient rich or starvation conditions; in an *atg18*Δ strain expressing Atg18^{FKKG}, Atg9 was seen in multiple dots similar to what was observed in a wild-type strain (data not shown).

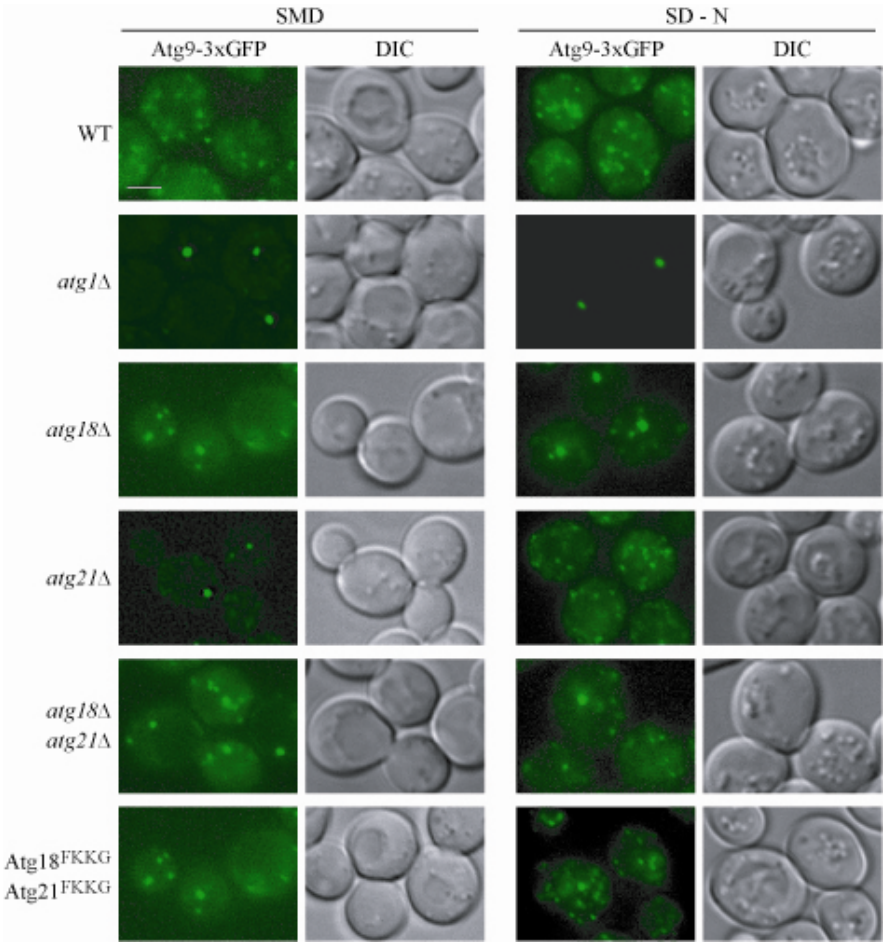

Figure 4.2. Atg18 and Atg21 have different effects on the retrograde transport of Atg9. The retrograde trafficking of Atg9 from the PAS to peripheral structures in nutrient-rich (SMD) but not starvation (SD-N) media is compromised by Atg18- and Atg21-FKKG mutants. Atg9-3xGFP was integrated into the *ura3* locus of the following strains: Wild type (SEY6210), *atg1*Δ, *atg18*Δ, *atg21*Δ, or *atg18*Δ *atg21*Δ; SEY6210 *atg18*Δ *atg21*Δ cells expressing Atg9-3xGFP were also transformed with plasmids expressing Atg18^{FKKG}-PA and Atg21^{FKKG}. The localization pattern of Atg9-3xGFP was analyzed by fluorescence microscopy in the above strains grown in rich medium to mid-log phase (SMD) or shifted to starvation conditions (SD-N) for 4 h. For every sample depicted in this figure, a projection of a stack of images covering the entire depth of the cell was collected and projections of the image stacks based on average intensity were acquired. One representative image for each sample is shown. DIC, differential interference contrast. Scale bar, 2.5 μm.

In contrast to the impaired localization of Atg9 in the absence of Atg18 in both rich and nitrogen starvation conditions, in an *atg21*Δ strain Atg9-3xGFP cycling was compromised only under rich conditions (Fig. 4.2). However, similar to what we observed in the case of the Atg18^{FKKG} mutant, the Atg21^{FKKG} mutant also had no effect

on Atg9 localization (data not shown). Thus, one of the mechanisms by which the formation of Cvt vesicles is blocked in the absence of Atg21 could be due to the limited supply of membrane that is delivered to the PAS via Atg9. Also, consistent with Atg21 not having a role in autophagy, this protein is required for Atg9 cycling only under rich conditions. In a strain bearing a double deletion of *ATG18* and *ATG21*, the localization pattern of Atg9-3xGFP resembled that seen in an *atg18*Δ strain (Fig. 4.2). In an *atg18*Δ *atg21*Δ strain expressing Atg18^{FKKG}-PA and Atg21^{FKKG}, Atg9-3xGFP was restricted to a few puncta in growing conditions, but this protein appeared to be normally localized in cells shifted to nitrogen-deprived medium. Co-localization of Atg9-3xGFP with the PAS marker RFP-Ape1 in an *atg18*Δ *atg21*Δ strain expressing Atg18^{FKKG}-PA and Atg21^{FKKG} during starvation, showed that at least some of these puncta coincided with RFP-Ape1 in both nutrient conditions (data not shown). These results show that the defect in autophagosome formation does not appear to be due to the mislocalization of Atg9, as steady state distribution of Atg9-3xGFP appeared to be normal under starvation conditions. However, a kinetic delay in Atg9 cycling under these conditions cannot be ruled out.

*atg18*Δ *atg21*Δ cells expressing Atg18 and Atg21 FKKG mutants are defective in the recruitment and/or dissociation of Atg8

Because autophagy is severely reduced in the presence of Atg18 and Atg21 FKKG mutants (Fig. 4.1A and B), we hypothesized that when expressed together, these mutant proteins may result in the mislocalization of some Atg proteins other than Atg9. Accordingly, we examined the localization of Atg8, which plays an important role in determining the size of the autophagosome (Xie, Nair et al. 2008). Atg8 is present in a

cytosolic pool and it is processed by the proteolytic removal of a C-terminal arginine by the cysteine protease Atg4. Atg8 then becomes membrane associated after lipidation; modification with PE is transient and the protein cycles back into the soluble pool following a second cleavage event by Atg4 (Kirisako, Ichimura et al. 2000). One study shows that the localization of Atg8 to the PAS under starvation conditions depends on ten Atg proteins; the absence of seven of these proteins—Atg3, Atg4, Atg7, Atg10, and the Atg12–Atg5-Atg16 complex—results in the compete lack of Atg8 localization to the PAS, whereas the loss of the other three proteins—Atg9 and the PtdIns(3)-kinase complex components Atg14 and Atg6—results in a partial loss of Atg8 recruitment to the PAS (Suzuki, Kubota et al. 2007). Under starvation conditions, the loss of Atg18 does not affect the recruitment of Atg8–PE to the PAS; instead there is a four-fold accumulation of Atg8–PE at the PAS relative to a wild-type strain (Suzuki, Kubota et al. 2007). Consistent with these results, in another study no differences in the localization of Atg8 in an *atg18*Δ strain were seen in both exponential growth and starvation conditions (Guan, Stromhaug et al. 2001). Atg21, on the other hand is required for the localization of GFP-Atg8 to the PAS under nutrient-rich conditions; GFP-Atg8 displays a diffuse cytosolic staining in the absence of Atg21 (Stromhaug, Reggiori et al. 2004).

We wanted to know the effect of FKKG mutation of Atg18 and Atg21 on GFP-Atg8 localization. First, we tested the roles of the single Atg18 FKKG mutation on the localization of GFP-Atg8. An *atg18*Δ strain bearing a GFP-Atg8 plasmid was transformed with wild-type Atg18-PA, empty plasmid or Atg18^{FKKG}-PA. The GFP-Atg8 localization pattern was observed in exponentially growing cells in rich medium or after cells were shifted to starvation conditions for 4 h. In wild-type cells (*atg18*Δ cells

expressing Atg18) grown in rich medium, GFP-Atg8 showed cytosolic staining as well as a concentrated perivacuolar dot (Fig. 4.3A). After 4 h in starvation conditions, GFP-Atg8 accumulated in the vacuole. In an *atg18*Δ strain, under both growing and starvation conditions, GFP-Atg8 was recruited to the PAS, in agreement with previous data. However, under starvation conditions the GFP-Atg8 fluorescence signal was concentrated into strong punctate dots essentially without cytosolic or vacuolar staining. Thus, Atg18 is not needed for the PAS recruitment of GFP-Atg8, but instead has a role in the dissociation of this protein from the PAS. The inability to form autophagosomes in an *atg18*Δ strain may reflect this block in Atg8 dissociation. The localization pattern of GFP-Atg8 in *atg18*Δ cells expressing Atg18^{FKKG}-PA was essentially the same as that seen in wild-type cells under both growing and starvation conditions.

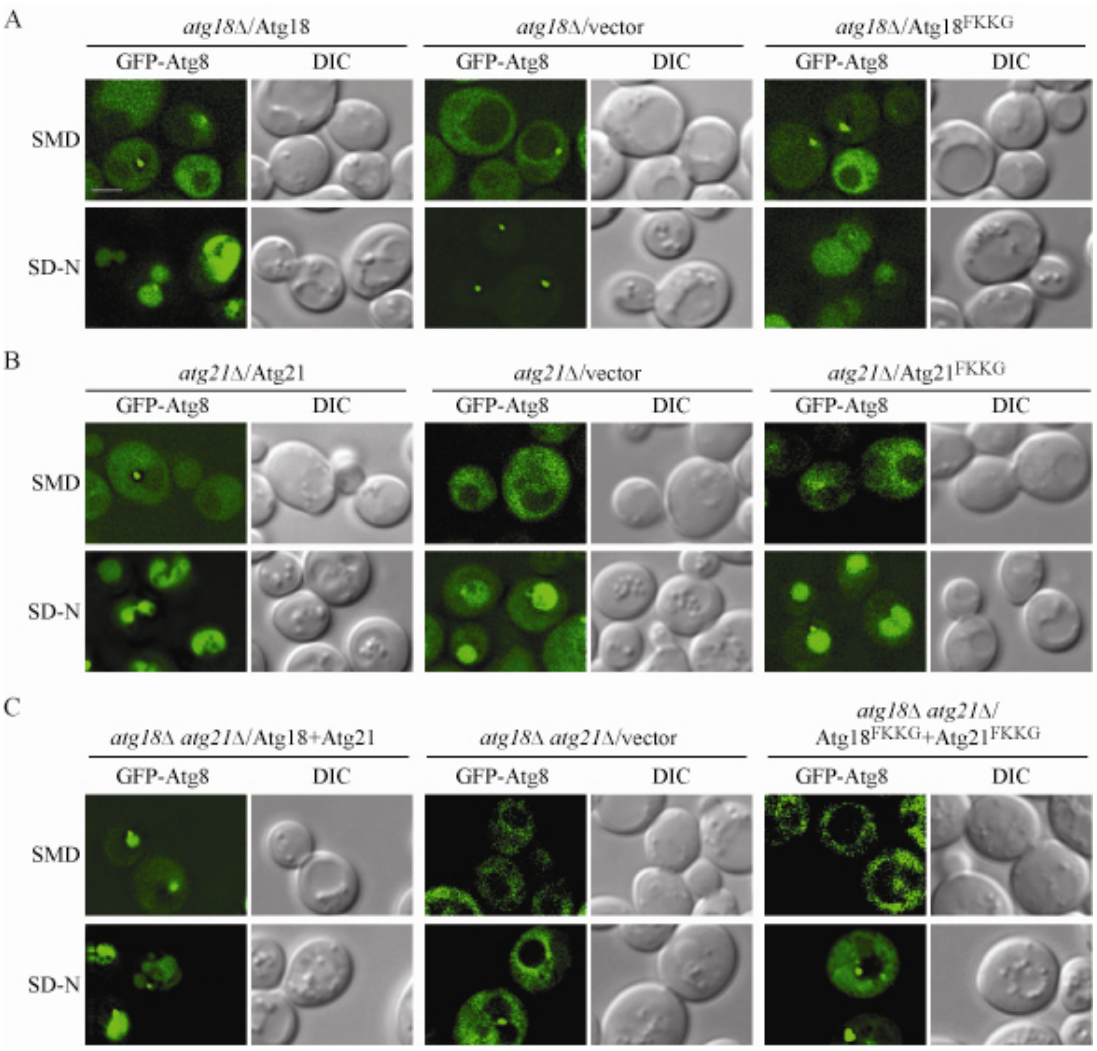

Figure 4.3. Atg18- and Atg21-FKKG mutants are defective in the recruitment of Atg8 to the PAS in nutrient rich media, and in both the recruitment to and the dissociation from the PAS under starvation conditions. (A) An *atg18*Δ or (B) *atg21*Δ strain was transformed with a centromeric plasmid expressing GFP-Atg8 and either a plasmid encoding (A) wild-type Atg18-PA, Atg18^{FKKG}-PA, (B) wild-type Atg21, Atg21^{FKKG}, or (A,B) empty vector. GFP-Atg8 localization patterns were monitored in nutrient-rich conditions and after a shift to starvation medium (SD-N) for 4 h. (C) An *atg18*Δ *atg21*Δ strain expressing GFP-Atg8 was transformed with plasmids expressing wild-type Atg18-PA and Atg21, empty vectors or Atg18^{FKKG}-PA and Atg21^{FKKG} and examined as above. DIC, differential interference contrast. Scale bar, 2.5 μm.

We also checked the effect of the Atg21 FKKG mutation on GFP-Atg8 localization. In *atg21*Δ cells expressing wild-type Atg21, GFP-Atg8 showed cytosolic staining as well as a concentrated perivacuolar dot in rich medium, and after 4 h in

starvation conditions, a fluorescence signal corresponding to GFP-Atg8 could be seen to accumulate in the vacuole (Fig. 4.3B). Consistent with previous observations, in the absence of Atg21, GFP-Atg8 perivauolar puncta were absent and this protein showed diffused cytosolic staining, in nutrient-rich conditions (Stromhaug, Reggiori et al. 2004). As Atg21 does not have a role in starvation-induced autophagy, under these conditions, the localization pattern of GFP-Atg8 appeared similar to that in wild-type cells (Fig. 4.3B). Under nutrient-rich conditions, $Atg21^{FKKG}$ was unable to recruit GFP-Atg8 to the PAS, thus providing a mechanistic explanation for the block in prApe1maturation via the Cvt pathway in *atg21*Δ cells expressing $Atg21^{FKKG}$. In agreement with the lack of a phenotype in the *atg21*Δ strain, $Atg21^{FKKG}$ did not affect the localization of GFP-Atg8 in nitrogen starvation conditions (Fig. 4.3B).

Next, we examined the effect of simultaneously expressing $Atg18^{FKKG}$-PA and $Atg21^{FKKG}$ on GFP-Atg8 localization in *atg18*Δ *atg21*Δ cells, under growing and starvation conditions. In *atg18*Δ *atg21*Δ cells, in nutrient-rich conditions, the GFP-Atg8 localization pattern appeared similar to that in an *atg21*Δ strain, showing a diffuse cytosolic fluorescence signal and a block in PAS recruitment (Fig. 4.3C). These observations suggest that in growing conditions, Atg21 is epistatic over Atg18 in the recruitment of Atg8. After 4 h in starvation conditions, the GFP-Atg8 in *atg18*Δ *atg21*Δ cells showed strong cytosolic staining and perivacuolar punctate dots (Fig. 4.3C). This phenotype suggests a defect in both the recruitment of GFP-Atg8 to, and dissociation from, the PAS; a defect in only recruitment would show cytosolic staining with no PAS dot, whereas a defect in dissociation alone would be reflected by the absence of cytosolic staining. Similar results were observed in *atg18*Δ *atg21*Δ cells

expressing both Atg18^{FKKG}-PA and Atg21^{FKKG}. In growing conditions, GFP-Atg8 was mostly cytosolic, whereas in starvation conditions, in accordance with our Pho8Δ60 activity and GFP-Atg8 processing results (Fig. 4.1A and B), vacuolar GFP-Atg8 fluorescence staining associated with autophagy was seldom seen; instead this protein showed both strong cytosolic staining and perivacuolar punctate structures (Fig. 4.3C). Overall, these results suggest that under starvation conditions, the wild-type localization of GFP-Atg8, and concomitantly normal autophagy, depends on the wild-type PtdIns(3)P binding ability of at least Atg18 or Atg21.

Finally, we wanted to test whether the aberrant localization of GFP-Atg8 in *atg18*Δ *atg21*Δ cells is due to a defect in the conjugation of Atg8 with PE. After Atg4-dependent processing, Atg8 is conjugated to PE via two enzymes: Atg7, the E1-like activating ezyme, and Atg3, an E2-like conjugating enzyme (Tanida, Mizushima et al. 1999; Ichimura, Kirisako et al. 2000; Tanida, Tanida-Miyake et al. 2001; Tanida, Tanida-Miyake et al. 2002). The conjugation of Atg8 with PE, which is required for its PAS localization, is facilitated by a multimeric complex that may function as an E3-like enzyme and is composed of three proteins, Atg12, Atg5 and Atg16 (Suzuki, Kirisako et al. 2001; Hanada, Noda et al. 2007). Atg8–PE can be resolved from Atg8 by carrying out SDS-PAGE electrophoresis in the presence of urea, and performing immunoblot analysis with the Atg8 antibody (Kirisako, Ichimura et al. 2000). Under growing conditions, the amount of conjugated Atg8 was significantly less in an *atg18*Δ *atg21*Δ strain expressing empty vectors or Atg18^{FKKG}-PA and Atg21^{FKKG} compared to that in the same strain expressing wild-type Atg18-PA and Atg21 (Fig. 4.S3). After starvation for 4 h, even though there was a considerable accumulation of the unconjugated form of Atg8 in

*atg18*Δ *atg21*Δ cells expressing empty vectors, or Atg18^{FKKG}-PA and Atg21^{FKKG}, there was no discernable difference in the amount of Atg8–PE relative to the wild type (Fig. 4.S3). Therefore, the autophagy defect in *atg18*Δ *atg21*Δ cells expressing Atg18- and Atg21-FKKG mutants was not simply due to the inability of the cells to form Atg8–PE.

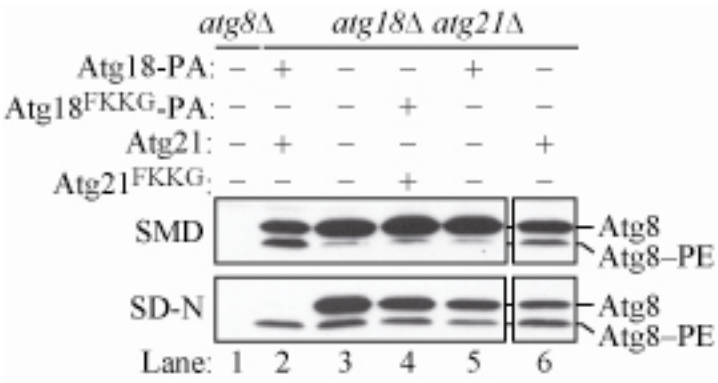

Figure 4.S3. Lipidation of Atg8 in *atg18*Δ *atg21*Δ cells. *atg8*Δ cells, or *atg18*Δ *atg21*Δ cells expressing empty vectors, wild-type Atg18-PA and/or Atg21 or Atg18^{FKKG}-PA and Atg21^{FKKG} were grown to mid-log phase and then shifted to nitrogen starvation media for 4 h. Atg8–PE was separated from Atg8 by carrying out electrophoresis in 12% SDS-PAGE in the presence of 6% urea (Kirisako, Ichimura et al. 2000). Immunoblot analysis was carried out using Atg8 antiserum.

*atg18*Δ *atg21*Δ cells expressing Atg18 and Atg21 FKKG mutants are defective in the PAS recruitment of Atg16 under starvation conditions

Having determined that the Atg18 and Atg21 FKKG mutants affect the localization pattern of Atg8, we wanted to extend our analysis to examine the localization of Atg16 in the presence of these mutants. We specifically chose to examine the localization of this protein for two reasons: first, Atg16 affects the recruitment of Atg8 to the PAS (Suzuki, Kubota et al. 2007) and second, the PAS localization of the Atg12–Atg5-Atg16 complex itself is blocked in *atg14*Δ or *vps34*Δ cells, suggesting a role for PtdIns(3)P in the PAS association of these molecules (Obara, Noda et al. 2008).

To examine the localization pattern of Atg16 by fluorescence microscopy, we chromosomally tagged Atg16 with GFP. Because in nutrient-rich conditions the fluorescence signal of Atg16-GFP in wild-type cells was very weak and could be detected in less than 10% of the cells, we chose to study its localization only under starvation conditions. After 4 h in nitrogen-depleted medium, Atg16-GFP showed cytosolic staining and a clear punctate perivacuolar dot in approximately 40% of the wild-type cells (Fig. 4.4A and B). Consistent with the notion that loss of Atg18 blocks the release of certain Atg proteins from the PAS such as Atg9, more than 60% of the *atg18Δ* cells accumulated Atg16-GFP puncta. In accordance with Atg21 not having a role in autophagy, the loss of this protein had no effect on the PAS localization of Atg16-GFP after 4 h starvation (Fig. 4.4A and B). The deletion of both Atg18 and Atg21, however, resulted in less than 20% of cells that showed Atg16-GFP perivacuolar puncta (Fig. 4.4A and B). Next, we examined the possible contribution of Atg18- and Atg21-lipid binding in the PAS localization of Atg16. *atg18*Δ *atg21*Δ cells transformed with Atg18-PA and Atg21, or Atg18^{FKKG}-PA and Atg21^{FKKG} showed approximately 50% or 22% Atg16-GFP puncta, respectively (Fig. 4.4C and D). Taken together, these results indicated that under starvation conditions the recruitment of Atg16 to the PAS was compromised in the absence of Atg18 and Atg21, and additionally that the lipid-binding motifs of these proteins were responsible for the PAS recruitment of Atg16.

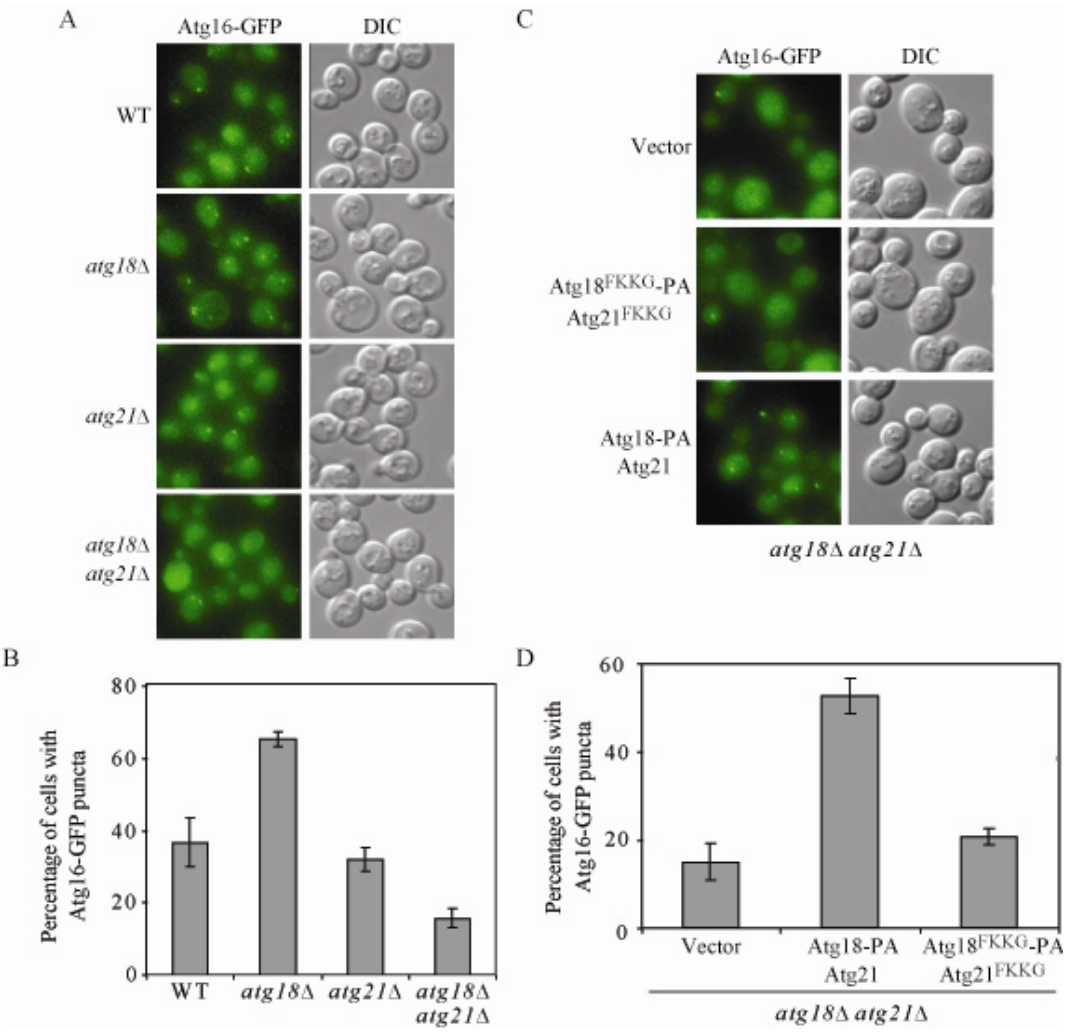

Figure 4.4. Atg18 and Atg21 lipid-binding mutants are defective in the recruitment of Atg16 to the PAS under starvation conditions. Each of the following strains was chromosomally tagged with Atg16-GFP: (A, B) wild-type (WT, SEY6210), *atg18*Δ, *atg21*Δ, and *atg18*Δ *atg21*Δ. (C, D) The *atg18*Δ *atg21*Δ strain was additionally transformed with plasmids expressing wild-type Atg18-PA and Atg21, the FKKG mutants, or empty vectors. (A, C) The Atg16-GFP localization pattern was examined by fluorescence microscopy and (B, D) the percentage of cells showing Atg16-GFP puncta in each of these strains after a 4 h shift to starvation conditions was quantified. The quantification shown here is from three independent experiments. Approximately 500 cells for each strain were analyzed for scoring the percentage of cells with fluorescent Atg16-GFP PAS puncta. Error bars represent the standard error of the mean. DIC, differential interference contrast. Scale bar, 2.5 μm.

Atg18 and Atg21 protect Atg8 from Atg4-mediated cleavage

Our current data suggest that Atg18 and Atg21 play a role in the PAS recruitment of Atg16; and in the case of Atg8, these proteins affect both its recruitment to, and

dissociation from, the PAS. To gain further insight into the functional relationship between Atg18 and Atg21 with Atg8, we utilized the multiple knockout (MKO) strain (Cao, Cheong et al. 2008). In this strain most of the autophagy-related genes are deleted and therefore it is deficient in the assembly of a functional PAS. The advantage of the MKO system is that it allows us to investigate a particular function or contribution of a subset of Atg proteins in the complete absence of the other Atg proteins that are not being examined.

Our MKO strain has endogenous, wild-type copies of the *VPS34* and *VPS15* genes, but not *VPS30/ATG6*, and therefore although it is not defective in PtdIns(3)P synthesis, it has a reduced amount of this lipid (Burda, Padilla et al. 2002). We started with an MKO strain expressing Atg3 (MKO (*ATG3*)), which is an E2-like enzyme that catalyzes the conjugation of Atg8–PE, and also expressing GFP-Atg8ΔR in which the C-terminal arginine residue has been removed; the latter allowed us to bypass the initial Atg4-mediated processing of Atg8. When we examined the localization of GFP-Atg8ΔR in this strain, we found that its fluorescence signal appeared to be evenly distributed in the cytosol (Fig. 4.5, Vector). In the presence of additional Atg8–PE conjugation components—Atg7, Atg10, Atg5 and Atg12 (Mizushima, Noda et al. 1998; Hanada, Noda et al. 2007; Cao, Cheong et al. 2008)—we observed that GFP-Atg8ΔR was localized to the vacuolar rim in addition to being distributed in the cytosol. When the MKO (*ATG3*) strain bearing these components was supplemented with Atg16, which enhances the efficiency of Atg8–PE conjugation (Mizushima, Noda et al. 1999), GFP-Atg8ΔR was recruited to distinct puncta and was also present around the vacuolar rim. In the presence of Atg4, the PE moiety is removed from Atg8. When Atg4 was additionally

expressed in the starting MKO (*ATG3*) strain containing Atg7, Atg10, Atg5, Atg12 and Atg16, GFP-Atg8ΔR-containing puncta and vacuolar rim staining disappeared, and became dispersed in the cytosol. Atg4 is normally present in the cell, and GFP-Atg8 can be detected as a punctum at the PAS in wild-type cells, suggesting that the MKO strain expressing the Atg8 and Atg12 conjugation proteins lacks some additional component(s) that regulate the second cleavage by Atg4.

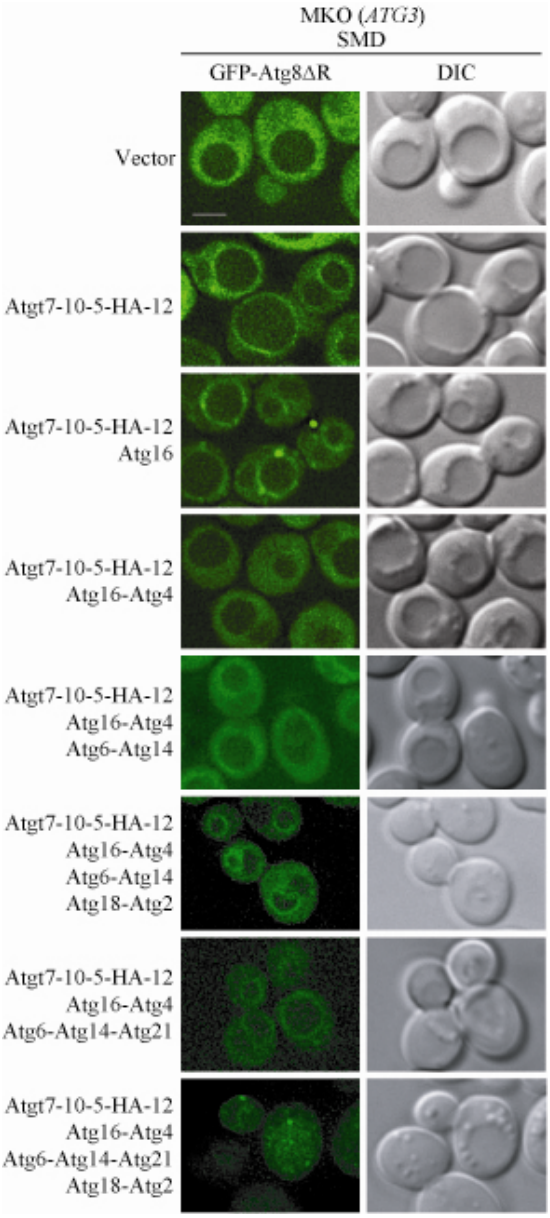

Figure 4.5. Atg18-Atg2 and Atg21 protect Atg8 from Atg4-mediated cleavage. A multiple knockout (MKO) strain expressing Atg3, the E2-like conjugating enzyme, and GFP-Atg8ΔR, a GFP-Atg8 chimera lacking the carboxyl terminal arginine residue of Atg8, was transformed with plasmids expressing different combinations of Atg proteins as indicated. The GFP-Atg8ΔR localization pattern in these different strains was monitored in nutrient-rich conditions by fluorescence microscopy. Similar results were observed in cells that were shifted to starvation conditions for 4 h (data not shown). DIC, differential interference contrast. Scale bar, 2.5 μm.

The addition of the PtdIns 3-kinase complex subunits Atg14 and Atg6, and either Atg18-Atg2 or Atg21, to the abovementioned system resulted in the relocation of GFP-

Atg8ΔR fluorescence back onto the vacuolar membrane (Fig. 4.5), presumably because these proteins were able to partially prevent the cleavage of PE from Atg8; however, these proteins alone did not restore the PAS localization of Atg8. In contrast, in the presence of both Atg18-Atg2 and Atg21 in addition to components from two conjugation systems and the PtdIns 3-kinase complex I, GFP-Atg8ΔR appeared as punctate dots in the presence of Atg4, suggesting that in wild-type cells, Atg18-Atg2 and Atg21 may play a role in protecting Atg8–PE from premature cleavage by Atg4 before autophagosome formation is complete. In this case, the vacuolar rim staining was not apparent, indicating that the inhibition of the second Atg4 cleavage reaction was restricted to the punctate GFP-Atg8ΔR. The use of the MKO strain and the presence of only a subset of Atg proteins did not prevent the initial cleavage of the Atg8 C-terminal arginine residue (Fig. 4.S4); the MKO (*ATG3*) strain retained normal Atg4 protease activity and the presence of the additional Atg components did not interfere with cleavage of GFP from Atg8 when fused at the C terminus. Thus, lack of Atg4 activity could not explain the restoration of GFP-Atg8ΔR puncta.

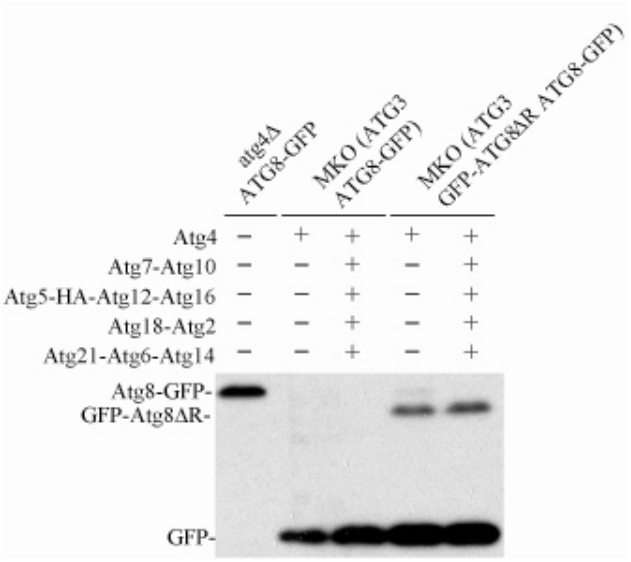

Figure 4.S4. The MKO strain is not defective for the initial cleavage of Atg8 by Atg4. *ATG8-GFP* under the control of the endogenous *ATG8* promoter was integrated into the *lys2* locus in the following strains: SEY6210 *atg4*Δ, an MKO strain expressing Atg3, or an MKO strain expressing GFP-Atg8ΔR and Atg3. The MKO strains were transformed with a plasmid expressing Atg4 alone, or in combination with plasmids expressing all the other components in the Atg8–PE and Atg12–Atg5 conjugation systems, Atg6-Atg14, Atg18-Atg2 and Atg21. Cells were grown to mid-log phase and collected, and protein extracts were subjected to SDS-PAGE followed by immunoblotting with anti-GFP antibody. Note that GFP-Atg8ΔR and Atg8-GFP migrate differently on an SDS-PAGE gel. Free GFP was derived from Atg8-GFP, but not GFP-Atg8ΔR. Similar results were obtained from cells that were shifted to starvation conditions for 2 h (data not shown).

The experiments described in Fig. 4.5 were carried out under growing conditions, but similar results were obtained when we performed this experiment in SD-N (data not shown). Taken together, our experimental results from Fig.s 4.3, 4.4 and 4.5 suggest a model wherein Atg18 and Atg21 facilitate the PAS localization of Atg8–PE via the recruitment of other proteins such as Atg16, and by protecting Atg8–PE from a second unregulated cleavage event catalyzed by Atg4.

Discussion

In this work we analyzed the physiological significance of the PtdIns(3)P-binding domains of two homologous proteins, Atg18 and Atg21, in the Cvt pathway and autophagy. Atg18 is required for both the Cvt pathway as well as for non-specific autophagy, whereas Atg21 is reported to only be required for the latter pathway (Barth, Meiling-Wesse et al. 2001; Guan, Stromhaug et al. 2001; Barth, Meiling-Wesse et al. 2002; Stromhaug, Reggiori et al. 2004). Under growing conditions, PtdIns(3)P is enriched on endosomes, on the vacuolar membrane and both the inner and outer membranes of autophagosomes; under starvation conditions, it is also found in the vacuole (Obara, Noda et al. 2008). The role of PtdIns(3)P in autophagy-related processes is still unclear, but it is absolutely required for both the Cvt and autophagy pathways. Mutations in the lipid kinase domain of Vps34 ($Vps34^{N736K}$), the sole PtdIns 3-kinase in the cell that is essential for the generation of PtdIns(3)P, results in a block in autophagy (Schu, Takegawa et al. 1993; Obara, Noda et al. 2008). Similarly, components of the PtdIns 3-kinase complex I, such as Atg6 and Atg14 are also essential for this process (Kametaka, Okano et al. 1998).

Atg18 and Atg21 bind PtdIns(3)P via conserved Phe-Arg-Arg-Gly (FRRG) motifs. In order to analyze the PtdIns(3)P–binding roles of these proteins, we generated point mutations within these motifs. Cells expressing $Atg18^{FKKG}$ or $Atg21^{FKKG}$ displayed defects in prApe1 maturation ((Stromhaug, Reggiori et al. 2004; Krick, Tolstrup et al. 2006; Obara, Sekito et al. 2008); Fig. 4.S1A), and in the case of $Atg18^{FKKG}$ the magnitude of autophagy (Obara, Sekito et al. 2008); Fig. 4.S1B). Because neither $Atg18^{FKKG}$ nor

Atg18^{FTTG} (Obara, Sekito et al. 2008) mutants completely abolished Pho8Δ60 activity, it is likely that the function of Atg18 depends on more than its ability to bind PtdIns(3)P. However, it cannot be ruled out that these mutants still retain some level of PtdIns(3)P binding. The Pho8Δ60 activity seen in the presence of Atg21^{FKKG} was similar to that seen in *atg21*Δ cells, suggesting that the contribution of Atg21 to autophagy may be through its PtdIns(3)P binding activity (Fig. 4.S1B). One important finding in the present study is that in *atg18*Δ *atg21*Δ cells expressing Atg18^{FKKG} and Atg21^{FKKG}, autophagy was almost completely eliminated, suggesting that the normal autophagy process requires the PtdIns(3)P-binding activity of at least one of the two proteins (Fig. 4.1A and B), and that either one is sufficient for essentially normal activity (Fig. 4.S1B).

Wild-type Atg18 and Atg21 localize in part to the phagophore assembly site (PAS) where they presumably carry out their function in autophagy. These proteins localize to several distinct structures in the cell such as the vacuolar membrane, the PAS and endosomes (Barth, Meiling-Wesse et al. 2001; Guan, Stromhaug et al. 2001; Barth, Meiling-Wesse et al. 2002; Stromhaug, Reggiori et al. 2004; Suzuki, Kubota et al. 2007; Krick, Henke et al. 2008; Obara, Sekito et al. 2008). The Atg18^{FKKG}-GFP and Atg21^{FKKG}-GFP mutants on the other hand, were not localized to membrane structures, but instead were dispersed throughout the cytosol in both growing (Fig. 4.S2B) and starvation conditions (Fig. 4.S2C) (Stromhaug, Reggiori et al. 2004; Krick, Tolstrup et al. 2006; Obara, Sekito et al. 2008). Thus, the localization of Atg18 and Atg21 to the vacuolar membrane and other punctate structures is dependent on their PtdIns(3)P binding domains. The lipid-binding FRRG motif is also conserved in the human Atg18 homolog WIPI-1. WIPI-1 binds PtdIns(3)P and forms puncta in an autophagy-dependent

manner in several cell lines, and the deletion of this four amino acid motif in WIPI-1 results in a mutant that has reduced PtdIns(3)P-binding and is incompetent for puncta formation (Proikas-Cezanne, Ruckerbauer et al. 2007).

Our microscopy examination of the localization pattern of Atg9, a protein that may play a role in the delivery of lipid to the PAS, revealed that the block in autophagy was not due to a defect in the steady state localization pattern of Atg9. The release of Atg9 from the PAS, part of its normal cycling, is dependent on Atg1, Atg13, Atg18, and Atg2 (Reggiori, Tucker et al. 2004), and in this work we have shown that the absence of Atg21 also resulted in the accumulation of this protein at the PAS in growing conditions (Fig. 4.2). Although the precise functions of these proteins remain to be fully elucidated, it appears that they may have roles in elongation of the phagophore (the initial sequestering compartment that forms the autophagosome) or vesicle completion, by allowing the dissociation of Atg9 from the PAS.

Atg8 is a ubiquitin-like protein subject to lipid-conjugation, whose steady state levels are significantly elevated during autophagy-inducing, starvation conditions (Kirisako, Baba et al. 1999). Atg8–PE is one of the last phagophore markers to be recruited to the PAS during autophagosome formation (Suzuki, Kubota et al. 2007), and the amount of Atg8 at the PAS controls the size of the autophagosome (Xie, Nair et al. 2008). Ag8–PE associates with the inner and outer membranes of the expanding phagophore; upon autophagic vesicle completion, Atg8–PE on the outer membrane of the autophagosome is cleaved by the action of the cysteine protease Atg4, whereas the Atg8 trapped in the inner membrane is degraded in the vacuole (Xie, Nair et al. 2008). In cells lacking Atg18, GFP-Atg8 was unable to dissociate from the PAS and was trapped at this

location in both growing and starvation conditions (Fig. 4.3). Atg21, on the other hand is required for the recruitment of GFP-Atg8 to the PAS only under nutrient-rich conditions (Fig. 4.3). In starvation conditions, neither Atg18^{FKKG} nor Atg21^{FKKG}, on their own, had any effect on Atg8 localization. When expressed together, Atg18^{FKKG}-PA and Atg21^{FKKG} showed a substantial defect both in Atg8 recruitment to, and release from, the PAS (Fig. 4.3). Although at this point the reason for the block in autophagosome formation in *atg18*Δ *atg21*Δ cells expressing the Atg18 ^{FKKG} and Atg21^{FKKG} mutants is not clear, the autophagy defect is not simply due to the inability of these cells to form Atg8–PE (Fig. 4.S3). This result supports a model where the PtdIns(3)P-binding domains of Atg18 and Atg21 can somehow substitute for each other in autophagosome formation by facilitating the normal localization of Atg8.

We further dissected the role of the Atg18- and Atg21-PtdIns(3)P-binding motifs by examining the localization of Atg16, a protein that is required for the PAS localization of Atg8, and whose own localization to the PAS depends on the PtdIns 3-kinase components (Suzuki, Kubota et al. 2007). We found that Atg18 and Atg21, via their PtdIns(3)P-binding motifs, regulate the PAS recruitment of Atg16 (Fig. 4.4). Prior to this work, it was unclear as to how Atg16 is targeted to the PAS, as it requires PtdIns(3)P for its PAS localization, but is independent of Atg18 (Suzuki, Kubota et al. 2007).

Finally, we resolved an apparent discrepancy between *in vitro* and *in vivo* results concerning the regulation of the Atg4 protease. Previous *in vitro* studies suggest that Atg7 and Atg3 are sufficient for correct conjugation of Atg8 (Ichimura, Imamura et al. 2004). Those analyses, however, rely on the use of Atg8ΔR and do not include Atg4, which is normally present in the cell. In contrast, Atg8–PE is not detected in an MKO

strain expressing these same components. The latter system, which included Atg4, suggested that additional components prevent the second Atg4-dependent cleavage of Atg8–PE from occurring prematurely, an aspect of autophagy regulation that has not been understood. We now show that in the absence of Atg4, Atg8–PE was located both in puncta (that would normally correspond to the PAS) and on the vacuole rim. The presence of Atg4 abolishes membrane association of Atg8, reflecting cleavage of the PE moiety. However, the additional presence of Atg18 and Atg21 (along with the Atg12–Atg5-Atg16 conjugation system and the Atg6-Atg14 PtdIns 3-kinase components) protected the punctate GFP-Atg8, but not that on the vacuole rim (Fig. 4.5). These data suggest that Atg18 and Atg21 function in some manner at the PAS to regulate the second Atg4-dependent cleavage event, in addition to their roles in recruiting Atg8–PE to this structure. Future studies are needed to provide additional information on the function of PtdIns(3)P binding and the role of Atg18 and Atg21 in autophagosome formation.

Materials and methods

Yeast strains and media

The yeast *Saccharomyces cerevisiae* strains used in this study are listed in Table 4.1. Knockout strains were constructed using the *loxP/Cre* system (Gueldener, Heinisch et al. 2002). Integration of the GFP tag at the 3' end of the *ATG16* open reading frame (ORF) was performed by a PCR-based procedure (Longtine, McKenzie et al. 1998). For integration of the Atg9-3xGFP fusion, the plasmid pATG9-3xGFP(306) was linearized with StuI and integrated at the *ura3* gene locus. GFP-Atg8ΔR(404) was was linearized with BstBI and introduced into the *ATG8* locus. The *TRP1* marker in YCY146 was replaced with the *E. coli kan*^{r} marker using a marker swap plasmid M3925 (*trp1::kanMX3*) digested with BamHI (Voth, Jiang et al. 2003).

Table 4.1. Yeast strains used in this study.

Strain	Descriptive name	Genotype	Source or reference
IRA029	*ATG9-3GFP*	SEY6210 *ATG9-3GFP::URA3*	(Monastyrska, He et al. 2008)
KTY148	*ATG16-GFP*	SEY6210 *ATG16-GFP::KAN*	This study
KTY162	*atg18Δ ATG16-GFP*	SEY6210 *atg18Δ::HIS3 ATG16-GFP::KAN*	This study
KTY164	*atg21Δ ATG16-GFP*	SEY6210 *atg21Δ::TRP1 ATG16-GFP::KAN*	This study
SEY6210	WT	*MATα ura3–52 leu2–3,112 his3-Δ200 trp1-Δ901 lys2–801 suc2-Δ9 GAL*	(Robinson, Klionsky et al. 1988)

TN121	WT	*MATa leu2-3,112 trp1 ura3-52 pho8::pho8Δ60 pho13Δ::URA3*	(Noda, Matsuura et al. 1995)
UNY23	*atg1Δ ATG9-3GFP*	IRA029 *atg1Δ::HIS3*	(Monastyrska, He et al. 2008)
YCY13	*atg21Δ ATG9-3GFP*	SEY6210 *ATG9-3GFP::URA3 atg21Δ:: HIS3*	This study
YCY14	*atg21Δ*	SEY6210 *atg21Δ::HIS3*	This study
YCY26	*atg18Δ*	SEY6210 *atg18Δ::KAN*	This study
YCY28	*atg18Δ atg21Δ*	SEY6210 *atg18Δ::KAN atg21Δ::HIS3*	This study
YCY31	*atg18Δ atg21Δ*	TN121 *atg18Δ atg21Δ*	This study
YCY35	*atg18Δ ATG9-3GFP*	SEY6210 *atg18Δ::KAN ATG9-3GFP::URA3*	This study
YCY50	*atg18Δ atg21Δ ATG9-3GFP*	SEY6210 *atg18Δ::KAN ATG9-3GFP::URA3 atg21Δ::HIS3*	This study
YCY66	*atg18Δ atg21Δ ATG16-GFP*	SEY6210 *atg18Δ::HIS3 ATG16-GFP::KAN atg21Δ::URA3*	This study
YCY79	*atg4Δ::LEU ATG8-GFP*	SEY6210 *atg4Δ::LEU ATG8-GFP::LYS*	This study
YCY146	MKO (*ATG3 GFP-ATG8ΔR*)	SEY6210 *atg1Δ, 2Δ, 4Δ, 5Δ, 6Δ, 7Δ, 8Δ, 9Δ, 10Δ, 11Δ, 12Δ, 13Δ, 14Δ, 16Δ, 17Δ, 18Δ, 19Δ, 20Δ, 21Δ, 23Δ, 24Δ, 27Δ, 29Δ GFP-ATG8ΔR::TRP1*	This study
YCY153	MKO (*ATG3 GFP-ATG8ΔR*)	YCY146 *GFP-ATG8ΔR::TRP1::KAN*	This study
YCY155	MKO (*ATG3 ATG8-GFP*)	YCY137 *ATG8-GFP::LYS*	This study
YCY156	MKO (*ATG3 GFP-ATG8ΔR*)	YCY153 *ATG8-GFP::LYS*	This study

Yeast cells were grown in rich medium (YPD; 1% yeast extract, 2% peptone, 2% glucose) or synthetic minimal medium (SMD; 0.67% yeast nitrogen base, 2% glucose, supplemented with the appropriate amino acids and vitamins). Cells were starved in synthetic medium lacking nitrogen (SD-N; 0.17% yeast nitrogen base without amino acids and ammonium sulfate, 2% glucose).

Plasmids

For constructing pATG18-PA(314) and pATG21-PA(314), the full-length *ATG18* and *ATG21* ORFs with 1 kb endogenous promoter were amplified from genomic DNA and cloned into the XhoI and XmaI sites of pNopPA(314) (He, Song et al. 2006). To clone pATG21-GFP(416), the full-length *ATG21* ORF with 1 kb endogenous promoter was PCR-amplified and cloned into the NotI and BamHI sites of pATG9-GFP(416) (pAPG9GFP(416)) (Noda, Kim et al. 2000). pATG18-GFP(416) was cloned by a two-step process: A silent mutation was first introduced into pATG18-PA(314) to remove an internal BamHI site in the *ATG18* ORF, leading to pATG18ΔBamHI-PA(314); the full-length *ATG18* ORF with 1 kb endogenous promoter was PCR-amplified from pATG18ΔBamHI-PA(314) and cloned into the same sites of pATG9-GFP(416). The full-length *ATG21* ORF with 1 kb endogenous promoter and 1 kb terminator was amplified from genomic DNA and cloned as a BamHI and SalI fragment into pRS415 or pRS414 to generate pATG21(415) or pATG21(414). PCR-based site-directed mutagenesis was used to substitute two arginines (RR) with two lysines (KK) in the corresponding wild-type plasmids, leading to pATG18FKKG-PA(314), pATG21FKKG-PA(314), pATG21FKKG-GFP(416), pATG18FKKG-GFP(416) and pATG21FKKG(415).

pATG7-ATG10-ATG5-HA-ATG12(416), pATG16(415), and pATG16-ATG4(415) were made based on plasmids pATG7(414), pATG10(414), pATG5(416), pHA-ATG12(416), pATG16(416),and pATG4(414) (Cao, Cheong et al. 2008). For constructing pATG7-ATG10-ATG5-HA-ATG12(416), an *ATG7* fragment from pATG7(414) was first cloned into the XmaI site of pRS416 to generate pATG7(416); *ATG10*, *ATG5* and *HA-ATG12* fragments were cloned sequentially into pATG7(416) using a single restriction enzyme each time. KpnI was used to introduce *ATG10*, BamHI for *ATG5*, and XhoI for *HA-ATG12*. pATG16(415) was constructed from pATG16(416) by replacing its backbone with that of pRS415 using PvuI. An *ATG4* fragment digested with SacI from pATG4(414) was cloned into the pATG16(415) vector linearized with the same enzyme, resulting in pATG16-ATG4(415).

To clone the multi-gene plasmids pATG18-ATG2(413), and pATG23-ATG27-ATG6-ATG14(414), single-gene plasmids expressing an individual *ATG* gene with its endogenous promoter and terminator regions were first constructed and tested for functionality. XbaI and SacI sites were used to clone pATG18(413), XhoI and XmaI for pATG2(413), XhoI for pATG23(414), KpnI for pATG27(414), SacI and BamHI for pATG6(414), and SalI and PstI for pATG14(414). The promoter, ORF and terminator inserts were then removed from the single-gene plasmids and cloned sequentially to generate plasmids pATG18-ATG2(413), and pATG23-ATG27-ATG6-ATG14(414). To generate pATG6-ATG14(414), a fragment containing both the *ATG6* and the *ATG14* inserts was PCR-amplified from pATG23-ATG27-ATG6-ATG14(414) and cloned into the NotI site of pRS414. The same fragment was inserted into the NotI site of pATG21(414), leading to pATG21-ATG6-ATG14(414).

pATG8-GFP(416) has been described previously (Kim, Huang et al. 2001). pATG8-GFP bearing the endogenous promoter of *ATG8* was digested using NotI and HindIII and a fragment containing the promoter of *ATG8* and the *ATG8* ORF fused to GFP were cloned into the pRS307 vector digested with the same enzymes. pAtg8-GFP(307) was linearized with BglII, and integrated into the lys2–801 locus.

The plasmids pATG9-3xGFP(306) (Monastyrska, He et al. 2008), M3925 (*trp1::kanMX3*) (Voth, Jiang et al. 2003) and pRS vectors (Sikorski and Hieter 1989) have been described previously. pGFP-ATG8(316) was a kind gift from Dr. Yoshinori Ohsumi (National Institute for Basic Biology, Okazaki, Japan).

Fluorescence microscopy

Fluorescence microscopy was performed as described previously (Cao, Cheong et al. 2008). Yeast cells were grown in YPD or SMD lacking the appropriate auxotrophic amino acids to mid-log phase before imaging. For starvation, cells were shifted to SD-N for 4 h. Images were captured with a 100× objective lens for all microscopy experiments except for those to localize Atg16-GFP, in which a 60× objective lens was used. Fluorescence signals were visualized on a fluorescence microscope (IX71; Olympus). The images were captured by a CCD camera (Photometrics CoolSNAP HQ; Roper Scientific) and deconvolved using DeltaVision software (Applied Precision). For the images showing the localization of Atg9-3xGFP, a stack of images covering the entire cell was collected, and a projection of the stack of images was created using the sum of signal intensities.

Other assays

The protein extraction, western blotting, prApe1 maturation, GFP-Atg8 processing and alkaline phosphatase (Pho8Δ60) assays have been described previously (Noda, Matsuura et al. 1995; Shintani, Huang et al. 2002).

References

Achsel, T., K. Ahrens, et al. (1998). "The human U5-220kD protein (hPrp8) forms a stable RNA-free complex with several U5-specific proteins, including an RNA unwindase, a homologue of ribosomal elongation factor EF-2, and a novel WD-40 protein." Mol Cell Biol **18**(11): 6756-66.

Barth, H., K. Meiling-Wesse, et al. (2001). "Autophagy and the cytoplasm to vacuole targeting pathway both require Aut10p." FEBS Lett **508**(1): 23-8.

Barth, H., K. Meiling-Wesse, et al. (2002). "Mai1p is essential for maturation of proaminopeptidase I but not for autophagy." FEBS Lett **512**(1-3): 173-9.

Burd, C. G. and S. D. Emr (1998). "Phosphatidylinositol(3)-phosphate signaling mediated by specific binding to RING FYVE domains." Mol Cell **2**(1): 157-62.

Burda, P., S. M. Padilla, et al. (2002). "Retromer function in endosome-to-Golgi retrograde transport is regulated by the yeast Vps34 PtdIns 3-kinase." J Cell Sci **115**(20): 3889-900.

Cao, Y., H. Cheong, et al. (2008). "In vivo reconstitution of autophagy in *Saccharomyces cerevisiae*." J Cell Biol **182**(4): 703-13.

Denisenko, O. N. and K. Bomsztyk (1997). "The product of the murine homolog of the Drosophila extra sex combs gene displays transcriptional repressor activity." Mol Cell Biol **17**(8): 4707-17.

Dove, S. K., R. C. Piper, et al. (2004). "Svp1p defines a family of phosphatidylinositol 3,5-bisphosphate effectors." EMBO J **23**(9): 1922-33.

Efe, J. A., R. J. Botelho, et al. (2007). "Atg18 regulates organelle morphology and Fab1 kinase activity independent of its membrane recruitment by phosphatidylinositol 3,5-bisphosphate." Mol Biol Cell **18**(11): 4232-44.

Gillooly, D. J., I. C. Morrow, et al. (2000). "Localization of phosphatidylinositol 3-phosphate in yeast and mammalian cells." EMBO J **19**(17): 4577-88.

Guan, J., P. E. Stromhaug, et al. (2001). "Cvt18/Gsa12 is required for cytoplasm-to-vacuole transport, pexophagy, and autophagy in *Saccharomyces cerevisiae* and *Pichia pastoris*." Mol Biol Cell **12**(12): 3821-38.

Gueldener, U., J. Heinisch, et al. (2002). "A second set of loxP marker cassettes for Cre-mediated multiple gene knockouts in budding yeast." Nucleic Acids Res **30**(6): e23.

Hanada, T., N. N. Noda, et al. (2007). "The Atg12-Atg5 conjugate has a novel E3-like activity for protein lipidation in autophagy." J Biol Chem **282**(52): 37298-302.

He, C., H. Song, et al. (2006). "Recruitment of Atg9 to the preautophagosomal structure by Atg11 is essential for selective autophagy in budding yeast." J Cell Biol **175**(6): 925-35.

Hu, Y., M. A. Benedict, et al. (1998). "Bcl-XL interacts with Apaf-1 and inhibits Apaf-1-dependent caspase-9 activation." Proc Natl Acad Sci U S A **95**(8): 4386-91.

Huang, W.-P., S. V. Scott, et al. (2000). "The itinerary of a vesicle component, Aut7p/Cvt5p, terminates in the yeast vacuole via the autophagy/Cvt pathways." J Biol Chem **275**(8): 5845-51.

Ichimura, Y., Y. Imamura, et al. (2004). "*In vivo* and *in vitro* reconstitution of Atg8 conjugation essential for autophagy." J Biol Chem **279**(39): 40584-92.
Ichimura, Y., T. Kirisako, et al. (2000). "A ubiquitin-like system mediates protein lipidation." Nature **408**(6811): 488-92.
Kametaka, S., T. Okano, et al. (1998). "Apg14p and Apg6/Vps30p form a protein complex essential for autophagy in the yeast, *Saccharomyces cerevisiae*." J Biol Chem **273**(35): 22284-91.
Kamura, T., S. Sato, et al. (1998). "The Elongin BC complex interacts with the conserved SOCS-box motif present in members of the SOCS, ras, WD-40 repeat, and ankyrin repeat families." Genes Dev **12**(24): 3872-81.
Katzmann, D. J., C. J. Stefan, et al. (2003). "Vps27 recruits ESCRT machinery to endosomes during MVB sorting." J Cell Biol **162**(3): 413-23.
Kihara, A., T. Noda, et al. (2001). "Two distinct Vps34 phosphatidylinositol 3-kinase complexes function in autophagy and carboxypeptidase Y sorting in *Saccharomyces cerevisiae*." J Cell Biol **152**(3): 519-30.
Kim, J., W.-P. Huang, et al. (2001). "Membrane recruitment of Aut7p in the autophagy and cytoplasm to vacuole targeting pathways requires Aut1p, Aut2p, and the autophagy conjugation complex." J Cell Biol **152**(1): 51-64.
Kim, J., W.-P. Huang, et al. (2002). "Convergence of multiple autophagy and cytoplasm to vacuole targeting components to a perivacuolar membrane compartment prior to *de novo* vesicle formation." J Biol Chem **277**(1): 763-73.
Kim, J., Y. Kamada, et al. (2001). "Cvt9/Gsa9 functions in sequestering selective cytosolic cargo destined for the vacuole." J Cell Biol **153**(2): 381-96.
Kirisako, T., M. Baba, et al. (1999). "Formation process of autophagosome is traced with Apg8/Aut7p in yeast." J Cell Biol **147**(2): 435-46.
Kirisako, T., Y. Ichimura, et al. (2000). "The reversible modification regulates the membrane-binding state of Apg8/Aut7 essential for autophagy and the cytoplasm to vacuole targeting pathway." J Cell Biol **151**(2): 263-76.
Klionsky, D. J., R. Cueva, et al. (1992). "Aminopeptidase I of *Saccharomyces cerevisiae* is localized to the vacuole independent of the secretory pathway." J Cell Biol **119**(2): 287-99.
Krick, R., S. Henke, et al. (2008). "Dissecting the localization and function of Atg18, Atg21 and Ygr223c." Autophagy **4**(7): 896-910.
Krick, R., J. Tolstrup, et al. (2006). "The relevance of the phosphatidylinositolphosphat-binding motif FRRGT of Atg18 and Atg21 for the Cvt pathway and autophagy." FEBS Lett **580**(19): 4632-8.
Legakis, J. E., W.-L. Yen, et al. (2007). "A cycling protein complex required for selective autophagy." Autophagy **3**(5): 422-32.
Li, D. and R. Roberts (2001). "WD-repeat proteins: structure characteristics, biological function, and their involvement in human diseases." Cell Mol Life Sci **58**(14): 2085-97.
Li, Q. and K. A. Suprenant (1994). "Molecular characterization of the 77-kDa echinoderm microtubule-associated protein. Homology to the beta-transducin family." J Biol Chem **269**(50): 31777-84.

Longtine, M. S., A. McKenzie III, et al. (1998). "Additional modules for versatile and economical PCR-based gene deletion and modification in *Saccharomyces cerevisiae*." Yeast **14**(10): 953-61.
Meiling-Wesse, K., H. Barth, et al. (2004). "Atg21 is required for effective recruitment of Atg8 to the preautophagosomal structure during the Cvt pathway." J Biol Chem **279**(36): 37741-50.
Mizushima, N., B. Levine, et al. (2008). "Autophagy fights disease through cellular self-digestion." Nature **451**(7182): 1069-75.
Mizushima, N., T. Noda, et al. (1999). "Apg16p is required for the function of the Apg12p-Apg5p conjugate in the yeast autophagy pathway." EMBO J **18**(14): 3888-96.
Mizushima, N., T. Noda, et al. (1998). "A protein conjugation system essential for autophagy." Nature **395**(6700): 395-8.
Monastyrska, I., C. He, et al. (2008). "Arp2 links autophagic machinery with the actin cytoskeleton." Mol Biol Cell **19**(5): 1962-75.
Munn, A. L. and H. Riezman (1994). "Endocytosis is required for the growth of vacuolar H(+)-ATPase-defective yeast: identification of six new *END* genes." J Cell Biol **127**(2): 373-86.
Noda, T., J. Kim, et al. (2000). "Apg9p/Cvt7p is an integral membrane protein required for transport vesicle formation in the Cvt and autophagy pathways." J Cell Biol **148**(3): 465-80.
Noda, T., A. Matsuura, et al. (1995). "Novel system for monitoring autophagy in the yeast *Saccharomyces cerevisiae*." Biochem Biophys Res Commun **210**(1): 126-32.
Obara, K., T. Noda, et al. (2008). "Transport of phosphatidylinositol 3-phosphate into the vacuole via autophagic membranes in *Saccharomyces cerevisiae*." Genes Cells **13**(6): 537-47.
Obara, K., T. Sekito, et al. (2008). "The Atg18-Atg2 complex is recruited to autophagic membranes via phosphatidylinositol 3-phosphate and exerts an essential function." J Biol Chem **283**(35): 23972-80.
Obara, K., T. Sekito, et al. (2006). "Assortment of phosphatidylinositol 3-kinase complexes--Atg14p directs association of complex I to the pre-autophagosomal structure in *Saccharomyces cerevisiae*." Mol Biol Cell **17**(4): 1527-39.
Proikas-Cezanne, T., S. Ruckerbauer, et al. (2007). "Human WIPI-1 puncta-formation: a novel assay to assess mammalian autophagy." FEBS Lett **581**(18): 3396-404.
Reggiori, F., K. A. Tucker, et al. (2004). "The Atg1-Atg13 complex regulates Atg9 and Atg23 retrieval transport from the pre-autophagosomal structure." Dev Cell **6**(1): 79-90.
Robinson, J. S., D. J. Klionsky, et al. (1988). "Protein sorting in *Saccharomyces cerevisiae*: isolation of mutants defective in the delivery and processing of multiple vacuolar hydrolases." Mol Cell Biol **8**(11): 4936-48.
Schu, P. V., K. Takegawa, et al. (1993). "Phosphatidylinositol 3-kinase encoded by yeast *VPS34* gene essential for protein sorting." Science **260**(5104): 88-91.
Shintani, T., W.-P. Huang, et al. (2002). "Mechanism of cargo selection in the cytoplasm to vacuole targeting pathway." Dev Cell **3**(6): 825-37.

Sikorski, R. S. and P. Hieter (1989). "A system of shuttle vectors and yeast host strains designed for efficient manipulation of DNA in *Saccharomyces cerevisiae*." Genetics **122**(1): 19-27.

Smith, T. F., C. Gaitatzes, et al. (1999). "The WD repeat: a common architecture for diverse functions." Trends Biochem Sci **24**(5): 181-5.

Stromhaug, P. E., F. Reggiori, et al. (2004). "Atg21 is a phosphoinositide binding protein required for efficient lipidation and localization of Atg8 during uptake of aminopeptidase I by selective autophagy." Mol Biol Cell **15**(8): 3553-66.

Suzuki, K., T. Kirisako, et al. (2001). "The pre-autophagosomal structure organized by concerted functions of *APG* genes is essential for autophagosome formation." EMBO J **20**(21): 5971-81.

Suzuki, K., Y. Kubota, et al. (2007). "Hierarchy of Atg proteins in pre-autophagosomal structure organization." Genes Cells **12**(2): 209-18.

Tanida, I., N. Mizushima, et al. (1999). "Apg7p/Cvt2p: A novel protein-activating enzyme essential for autophagy." Mol Biol Cell **10**(5): 1367-79.

Tanida, I., E. Tanida-Miyake, et al. (2002). "Human Apg3p/Aut1p homologue is an authentic E2 enzyme for multiple substrates, GATE-16, GABARAP, and MAP-LC3, and facilitates the conjugation of hApg12p to hApg5p." J Biol Chem **277**(16): 13739-44.

Tanida, I., E. Tanida-Miyake, et al. (2001). "The human homolog of *Saccharomyces cerevisiae* Apg7p is a Protein-activating enzyme for multiple substrates including human Apg12p, GATE-16, GABARAP, and MAP-LC3." J Biol Chem **276**(3): 1701-6.

Voth, W. P., Y. W. Jiang, et al. (2003). "New 'marker swap' plasmids for converting selectable markers on budding yeast gene disruptions and plasmids." Yeast **20**(11): 985-93.

Xie, Z., U. Nair, et al. (2008). "Atg8 controls phagophore expansion during autophagosome formation." Mol Biol Cell **19**(8): 3290-8.

CHAPTER 5

Atg26 is not involved in autophagy-related pathways in *Saccharomyces cerevisiae*

Abstract

Autophagy is a degradative pathway conserved among eukaryotes. It is a major route for degradation of long-lived proteins and entire organelles, such as peroxisomes. Atg26, a sterol glucosyltransferase, is specifically required for micro- and macropexophagy, but not for starvation-induced bulk autophagy in *Pichia pastoris*. Here we study the requirement of *Saccharomyces cerevisiae* Atg26 in the Cvt pathway, nonspecific autophagy and pexophagy. Our results show that the *S. cerevisiae atg26Δ* strain is not defective in prApe1 maturation, macroautophagy or peroxisome degradation, in contrast to the situation seen in *Pichia pastoris*. These studies highlight the importance of examining mutants in multiple organisms.

Introduction

Eukaryotic cells utilize autophagy to adapt to environmental changes such as alterations in available nutrients or other types of stress. Microautophagy and macroautophay are two mechanisms for sequestering cytoplasmic components and organelles (Klionsky 2005). Microautophagy involves the engulfment of cytoplasm and organelles by the lysosomal/vacuolar membrane followed by their internalization and degradation. Macroautophagy is a vesicular process involving the formation of double-membrane vesicles called autophagosomes that sequester cytosol and organelles. The autophagosomes then fuse with the lysosome/vacuole and release the inner single-membrane vesicle or autophagic body into the lysosome/vacuole lumen, resulting in the breakdown and subsequent recycling of the cargo. Although these processes are generally considered to be nonselective, there are selective types of autophagy, such as the cytoplasm to vacuole targeting (Cvt) pathway and pexophagy. The Cvt pathway is a biosynthetic pathway for delivery of the resident vacuolar hydrolases aminopeptidase 1 (Ape1) and α-mannosidase (Ams1) (Yorimitsu and Klionsky 2005). Pexophagy, or peroxisome degradation, may occur through selective micro- or macroautophagy as well as nonselective autophagy (Dunn, Cregg et al. 2005). There is extensive mechanistic and genetic overlap among these different autophagic pathways, and several pexophagy genes from *Pichia pastoris* have been found to have orthologues involved in Cvt and nonspecific autophagy in *Saccharomyces cerevisiae.*

A sterol glucosyltransferase, Atg26 (Ugt51/Paz4), is specifically required for micro- and macropexophagy, but not for starvation-induced macroautophagy in *Pichia*

pastoris (Oku, Warnecke et al. 2003). Upon induction of micropexophagy, it localizes to a cup-shaped membrane apparatus, the micropexophagic membrane apparatus (MIPA) depending on its GRAM (glucosyltransferase, Rab-like GTPase activators, and myotubularins) domain (Oku, Warnecke et al. 2003). PpAtg26 is also required for the formation of the MIPA structure (Yamashita, Oku et al. 2006). The three domains of PpAtg26, pleckstrin homology (PH), GRAM and catalytic UDP-glucosyl transferase (UDPGT) domains, are all essential for microautophagy (Oku, Warnecke et al. 2003). However, in the alkane-utilizing yeast *Yarrowia lipolytica*, it is not required for pexophagy (Stasyk, Nazarko et al. 2003). Because the *S. cerevisiae* Atg26 protein (ScAtg26) possesses all three, PH, GRAM, and UDPGT, domains, which share significant sequence identities, 46%, 43.3%, and 62.5% respectively, with those in PpAtg26, we were interested to know whether the ScAtg26 function was conserved. In this study, we determined the involvement of ScAtg26 in the Cvt pathway, macroautophagy and pexophagy. Our results indicate that ScAtg26 is not required for any of these pathways in *S. cerevisiae*; its requirement for pexophagy might be unique to *P. pastoris*.

Results and discussions

The *S. cerevisiae atg26*Δ strain is not defective for the Cvt pathway.

The precursor form of the vacuolar resident hydrolase aminopeptidase 1 (prApe1) is synthesized in the cytosol and then delivered to the vacuole via the Cvt pathway under nutrient-rich conditions. The prApe1 is activated upon cleavage of its propeptide in the vacuolar lumen. We first examined the role of Atg26 in the Cvt pathway by monitoring prApe1 processing under rich conditions. As a control, we used *atg11*Δ cells, which are defective for the Cvt pathway. As expected, *atg11*Δ cells accumulated only the precursor form of Ape1, whereas the wild type cells showed almost complete maturation of prApe1 (Fig. 5.1A). In *atg26*Δ cells, prApe1 maturation was comparable with wild type, which indicates that Atg26 is not required for the Cvt pathway. We extended the analysis of the Cvt pathway by monitoring the localization of GFP-Ape1 in *atg26*Δ cells under rich conditions. Cells expressing GFP-Ape1 from its endogenous promoter were labeled with the dye FM 4-64 to stain the vacuole. In wild type cells, the GFP signal was concentrated in the vacuole lumen, in agreement with the localization of Ape1 as a resident vacuolar hydrolase (Fig. 5.1B). In contrast, in *atg1*Δ cells, GFP-Ape1 was arrested as a perivacuolar dot when the Cvt pathway was blocked; this location presumably corresponds with the phagophore assembly site/pre-autophagosomal structure. Similar to the result seen in wild type cells, GFP-Ape1 in *atg26*Δ cells was localized inside the vacuoles. Taken together, these results suggest that *S. cerevisiae* Atg26 is not required for the Cvt pathway.

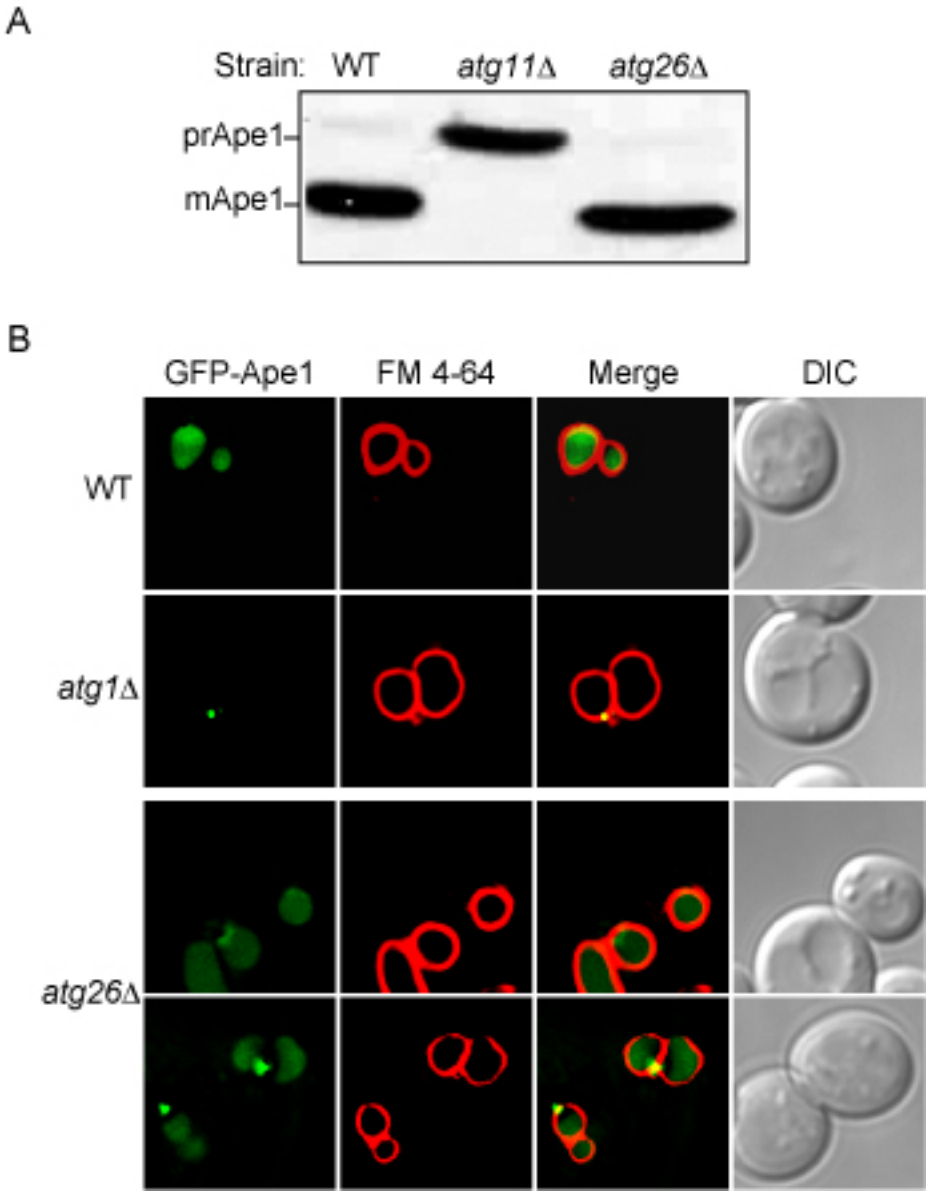

Figure 5.1. *atg26*Δ cells are not defective in the Cvt pathway. (A) Protein extracts from wild type (BY4742), *atg11*Δ and *atg26*Δ cells grown in rich condition were resolved by SDS-PAGE. Western blot was performed with anti-Ape1 antiserum. (B) Wild type, *atg1*Δ and *atg26*Δ cells expressing GFP-Ape1 under its own promoter were grown to mid-log phase, labeled with FM 4-64 and observed by fluorescence microscopy. DIC, differential interference contrast.

The ScAtg26 protein is not required for macroautophagy.

We next examined the role of Atg26 in macroautopahgy by an alkaline phosphatase assay. A truncated form of the vacuolar alkaline phosphatase (Pho8), Pho8Δ60, can only be transported to the vacuole through autophagy (Warnecke, Erdmann et al. 1999). Once delivered to the vacuole, it is proteolytically processed to remove a C-terminal propeptide, and acquires its phosphatase activity. Thus, we can quantitatively measure autophagic activity by monitoring Pho8Δ60-dependent alkaline phosphatase activity. Wild type, *atg1*Δ and *atg26*Δ cells were grown in rich medium to mid-log phase, and then shifted to starvation medium for four hours. As expected, after starvation there was an induction of alkaline phosphatase activity in wild type cells, whereas *atg1*Δ cells that are defective for autophagy did not show any increase in activity (Fig. 5.2). The *atg26*Δ cells exhibited an induction of Pho8Δ60-dependent alkaline phosphatase activity comparable with the wild type cells. This result suggests that *S. cerevisiae* Atg26 is not essential for macroautophagy, in agreement with the data from *P. pastoris* (Oku, Warnecke et al. 2003).

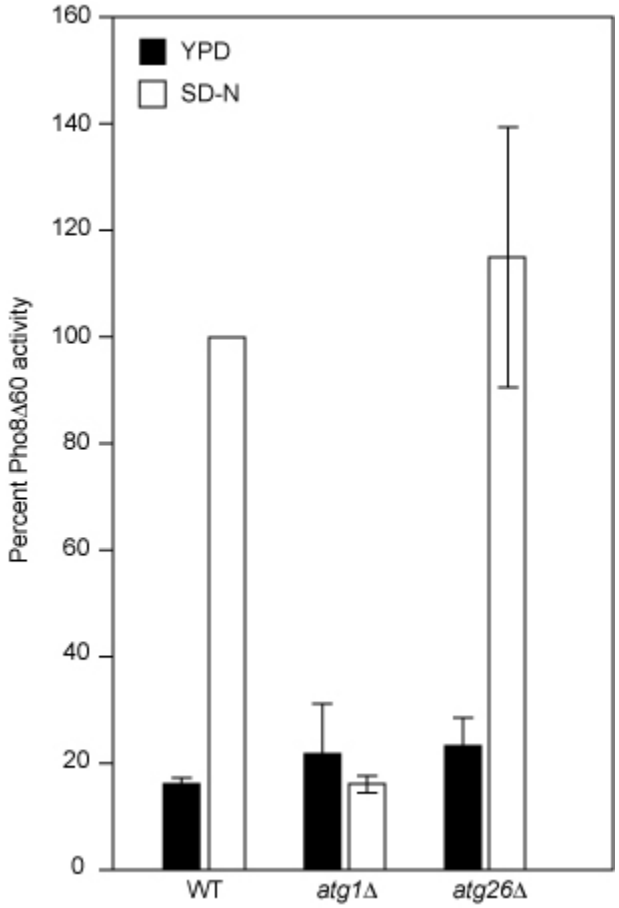

Figure5.2. Atg26 is not required for macroautophagy. Wild type (TN124), *atg1*Δ (HAY572) and *atg26*Δ (YCY6) cells were shifted from SMD to SD-N medium for 4 h. Autophagy was measured by the Pho8Δ60 assay as described in Materials and Methods. Activity in the wild type strain after starvation was set to 100% and activity in the other strains normalized relative to wild type. Error bars represent the S.D. from three separate experiments.

The *S. cerevisiae atg26*Δ strain does not display defects in pexophagy.

Our data indicated that ScAtg26 is not required for nonspecific autophagy or for one type of specific autophagy, the Cvt pathway; however, this protein is required for micro- and macropexophagy in *P. pastoris* (Oku, Warnecke et al. 2003). Accordingly, we examined the role of Atg26 in pexophagy. When the yeast *S. cerevisiae* is grown on oleic acid as the sole carbon source, peroxisome biogenesis is induced. When the culture is

shifted to a glucose-rich, nitrogen-limiting medium (SD-N), the excess peroxisomes become superfluous and degradation is induced. We first measured pexophagy in wild type, *atg11*Δ, and *atg26*Δ cells by following the degradation of the peroxisome matrix protein Fox3. *Atg11*Δ cells were blocked in Fox3 degradation (Fig. 5.3A). In contrast, Fox3 was degraded rapidly in wild type cells and was almost undetectable after six hours in SD-N. Degradation of Fox3 in *atg26*Δ cells was comparable with that seen in the wild type strain.

We next followed peroxisome degradation by visualizing green fluorescent protein (GFP) that was tagged with the peroxisome targeting sequence SKL (Fig. 5.3B). Wild type, *atg1*Δ, and *atg26*Δ cells expressing GFP-SKL were shifted from oleic acid to SD-N, and samples were taken every three hours for imaging. The number of peroxisomes was reduced significantly after the shift to SD-N in wild type and *atg26*Δ cells, whereas the level of peroxisomes in *atg1*Δ cells was largely unchanged. This result agrees with the data from the Fox3 degradation experiment. Together, these experiments indicate that *S. cerevisiae* Atg26 is not required for pexophagy.

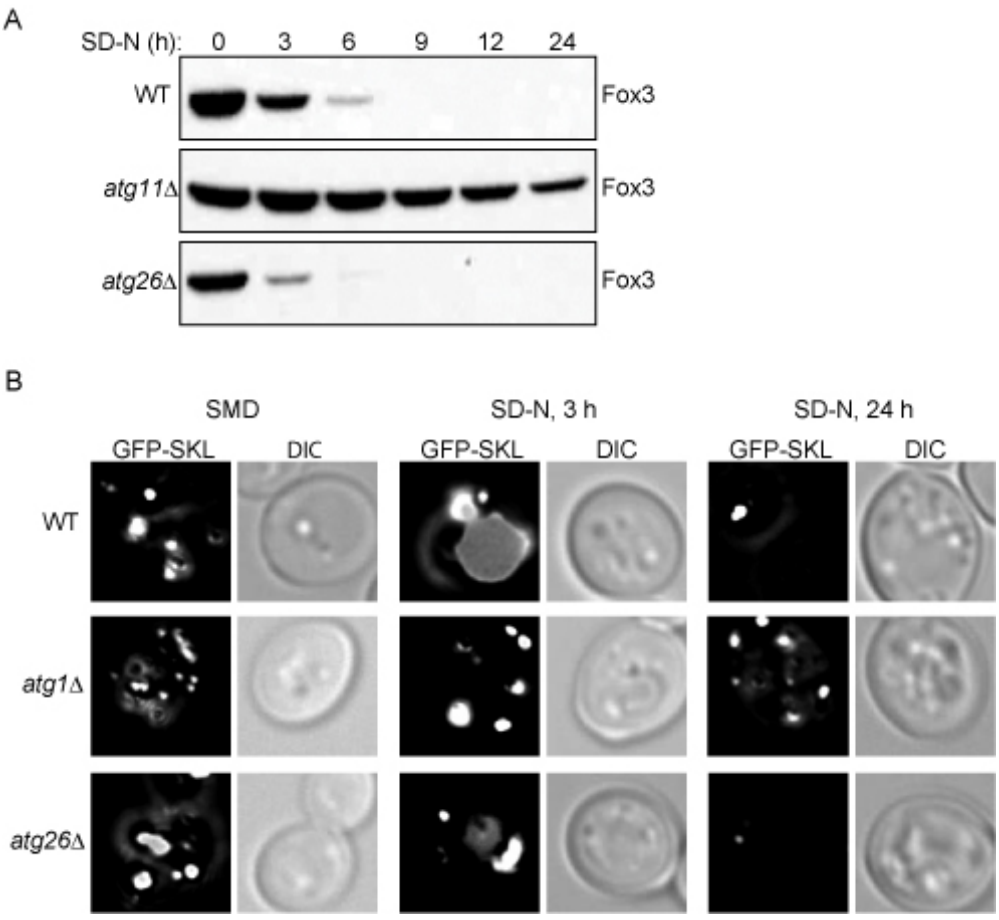

Figure 5.3. Atg26 is not required for pexophagy. (A) Wild type (BY4742), *atg11*Δ and *atg26*Δ cells were shifted from peroxisome-inducing oleic acid medium to SD-N for 24 h. Every 3 h, protein extracts were prepared and subjected to immunoblot analysis using anti-Fox3 antiserum. (B) Wild type, *atg1*Δ and *atg26*Δ cells expressing GFP-SKL were shifted from peroxisome-inducing oleic acid medium to SD-N for 24 h. At the indicated times, samples were taken and examined by fluorescence microscopy.

In this study, we reported that the *S. cerevisiae* protein Atg26 is not involved in the Cvt pathway, macroautophagy or pexophagy. It seems that the role of PpAtg26 in pexophagy is unique to *P. pastoris,* although the C-terminal UDP-glucosyl transferase domain has very high sequence identity between these two yeasts. It could be that the amount of sterol glucoside (SG) in *S. cerevisiae* is too low to have any effect on these autophagy-related pathways (Warnecke, Erdmann et al. 1999). SG synthesis is higher in

P. pastoris, and the SG content might influence MIPA formation and other membrane events in *P. pastoris,* which contributes to the involvement of PpAtg26 in pexophagy; however, the role of the *S. cerevisiae* Atg26 protein, remains to be elucidated.

Materials and methods

Strains, plasmids and media

The *S. cerevisiae* strains used in this study are listed in Table 5.1. Plasmids pRS315-GFP-APE1 and pCuGFP-SKL416 have been described previously (Guan, Stromhaug et al. 2001; Shintani, Huang et al. 2002).

Yeast strains were grown in YPD (1% yeast extract, 2% peptone, and 2% glucose) or synthetic minimal medium (SMD: 0.67% yeast nitrogen base, 2% glucose, and auxotrophic amino acids and vitamins as required). For nitrogen starvation, SD-N medium (0.17% yeast nitrogen base without ammonium sulfate, amino acids and 2% glucose) was used. Peroxisomes were induced by growth in oleic acid medium (YTO: 0.67% YNB, 0.1% Tween 40, and 0.1% oleic acid).

Table 5.1. Yeast strains used in this study.

Strain	Genotype	Source or reference
BY4742	*MATα his3*Δ *leu2*Δ *lys2*Δ *ura3*Δ	ResGen/Invitrogen (Carlsbad, CA)
*atg26*Δ	BY4742 *atg26*Δ*::KAN*	ResGen/Invitrogen
*atg11*Δ	BY4742 *atg11*Δ*::KAN*	ResGen/Invitrogen
*atg1*Δ	BY4742 *atg1*Δ*::KAN*	ResGen/Invitrogen
TN124	*MATa leu2-3,112 trp1 ura3-52*	(Abeliovich, Zhang et al. 2003)
	*Pho8::pho8*Δ*60 pho13*Δ*::LEU2*	
HAY572	TN124 *atg1*Δ*::URA3*	(Noda, Matsuura et al. 1995)
YCY6	TN124 *atg26*Δ*::URA3*	This study

Fluorescence microscopy

Yeast cells were grown to mid-log phase in the appropriate medium before imaging. To label the vacuolar membrane, cells were stained with 0.8 mM FM 4-64 (Molecular Probes, Eugene, OR) for 15 min. Cells were then washed and incubated in the same medium for 30 min. Fluorescence microscopy observation was performed as described previously (Cheong, Yorimitsu et al. 2005).

Alkaline phosphatase and pexophagy assays

The alkaline phosphatase (Pho8Δ60) and pexophagy assays were performed as described previously (Noda, Matsuura et al. 1995; Hutchins, Veenhuis et al. 1999).

References

Abeliovich, H., C. Zhang, et al. (2003). "Chemical genetic analysis of Apg1 reveals a non-kinase role in the induction of autophagy." Mol Biol Cell **14**(2): 477-90.

Cheong, H., T. Yorimitsu, et al. (2005). "Atg17 regulates the magnitude of the autophagic response." Mol Biol Cell **16**(7): 3438-53.

Dunn, W. A. Jr., J. M. Cregg, et al. (2005). "Pexophagy: the selective autophagy of peroxisomes." Autophagy **1**(2): 75-83.

Guan, J., P. E. Stromhaug, et al. (2001). "Cvt18/Gsa12 is required for cytoplasm-to-vacuole transport, pexophagy, and autophagy in *Saccharomyces cerevisiae* and *Pichia pastoris*." Mol Biol Cell **12**(12): 3821-38.

Hutchins, M. U., M. Veenhuis, et al. (1999). "Peroxisome degradation in *Saccharomyces cerevisiae* is dependent on machinery of macroautophagy and the Cvt pathway." J Cell Sci **112**: 4079-87.

Klionsky, D. J. (2005). "The molecular machinery of autophagy: unanswered questions." J Cell Sci **118**(1): 7-18.

Noda, T., A. Matsuura, et al. (1995). "Novel system for monitoring autophagy in the yeast *Saccharomyces cerevisiae*." Biochem Biophys Res Commun **210**(1): 126-32.

Oku, M., D. Warnecke, et al. (2003). "Peroxisome degradation requires catalytically active sterol glucosyltransferase with a GRAM domain." EMBO J **22**(13): 3231-41.

Shintani, T., W.-P. Huang, et al. (2002). "Mechanism of cargo selection in the cytoplasm to vacuole targeting pathway." Dev Cell **3**(6): 825-37.

Stasyk, O. V., T. Y. Nazarko, et al. (2003). "Sterol glucosyltransferases have different functional roles in *Pichia pastoris* and *Yarrowia lipolytica*." Cell Biol Int **27**(11): 947-52.

Warnecke, D., R. Erdmann, et al. (1999). "Cloning and functional expression of *UGT* genes encoding sterol glucosyltransferases from *Saccharomyces cerevisiae*, *Candida albicans*, *Pichia pastoris*, and *Dictyostelium discoideum*." J Biol Chem **274**(19): 13048-59.

Yamashita, S., M. Oku, et al. (2006). "PI4P-signaling pathway for the synthesis of a nascent membrane structure in selective autophagy." J Cell Biol **173**(5): 709-17.

Yorimitsu, T. and D. J. Klionsky (2005). "Autophagy: molecular machinery for self-eating." Cell Death Differ **12**: 1542-52.

CHAPTER 6

Conclusions and contributions

In this thesis, I have described my contributions to our understanding of multiple components and different steps of autophagy-related pathways using *Saccharomyces cerevisiae* as a model organism. First, I constructed a multiple *ATG* gene knockout (MKO) strain and further converted it into a yeast two-hybrid (Y2H) host strain, providing valuable tools for the autophagy research community. Second, using the MKO strain, I reconstituted different steps of autophagy *in vivo* and determined minimum components for cargo packaging, initial starvation-specific PAS assembly, Atg12–Atg5 conjugation and Atg8–PE conjugation. Third, I demonstrated the advantage of using the MKO strains for protein-protein interactions and complex formation. I helped further our understanding of Atg9 self-interaction in autophagy and identified a new interaction between Atg29 and Atg31. Fourth, I analyzed the physiological significance of the PtdIns(3)P-binding domains of two homologous proteins, Atg18 and Atg21, in the Cvt pathway and autophagy, and advanced our knowledge of the role of PtdIns(3)P-binding proteins in autophagy.

In Chapter 2, I have described the construction of the MKO stain and reconstitution of different steps in the Cvt pathway and autophagy. I knocked out 24 *ATG*

genes by multiple rounds of deletion and marker rescue using a *loxP-Cre* system (Gueldener, Heinisch et al. 2002; Cao, Cheong et al. 2008). The MKO strain YCY123 is defective in autophagy-related pathways, but not other vacuolar protein targeting pathways. The strain has no obvious unexpected defect other than a slight growth delay (Cao, Cheong et al. 2008). As a proof of principle, I first reconstituted a relatively well-characterized step in the Cvt pathway, the cargo recognition and packaging step. I reproduced the temporal order of this step: The adaptor protein Atg11 cannot colocalize with the cargo prApe1 without the receptor Atg19, and the three proteins are necessary and sufficient for this cargo packaging event. Beyond that, my data suggest that the cargo complex is not sufficient by itself to efficiently target to a perivacuolar site—additional Atg proteins may be required for the delivery of the cargo complex to the PAS (Cao, Cheong et al. 2008). With regard to starvation-specific PAS formation, we found that Atg17 is not sufficient for starvation-specific PAS formation; rather, the Atg17-interacting proteins Atg1 and Atg13, along with Atg17 appear to be required and sufficient for the initial PAS assembly during starvation. Other factors in the Atg1 complex, such as Atg11 and Atg29, further enhance assembly of the PAS (Cao, Cheong et al. 2008). Analyzing the initial starvation-specific PAS assembly can be viewed as part of a bigger project for determining the temporal order of protein arrival at the PAS, and the MKO strain will continue to be useful for studying PAS assembly.

Additionally, I reconstituted Atg12–Atg5 conjugation and Atg8–phosphatidylethanolamine (PE) conjugation *in vivo*, and provided new insights into the regulation of Atg8–PE by Atg4. Both conjugation systems have been reconstituted *in vitro*, so the minimum components have been identified for these reactions (Ichimura,

Imamura et al. 2004; Hanada, Noda et al. 2007; Shao, Gao et al. 2007; Fujioka, Noda et al. 2008). I wanted to know whether the *in vitro* analyses represented the *in vivo* situation. By adding back different combinations of Atg proteins to the MKO strain, I find that, consistent with the published data, Atg5, Atg7, Atg10 and Atg12 are necessary and sufficient for Atg12–Atg5 conjugation, and Atg16 facilitates formation of the conjugate. I further find that components in the Atg8–PE conjugation system also enhance the conjugation reaction, a connection that was not previously known (Cao, Cheong et al. 2008). Even more surprising, even when all eight of the proteins involved in both conjugation systems are expressed, Atg8–PE is still not detected (Cao, Cheong et al. 2008). In contrast, in wild-type cells where Atg4 is present, Atg8–PE is readily detectable in both growing and starvation conditions. However, when Atg4 is removed from the reaction (blocking deconjugation, and thus favoring accumulation of Atg–PE) in the MKO strain, and a modified Atg8ΔR is used to bypass the need for the initial cleavage by Atg4, a significant amount of Atg8–PE is detected. The presence of the Atg12–Atg5 conjugate further increases Atg8–PE formation in this setting (Cao, Cheong et al. 2008). Thus, Atg4 determines the balance between Atg8 and Atg8–PE and its activity is probably dysregulated in the MKO strain. A remaining question is what factor(s) may regulate Atg4 activity in terms of the timing and location of the deconjugation. The next set of experiments is to add back additional Atg components to restore Atg8–PE formation in the presence of Atg4. Also, the MKO system where Atg8ΔR, Atg3 and Atg7 are sufficient for Atg8–PE formation may be used as readout for studying the direct effects of environmental cues (e.g., drugs and oxidative stress) on Atg8 conjugation and ultimately on autophagy.

The MKO strain can also be used to reconstitute other steps or aspects of autophagy, such as Atg9 cycling. It might even be possible to heterogeneously express mammalian Atg proteins and reconstitute various aspects of autophagy. Besides reconstitution, the MKO strain can be a valuable tool for studying protein-protein interactions and complex formation. For example, it can be used to determine whether a particular interaction among Atg proteins is direct or not.

In Chapter 3, I took one step further in construction of the MKO strain. To supplement the existing MKO strain and make protein-protein interaction analyses faster and more efficient, I converted the MKO strain into a Y2H host strain. I knocked out *GAL4*, *GAL80* and *ADE2* open reading frames in strain YCY123, and integrated into the genome three reporter genes *GAL1-HIS3*, *GAL2-ADE2* and *GAL7-lacZ* by multiple rounds of plasmid-based integration and 5-FOA selected marker excision. I tested the three reporter genes with known interactions, such as Atg9 self-interaction and some of those that occur within the Atg1 complex. I find that consistent with data shown in Appendix A, Atg9 self-interacts in the absence of other Atg proteins by the Y2H approach. I also find that Atg1 interacts with Atg11, Atg13 and Atg17 similar to previous reports (Kamada, Funakoshi et al. 2000; Kim, Kamada et al. 2001; Cheong, Yorimitsu et al. 2005). Using the MKO Y2H strain, I identified a new "direct" (i.e., not involving other known Atg proteins) interaction between Atg29 and Atg31, and I further verified the interaction by coimmunoprecipitation using a wild-type strain and the MKO strain.

Atg29 and Atg31 are required for nonspecific autophagy, but not for the Cvt pathway (Kawamata, Kamada et al. 2005; Kabeya, Kawamata et al. 2007). Not much is known about the actual function of the two proteins except that they both interact with

Atg17 and function in the initial PAS assembly during starvation conditions (Kawamata, Kamada et al. 2005; Kabeya, Kawamata et al. 2007; Kawamata, Kamada et al. 2008). My data provided additional information about the presumed ternary complex, and further studies are needed to test whether Atg29-Atg17 and Atg31-Atg17 interactions are direct. To understand the significance of the Atg29-Atg31 interaction, we need to map interaction domains between the two, and a mutant that blocks their interaction may help us further characterize the two proteins. Using a set of intermediate MKO strains, I helped Dr. Heesun Cheong identify Atg proteins that are necessary and sufficient for Atg29 phosphorylation, and I found that Atg1, Atg13, Atg17 and Atg31 are the only Atg proteins required for this modification (data not shown). Meanwhile, during my analyses of the Atg29-Atg31 interaction, I found Atg31 is phosphorylated (data not shown). Currently, the significance of this phosphorylation is unknown. A mutant that blocks Atg31 phosphorylation, together with a mutant that loses Atg29-Atg31 interaction, will at least give us some information about the regulation of nonspecific autophagy.

In Chapter 4, I looked into the functions of Atg18, Atg21 and their PtdIns(3)P-binding FRRG motifs in autophagy and the Cvt pathway. Our results suggest that the PtdIns(3)P binding motifs of Atg18 and Atg21 can compensate for one another in the recruitment of Atg proteins that are dependent on PtdIns(3)P for their PAS localization, and in this manner allow autophagy to proceed. Using the MKO strain, we further found that Atg18 and Atg21 facilitate the recruitment of Atg8–PE to the PAS and protect it from Atg4-mediated cleavage.

With Dr. Usha Nair, we generated mutations within the FRRG motifs of Atg18 and Atg21 (FRRG to FKKG) and examined the effects of these mutations on the Cvt

pathway and autophagy. Consistent with previous analyses, cells in rich medium expressing Atg18^{FKKG} or Atg21^{FKKG} show a substantial or a complete block in the Cvt pathway, respectively, but single FKKG mutation has little or no effect on autophagy (Stromhaug, Reggiori et al. 2004; Krick, Tolstrup et al. 2006; Obara, Noda et al. 2008). Because Atg18 and Atg21 are homologous proteins, we considered the possibility that they, as well as their lipid-binding functions, are partially redundant. As predicted, *atg18*Δ *atg21*Δ cells expressing both of the Atg18^{FKKG} and Atg21^{FKKG} mutants show a severe block in autophagy. Our data suggest that although Atg18 and Atg21 are not functionally identical, wild-type PtdIns(3)P binding activity of at least one of these proteins is required for, and largely sufficient for, autophagy in the absence of the other.

As Atg18 and components of the PtdIns 3-kinase complex I have a role in the retrieval of Atg9 from the PAS (Reggiori, Tucker et al. 2004), we hypothesized that Atg21 might have a similar function and their PtdIns(3)P-binding FRRG motifs be required for the retrograde movement of Atg9. Our data suggest that the absence of Atg21 also results in an accumulation of Atg9 at the PAS in growing conditions. But the FKKG mutation on either Atg18 or Atg21 has little effect on Atg9 localization. Moreover, *atg18*Δ *atg21*Δ cells expressing Atg18^{FKKG} and Atg21^{FKKG} display normal Atg9 distribution in starvation conditions. Together, these data suggest that the autophagy block observed with the double FKKG mutants is not due to a defect in the steady state localization pattern of Atg9.

Rather, the autophagy defect in cells expressing Atg18^{FKKG} and Atg21^{FKKG} together corresponds to defects in the PAS recruitment of Atg16 and Atg8. In cells lacking Atg18, GFP-Atg8 cannot be released from the PAS, whereas in *atg21*Δ cells

GFP-Atg8 is not recruited to the PAS. On the other hand, a single FKKG mutation on Atg18 or Atg21 has no effect on GFP-Atg8 localization in starvation, but when combined, cells display a substantial defect both in Atg8 recruitment to, and release from, the PAS. We further examined the localization of Atg16, a protein required for PAS localization of Atg8 and dependent on the PtdIns 3-kinase components for its own localization, in the presence of both Atg18^{FKKG} and Atg21^{FKKG} mutants. We found that the PtdIns(3)P-binding motifs of Atg18 and Atg21 are important for efficient PAS localization of Atg16 in starvation. Altogether, our data supports a model where the PtdIns(3)P-binding motifs of Atg18 and Atg21 can somehow substitute for each other in recruiting Atg8 and Atg16 to the PAS efficiently under starvation conditions.

To gain further insights into the functional relationship between Atg18 and Atg21 with Atg8, we utilized the MKO strain. Instead of using western-blot to analyze Atg8–PE formation, we examined GFP-Atg8 puncta formation using fluorescence microscopy. Consistent with our Atg8–PE reconstitution data in Chapter 2 and recently published results on Atg16 by another group, we found that GFP-Atg8ΔR by itself is cytosolic; with Atg3, Atg7 Atg10 and Atg12 expressed, it is conjugated to PE and mislocalized to the vacuolar rim; additional expression of Atg16 recruits it to distinct punctate structures. However, when Atg4 is expressed in addition to all those components, Atg8–PE is no longer detected, and there is a similar disappearance of GFP-Atg8ΔR-containing puncta and vacuolar rim staining. So, an additional component(s) that regulates Atg4-mediated deconjugation of Atg8–PE and loss of GFP-Atg8 puncta are lacking in the above system.

Additional expression of Atg18-Atg2 and Atg21 (along with the PtdIns 3-kinase complex subunits Atg14 and Atg6) in the abovementioned system results in the

relocation of GFP-Atg8ΔR fluorescence back to punctate structures in the presence of Atg4, suggesting that Atg18-Atg2 and Atg21 somehow protect Atg8–PE from premature cleavage by Atg4. These data provide the first evidence for an *in vivo* mechanism that regulates the cleavage of Atg8–PE.

In Chapter 6, I have described the characterization of *S. cerevisiae* Atg26. Different from *Pichia pastoris* Atg26, which is essential for micro- and macropexophagy but not for starvation-induced autophagy, ScAtg26 is not required for the Cvt pathway, pexophagy or nonspecific autophagy. These studies highlight the importance of analyzing homologous proteins in different species.

In Appendix A, I have described a usage of the MKO strain in studying Atg9 self-interaction (He, Baba et al. 2008). Atg9-3GFP forms clusters in both wild-type and the MKO cells, suggesting a self-interaction exists. Then the MKO strain was used to show Atg9 self-interacts in the absence of other Atg proteins by coimmunoprecipitation. Mutational analyses reveal that amino acids 766 to 770 (LGYVC) are important for Atg9 self-interaction and its function in the Cvt pathway and autophagy. I introduced alanine mutations at each conserved residue in the region 766-770, and found that every mutation interferes with the function of Atg9 in the Cvt pathway and autophagy. Furthermore, the MKO strain allowed us to study the formation of the Atg9 complex. The Atg9Δ766-770 mutant is unable to self-interact, but still runs at a much higher molecular weight than a monomer in a native gel analysis, suggesting proteins other than Atg proteins may be stably present in the Atg9 complex.

In summary, most of the work presented in this thesis relates to a multiple *ATG* gene knockout strain, and furthers our understanding of various questions in autophagy

and the Cvt pathway. As the list of yeast *ATG* genes and other genes involved in autophagy expands, along with homologues of *ATG* genes being identified and characterized in higher eukaryotes, our understanding of the molecular mechanisms of autophagy and its implications will continue to grow and deepen. The work in *Saccharomyces cerevisiae* will continue to be the cornerstone and inspiration for autophagy research in mammalian systems.

References

Cao, Y., H. Cheong, et al. (2008). "In vivo reconstitution of autophagy in *Saccharomyces cerevisiae*." J Cell Biol **182**(4): 703-13.

Cheong, H., T. Yorimitsu, et al. (2005). "Atg17 regulates the magnitude of the autophagic response." Mol Biol Cell **16**(7): 3438-53.

Fujioka, Y., N. N. Noda, et al. (2008). "In vitro reconstitution of plant Atg8 and Atg12 conjugation systems essential for autophagy." J Biol Chem **283**(4): 1921-8.

Gueldener, U., J. Heinisch, et al. (2002). "A second set of loxP marker cassettes for Cre-mediated multiple gene knockouts in budding yeast." Nucleic Acids Res **30**(6): e23.

Hanada, T., N. N. Noda, et al. (2007). "The Atg12-Atg5 conjugate has a novel E3-like activity for protein lipidation in autophagy." J Biol Chem **282**(52): 37298-302.

He, C., M. Baba, et al. (2008). "Self-interaction is critical for Atg9 transport and function at the phagophore assembly site during autophagy." Mol Biol Cell **19**(12): 5506-16.

Ichimura, Y., Y. Imamura, et al. (2004). "*In vivo* and *in vitro* reconstitution of Atg8 conjugation essential for autophagy." J Biol Chem **279**(39): 40584-92.

Kabeya, Y., T. Kawamata, et al. (2007). "Cis1/Atg31 is required for autophagosome formation in *Saccharomyces cerevisiae*." Biochem Biophys Res Commun **356**(2): 405-10.

Kamada, Y., T. Funakoshi, et al. (2000). "Tor-mediated induction of autophagy via an Apg1 protein kinase complex." J Cell Biol **150**(6): 1507-13.

Kawamata, T., Y. Kamada, et al. (2008). "Organization of the pre-autophagosomal structure responsible for autophagosome formation." Mol Biol Cell **19**(5): 2039-50

Kawamata, T., Y. Kamada, et al. (2005). "Characterization of a novel autophagy-specific gene, *ATG29*." Biochem Biophys Res Commun **338**(4): 1884-9.

Kim, J., Y. Kamada, et al. (2001). "Cvt9/Gsa9 functions in sequestering selective cytosolic cargo destined for the vacuole." J Cell Biol **153**(2): 381-96.

Krick, R., J. Tolstrup, et al. (2006). "The relevance of the phosphatidylinositolphosphat-binding motif FRRGT of Atg18 and Atg21 for the Cvt pathway and autophagy." FEBS Lett **580**(19): 4632-8.

Obara, K., T. Noda, et al. (2008). "Transport of phosphatidylinositol 3-phosphate into the vacuole via autophagic membranes in *Saccharomyces cerevisiae*." Genes Cells **13**(6): 537-47.

Reggiori, F., K. A. Tucker, et al. (2004). "The Atg1-Atg13 complex regulates Atg9 and Atg23 retrieval transport from the pre-autophagosomal structure." Dev Cell **6**(1): 79-90.

Shao, Y., Z. Gao, et al. (2007). "Stimulation of ATG12-ATG5 conjugation by ribonucleic acid." Autophagy **3**(1): 10-6.

Stromhaug, P. E., F. Reggiori, et al. (2004). "Atg21 is a phosphoinositide binding protein required for efficient lipidation and localization of Atg8 during uptake of aminopeptidase I by selective autophagy." Mol Biol Cell **15**(8): 3553-66.

Appendix A

Self-interaction is critical for Atg9 transport and function at the phagophore assembly site during autophagy

Abstract

Autophagy is the degradation of a cell's own components within lysosomes (or the analogous yeast vacuole), and its malfunction contributes to a variety of human diseases. Atg9 is the sole integral membrane protein required in formation of the initial sequestering compartment, the phagophore, and is proposed to play a key role in membrane transport; the phagophore presumably expands by vesicular addition to form a complete autophagosome. It is not clear through what mechanism Atg9 functions at the phagophore assembly site (PAS). Here we report that Atg9 molecules self-associate independently of other known autophagy proteins in both nutrient-rich and starvation conditions. Mutational analyses reveal that self-interaction is critical for anterograde transport of Atg9 to the PAS. The ability of Atg9 to self-interact is required for both selective and non-selective autophagy at the step of phagophore expansion at the PAS. Our results support a model in which Atg9 multimerization facilitates membrane flow to the PAS for phagophore formation.

Introduction

Autophagic degradation of unneeded or damaged cellular components is essential for various cellular functions including proper homeostasis. Along these lines, the malfunction of autophagy is implicated in a variety of diseases, including cancer, neurodegeneration, cardiac disorders and pathogen infection (Shintani and Klionsky 2004). During autophagy, cytosolic proteins and organelles are engulfed into a double-membrane vesicle, the autophagosome, which then fuses with a lysosome (or the vacuole in fungi and plants) where its cargos are degraded. The autophagy-related (Atg) protein Atg9 plays a central role in the nucleation step during autophagosome formation in eukaryotes ranging from yeast to mammals (Noda, Kim et al. 2000; Young, Chan et al. 2006). Being the only identified integral membrane protein that is absolutely required in autophagosome formation, Atg9 is proposed to be the "carrier" of lipids to the phagophore assembly site (PAS, also known as the preautophagosomal structure) (Kim, Huang et al. 2002). Atg9 is absent from the completed autophagosomes, suggesting that the protein is retrieved upon vesicle completion. Previous work done in the yeast *Saccharomyces cerevisiae* has shown that Atg9 interacts with multiple autophagy-related proteins via its two cytosol-facing termini (Reggiori, Shintani et al. 2005; He, Song et al. 2006; Legakis, Yen et al. 2007; Yen, Legakis et al. 2007). However, the physiological role of such a multi-subunit complex in autophagy and the function of Atg9 in this complex are still unclear.

Selective autophagy, such as pexophagy (degradation of excess peroxisomes), mitophagy (clearance of damaged mitochondria) and the cytoplasm to vacuole targeting

(Cvt) pathway, targets specific cargos (Xie and Klionsky 2007). The Cvt pathway occurs during vegetative growth in yeast, in which two vacuolar hydrolases, α-mannosidase and the precursor form of aminopeptidase I (Ape1 [prApe1]), are transported to the vacuole where prApe1 is processed into mature Ape1. Non-selective, bulk autophagy occurs at a basal level and is induced by developmental signals and/or stress conditions (Levine and Klionsky 2004). For instance, during starvation, nutrients are provided to ensure cell survival through elevated autophagic degradation of bulk cytoplasm and subsequent release of the breakdown products from the lysosome. Previous studies in yeast show a cycling route of Atg9 transport between the PAS and some peripheral compartments including mitochondria, during vegetative growth: the anterograde transport of Atg9 to the PAS facilitated by Atg9 binding partners may deliver lipids to the PAS, and the retrieval of Atg9 from the PAS may recycle the protein back to the membrane origin for the next round of delivery (Reggiori, Tucker et al. 2004; He, Song et al. 2006). Nevertheless, to date little is known about the mechanism targeting Atg9 to the PAS during starvation-induced bulk autophagy.

Unlike other intracellular trafficking vesicles that usually bud from the surface of a preexisting organelle, an autophagosome is thought to assemble by fusion of new membrane fragments with the phagophore, the initial sequestering compartment, at the PAS. However, the membranous structure at the PAS, or the expanding phagophore, has not been clearly elucidated; how small membranes are incorporated into this structure remains unknown. In this paper, we present data that Atg9 interacts with itself in both nutrient-rich and starvation conditions independent of other Atg proteins. The self-interaction, which is mediated by the C terminus of the protein, promotes the trafficking

of Atg9 from its origins to the PAS and is required for both selective and non-selective starvation-induced autophagy. Through examining the expansion of Atg9-containing phagophores by fluorescence and immunoelectron microscopy, we found that the ability of Atg9 to multimerize is an essential function during formation of a normal phagophore at the PAS. Our data provide new conceptual insights to the molecular mechanism governing Atg9 anterograde transport and assembly of the PAS during bulk autophagy, and hence refine the cycling model of Atg9 transport.

Results

Atg9 self-interacts independent of other autophagy proteins or nutrient status

Previously we showed that Atg9 is located at the PAS and multiple peripheral punctate sites (Reggiori, Tucker et al. 2004). To determine whether Atg9 directly self-interacts, we took advantage of a new reagent, a yeast strain lacking twenty-four known *ATG* genes that function in *S. cerevisiae*, referred to as the multiple knockout (MKO) strain (Cao et al., 2008). Analyses by fluorescence microscopy revealed that Atg9-GFP fusion proteins were indeed organized in clusters (detected as large puncta) in this strain, as well as in the wild-type strain (Fig. A.1A), while expressing GFP alone did not lead to observable cluster formation (Fig. A.S1). These findings led us to propose that Atg9 may form clusters through direct self-association involving none of the other known Atg proteins. To test this hypothesis, we coexpressed Atg9 proteins fused with two different tags, GFP and DsRed, in MKO and wild-type strains. As shown in Fig. A.1B, the Atg9-GFP and Atg9-DsRed fusion proteins were colocalized in the cell as assessed by fluorescence microscopy.

Table A.1. Yeast strains used in this study.

Strain	Genotype	Reference
BY4742	*MATα ura3Δ leu2Δ his3Δ lys2Δ*	Invitrogen
CCH001	SEY6210 *atg9Δ::HIS5 atg1Δ::LEU2*	(He, Song et al. 2006)
CCH002	YTS158 *atg9Δ::HIS5*	(He, Song et al. 2006)
CCH010	YCY123 *ATG9-3GFP::URA3 ATG9-3DsRed::LEU2*	This study
CCH011	SEY6210 *ATG9-3GFP::URA3 ATG9-3DsRed::LEU2*	This study
CCH019	SEY6210 *ATG9-TAP::TRP1*	This study
CCH020	JLY68 *atg9Δ::LEU2*	This study
CCH025	SEY6210 *RFP-APE1::LEU2 atg9Δ::HIS3*	This study
CCH026	SEY6210 *ATG14-GFP::TRP1 RFP-APE1::LEU2 atg9Δ::HIS3*	This study
CCH027	SEY6210 *atg9Δ::TAP(URA3)*	This study
JKY007	SEY6210 *atg9Δ::HIS3*	(Noda, Kim et al. 2000)
JLY68	SEY6210 *ATG23-PA::HIS5 ATG27-HA::TRP1*	(Legakis, Yen et al. 2007)
PJ69-4A	*MATα leu2-3,112 trp1-Δ901 ura3-52 his3-Δ200 gal4Δ gal80Δ LYS2::GAL1-HIS3 GAL2-ADE2 met2::GAL7-lacZ*	(James, Halladay et al. 1996)
SEY6210	*MATα ura3-52 leu2-3,112 his3-Δ200 trp1-Δ901 lys2-801 suc2-Δ9 mel GAL*	(Robinson, Klionsky et al. 1988)
UNY102	SEY6210 *TAP-ATG1*	(Yorimitsu, Nair et al. 2006)
YCY123	SEY6210 *atg1Δ, 2Δ, 3Δ, 4Δ, 5Δ, 6Δ, 7Δ, 8Δ, 9Δ, 10Δ, 11Δ, 12Δ, 13Δ, 14Δ, 16Δ, 17Δ, 18Δ, 19Δ, 20Δ, 21Δ, 23Δ, 24Δ, 27Δ, 29Δ*	(Cao et al., 2008)
YCY135	YCY123 *ATG9-3GFP::URA3*	This study
YTS158	BY4742 *pho8::pho8Δ60 pho13Δ::KAN*	(He, Song et al. 2006)

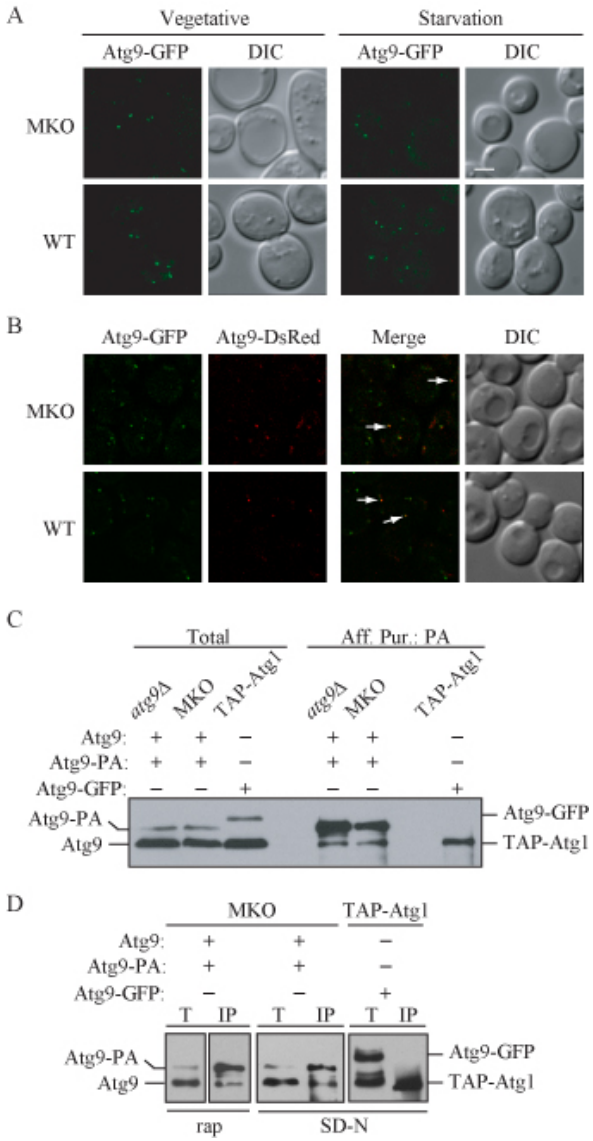

Figure A.1. Atg9 self-associates independent of other Atg components or nutrient status. (A) Atg9 forms clusters independent of other Atg proteins under both nutrient rich and nitrogen starvation conditions. Wild-type (SEY6210; WT) or multiple knockout (YCY123; MKO) strains were transformed with a plasmid expressing Atg9-GFP driven by the Atg9 native promoter. Cells cultured in nutrient-rich medium (Vegetative) or nitrogen-starved for 3 h (Starvation) were visualized by fluorescence microscopy. (B) Atg9 molecules colocalize. WT (CCH011) or MKO (CCH010) strains expressing integrated Atg9-3GFP and Atg9-3DsRed fusions were grown to mid-log phase, subject to mild formaldehyde fixation and imaged by fluorescence microscopy. The arrows mark examples of the sites where the two chimeras colocalize. (C) Atg9 is coprecipitated by Atg9-protein A (PA) independent of other Atg proteins. *atg9*Δ (JKY007) or MKO strains cotransformed with centromeric plasmids containing Atg9 and the Atg9-PA fusion driven by the Atg9 native promoter were used for affinity isolation. Cells were cultured in nutrient rich medium (SMD). A strain (UNY102) expressing chromosomally tagged TAP-Atg1 and plasmid-borne Atg9-GFP was used as a control in (C) and (D). Total lysates (Total) and eluted polypeptides (Aff. Pur.) were separated by SDS-PAGE and blotted with anti-Atg9 antiserum in (C) and (D). (D) Atg9 self-interaction in nutrient-deprived conditions is independent of other Atg components. The MKO strain expressing plasmid-borne, native promoter-driven Atg9 and Atg9-PA was used for affinity isolation. Cells were subjected to rapamycin treatment for 2 h (rap) or nitrogen starvation for 3 h (SD-N). T, total lysates; IP, immunoprecipitates. DIC, differential interference contrast. Scale bar, 2 μm.

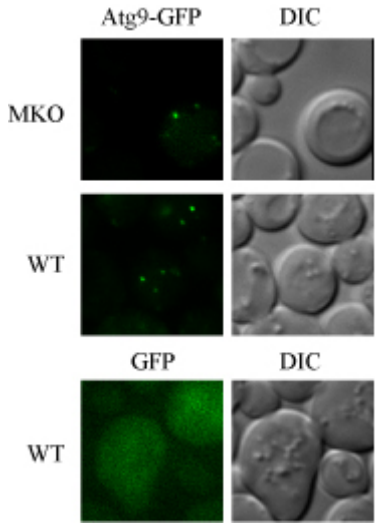

Figure A.S1. The GFP tag does not cause observable aggregation or puncta formation. The MKO or wild-type strain expressing plasmid borne, native promoter-driven Atg9-GFP, and the wild-type strain expressing plasmid borne, *CUP1* promoter-driven GFP alone were grown in nutrient-rich medium to mid-log phase and imaged by fluorescence microscopy. DIC, differential interference contrast.

Next, we used a biochemical co-immunoprecipitation approach to test the self-interaction of Atg9. As shown in Fig. A.1C, Atg9 was coprecipitated with Atg9-protein A (PA) in the MKO strain as well as in the wild-type strain in nutrient-rich conditions. As a negative control, we examined the ability of tandem affinity purification (TAP)-tagged Atg1 to co-immunoprecipitate Atg9-GFP; in this case, we could not examine endogenous Atg9 due to its migration at the same position as TAP-Atg1 during SDS-PAGE. In contrast to the result with Atg9-PA, Atg9-GFP was not recovered with TAP-tagged Atg1; Atg1 interacts with various other proteins including Atg13 but not Atg9, and we verified that TAP-Atg1 was able to co-immunoprecipitate Atg13 (Fig. A.S2A). Similarly, Atg9-PA was not able to co-immunoprecipitate Atg1 (Fig. A.S2B). Along with our previously published yeast two-hybrid results suggesting Atg9 self-interaction (Reggiori, Shintani et

al. 2005), these data demonstrated that multiple Atg9 molecules were able to form a complex without any other known Atg proteins.

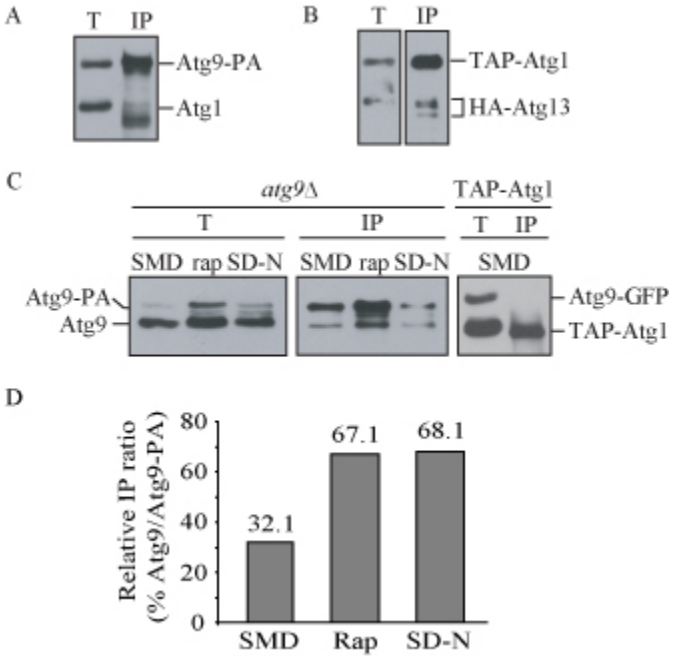

Figure A.S2. (A) TAP-Atg1 coprecipitates HA-Atg13. The TAP-Atg1 strain (UNY102) transformed with a centromeric plasmid containing native promoter-driven HA-Atg13 was used in the affinity isolation. Total lysates and eluates were analyzed by SDS-PAGE and detected with anti-HA antibody. (B) Atg1 is not coprecipitated with Atg9-PA. The wild-type strain (SEY6210) transformed with a centromeric plasmid expressing native promoter-driven Atg9-PA was used for affinity isolation. Total lysates (T) and eluates (IP) were analyzed by SDS-PAGE and detected with anti-Atg1 antiserum. (C) Atg9 self-interacts independent of nutrient status. An *atg9*Δ strain (JKY007) expressing plasmid-borne, native promoter-driven Atg9 and Atg9-PA was used for affinity isolation. Cells were grown in nutrient-rich medium (SMD), nutrient-rich medium with rapamycin (rap), or nitrogen-starvation medium (SD-N). As a negative control, a TAP-Atg1 strain (UNY102) expressing plasmid-borne native promoter-driven Atg9-GFP was grown in nutrient-rich medium and analyzed by affinity isolation. (D) Band intensity shown in (C) was quantified using the ImageJ software (http://rsb.info.nih.gov/ij/), as percentage of Atg9 precipitated by Atg9-PA in the IP fraction.

Atg9 clustering occurs not only in nutrient-rich conditions but also during nitrogen starvation (Fig. A.1A). To explore whether the same Atg9 complex forms during bulk autophagy, the MKO cells were subjected to nitrogen starvation or treatment with rapamycin, a drug that partly mimics starvation conditions and induces bulk autophagy.

Atg9 was coprecipitated with Atg9-PA in both conditions in the MKO strain (Fig. A.1D). As before, Atg9-GFP was not co-isolated with TAP-tagged Atg1. Similar results were obtained using wild-type cells (Fig. A.S2C). In addition, we found that Atg9 self-interaction is enhanced during starvation, based on quantification of the relative Atg9 amount precipitated by Atg9-PA (Fig. A.S2D), implicating an important role of self-interaction during autophagosome formation. Collectively, we concluded that Atg9 self-interacts independent of any other known Atg proteins in both nutrient-rich and starvation conditions, which may correlate with a role for Atg9 in both selective and non-selective bulk autophagy.

An Atg9 C-terminal mutant disrupts its ability to multimerize

Next, we wanted to study the physiological function of Atg9 self-interaction in autophagy. Accordingly, we first mapped the interaction domain by the yeast two-hybrid approach. In the presence of full-length Atg9, the Atg9 C-terminal domain supported the growth of two-hybrid cells on selective plates lacking histidine as well as full-length Atg9, whereas the N terminus was not able to do so (Fig. A.2A), indicating that Atg9 self-interaction is mediated through the C terminus. To narrow down the critical region, we further constructed a series of Atg9 C-terminal deletion mutants (Fig. A.2B) and analyzed them using the co-immunoprecipitation assay. Atg9, Atg9Δ870-997 and Atg9Δ787-997, but not Atg9Δ766-785 or Atg9Δ766-997, were pulled-down by full-length Atg9-PA (Fig. A.2C and unpublished data), suggesting that amino acids included in the region of 766-786 were required for self-interaction. Atg9 and the PA vector were coexpressed as control and no detectable Atg9 was coprecipitated by PA. Based on this

result, we generated four additional mutants each lacking five consecutive amino acids within the sequence of amino acids 766-786. By co-immunoprecipitation assays we determined that Atg9Δ766-770 was unable to interact with Atg9, whereas the other mutants displayed a normal interaction (Fig. A.2D and unpublished data). We note that amino acids 766-770 are highly conserved through evolution (Fig. A.2E).

Since Atg9 interacts with several other known Atg proteins, we further tested the ability of Atg9Δ766-770 to bind these other binding partners by yeast two-hybrid assays. Although Atg9Δ766-770 had a significantly compromised interaction with Atg9, it was still able to bind to its other binding partners, including Atg23, Atg27, Atg18 and Atg11, with apparently normal affinity (Fig. A.2F). In addition, we verified that the interaction between Atg9Δ766-770 and Atg23 was not impaired based on co-immunoprecipitation; we used a vector expressing PA alone as a negative control (Fig. A.2G). Therefore, the C-terminal mutant Atg9Δ766-770 specifically disrupts the self-interaction of Atg9 and was used for the following functional analyses.

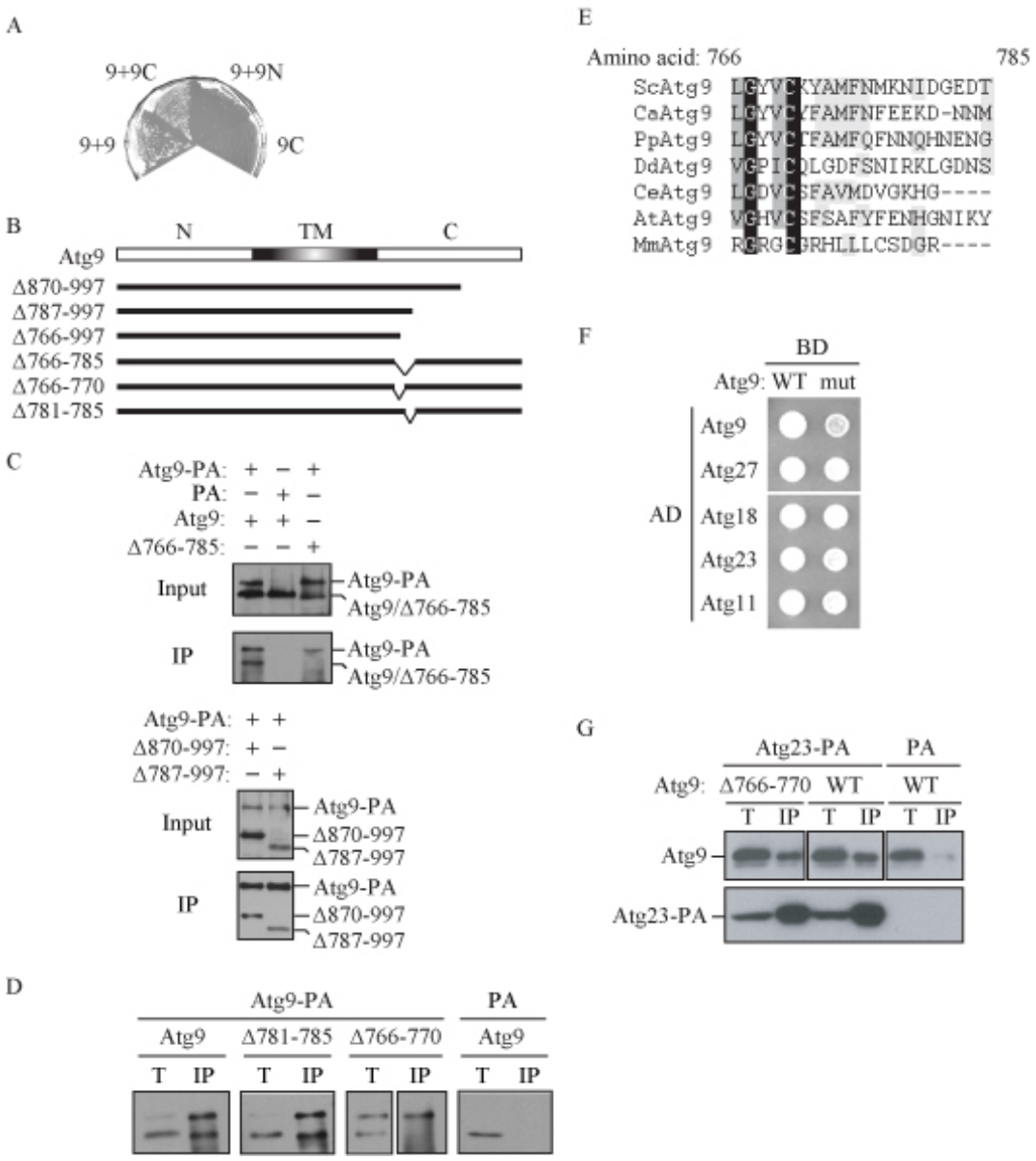

Figure A.2. An Atg9 C-terminal mutant disrupts the ability to multimerize. (A) Atg9 self-interaction is mediated through its C terminus. Yeast two-hybrid cells (PJ69-4A) expressing full-length Atg9 with either full-length Atg9 (9+9), the Atg9 C terminus (9+9C) or the N terminus (9+9N), or expressing the Atg9 C terminus alone were grown for 6 d on plates lacking histidine. (B) Schematic representation of Atg9 truncation mutants. N, N terminus; TM, transmembrane domain; C, C terminus. (C) Atg9Δ870-997 and Atg9Δ787-997, but not Atg9Δ766-785, are coprecipitated with full-length Atg9. The MKO strain (YCY123) cotransformed with centromeric plasmids expressing native promoter-driven Atg9-PA and Atg9, Atg9Δ870-997, Atg9Δ787-997, or Atg9Δ766-785, were used for affinity isolation. Total lysates (Input) and eluted polypeptides (IP) were separated by SDS-PAGE and detected with anti-Atg9 antiserum. The MKO strain cotransformed with plasmids encoding Atg9 and PA alone was used as a control in (C) and (D). (D) An Atg9 mutant with a five-amino acid deletion (Atg9Δ766-770) loses self-interaction. MKO cells expressing plasmid-borne Atg9-PA with Atg9, Atg9Δ781-785, or Atg9Δ766-770, driven by the Atg9 native promoter, were used for affinity isolation. (E) Alignment of Atg9 amino acids 766-785. Sequences from *S. cerevisiae*, *C. albicans*, *P. pastoris*, *D. discoideum*, *C. elegans*, *A. thaliana* and *M. musculus* Atg9 were aligned using the ClustalW program. Amino acid identities, and high and low similarities are highlighted in

black, dark gray and light gray, respectively. (F) Atg9Δ766-770 specifically loses self-interaction but not interactions with other Atg9 binding partners. The two-hybrid strain (PJ69-4A) was cotransformed with plasmids expressing the DNA binding domain-fused wild-type Atg9 (WT) or Atg9Δ766-770 (mut) and a series of known Atg9 binding partners fused with the activation domain. Interactions were monitored by the ability of cells to grow on plates lacking histidine for 5 d. (G) Atg9Δ766-770 interacts with Atg23 similar to wild-type Atg9. An *atg9*Δ strain expressing an integrated Atg23-PA fusion (CCH020) was transformed with a 2-micron plasmid containing wild-type Atg9-triple hemagglutinin (3HA) or Atg9Δ766-770-3HA. Total lysates (T) and eluates (IP) were separated by SDS-PAGE and detected by anti-HA or anti-PA antibody. An *atg9*Δ strain expressing plasmid-borne Atg9-3HA and PA was used as a control.

Atg9 self-interaction is required for autophagy progression

To study the function of Atg9 self-interaction in autophagy, we adopted several established assays using the Atg9Δ766-770 mutant. The processing of prApe1 into mature Ape1 results in a migration shift during SDS-PAGE and can be monitored as an indicator for selective autophagy. As shown in Fig. A.3A, Atg9Δ766-770, which impaired the self-interaction of Atg9, blocked the maturation of prApe1; whereas the other three deletion mutants, which had no effect on Atg9 self-interaction, retained the capacity of prApe1 maturation similar to wild-type Atg9, although all of the Atg9 mutants displayed a level of stability at least equivalent to that of the wild-type protein. This indicated that the self-interaction of Atg9 is indispensable for selective autophagy.

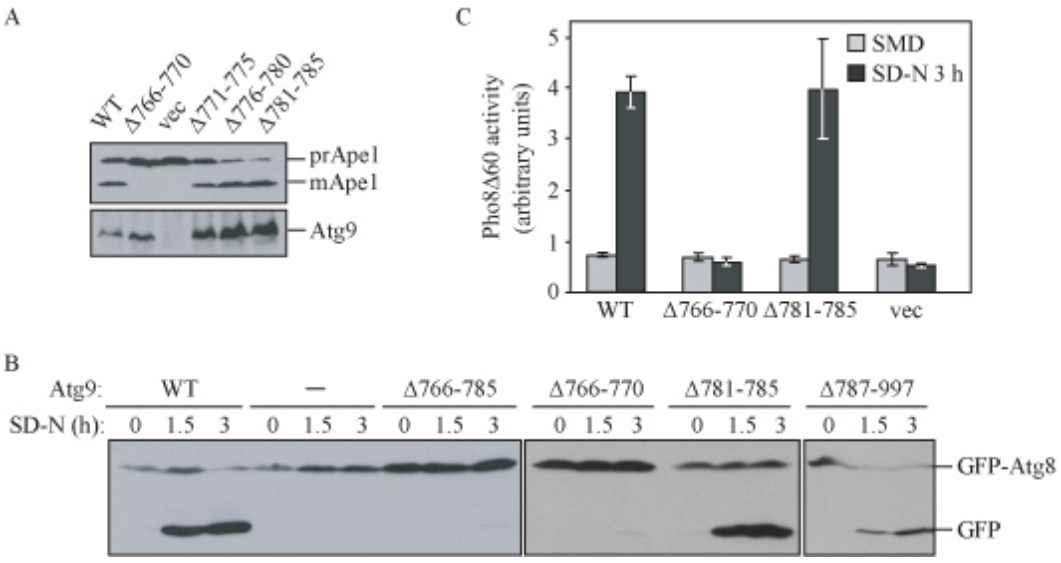

Figure A.3. Atg9 self-interaction is required for autophagy activity in both nutrient-rich and starvation conditions. (A) Precursor Ape1 maturation is blocked in cells expressing Atg9Δ766-770. An *atg9*Δ strain (JKY007) was transformed with an empty vector, or a plasmid expressing wild-type Atg9 or a series of truncation mutants (Δ766-770, Δ771-775, Δ776-780, Δ781-785) driven by the Atg9 native promoter. Protein extracts were analyzed by western blotting using antiserum to Ape1 or Atg9. (B) GFP-Atg8 processing is impaired by deletion of residues 766-770 of Atg9. The *atg9*Δ strain (JKY007) was cotransformed with a GFP-Atg8 plasmid and an empty vector (-), or a plasmid expressing wild-type Atg9 or a series of truncation mutants (Δ766-785, Δ766-770, Δ781-785, Δ787-997). Cells were grown in nutrient rich medium to mid-log phase then shifted to nitrogen starvation conditions (SD-N). Aliquots were taken at the indicated time points and analyzed by Western blotting using anti-GFP antibody. (C) Pho8Δ60 activity is reduced in Atg9Δ766-770-expressing cells. The *atg9*Δ strain (CCH002) transformed with a plasmid expressing native promoter-driven wild-type Atg9 (WT), Atg9Δ766-770, Atg9Δ781-785, or an empty vector (vec), were grown in nutrient-rich medium (SMD) to mid-log phase then shifted to starvation medium (SD-N) for 3 h. The Pho8Δ60 activity was measured according to Materials and methods. Error bars indicate the standard deviation of three independent experiments.

We also observed that Atg9 self-interaction occurs under nitrogen starvation conditions, which suggests that a protein complex containing multiple Atg9 proteins may be involved in bulk autophagy. To test this hypothesis, we carried out two assays to measure bulk autophagy activity when Atg9 self-interaction was altered. Atg8 is conjugated to phosphatidylethanolamine (PE) and remains associated with the completed autophagosome, and thus is a marker for autophagy progression (Kirisako, Baba et al. 1999; Huang, Scott et al. 2000). During autophagy, the GFP-tagged Atg8 is transported

to the vacuole where Atg8 is rapidly degraded, while the GFP moiety remains relatively stable. Thus, the accumulation of free GFP detected by western blot reflects autophagy activity (Shintani and Klionsky 2004). We assayed GFP-Atg8 processing with the mutants mentioned above, and found that only with Atg9Δ766-770 and Atg9Δ766-785, both of which affected Atg9 self-interaction (Fig. A.2D and unpublished data), GFP-Atg8 processing was blocked. With two other mutants Atg9Δ781-785 and Atg9Δ787-997 that did not affect Atg9 self-interaction, GFP-Atg8 was processed similar to cells expressing wild-type Atg9 (Fig. A.3B). These data demonstrated that loss of Atg9 self-interaction caused a defect in bulk autophagy. To quantitatively confirm this result, we measured the Pho8Δ60 enzymatic activity. Pho8Δ60 is a truncated form of alkaline phosphatase that can be delivered to the vacuole only via autophagy (Noda, Matsuura et al. 1995). Approximately four-fold induction of Pho8Δ60 activity by starvation was observed with wild-type Atg9 and Atg9Δ781-785, whereas the empty vector and Atg9Δ766-770 showed only the basal level of Pho8Δ60 activity (Fig. A.3C). We further introduced alanine mutations at each conserved residue (Fig. A.2E) in the region 766-770, and found that these mutations also caused defects in the Cvt pathway and bulk autophagy (Table A.2). Thus, even point mutations in the highly conserved interaction domain interfere with Atg9 function. Taken together, these results indicate that Atg9 self-interaction is also functionally essential for bulk autophagy. Thus our data revealed a previously unknown mechanism of Atg9 shared in both selective and bulk autophagy, involving formation of a multiple Atg9-containing complex that depends on interaction between Atg9 proteins.

Table A.2. Point mutations to alanine in Atg9 amino acids 766-770 affect autophagy.

	Cvt	Autophagy
LGYVC	+	+
L to A	-	-
G to A	-	-
V to A	-	-
C to A	-	+/-
V to A C to A	-	-

-, complete block; +/-, partial block

Self-interaction promotes anterograde transport of Atg9 and formation of intact phagophores

We decided to investigate the underlying mechanisms of the functional defects seen with the Atg9Δ766-770 mutant. In the absence of Atg9, a number of Atg proteins are not correctly localized to the PAS, including Atg2, Atg14 and Atg18 (Suzuki, Kubota et al. 2007). Therefore it is possible that formation of a multimeric Atg9 complex is required for recruitment of these proteins to the PAS. To examine this possibility, we visualized the localization of Atg2, Atg18 and Atg14 in cells expressing wild-type Atg9 or Atg9Δ766-770. As shown in Fig. A.4, in the presence of either wild-type Atg9 or Atg9Δ766-770, Atg2, Atg18 and Atg14 localized to a primary perivacuolar punctum, which colocalized with RFP-Ape1 and corresponded to the PAS. These data suggested that PAS recruitment of Atg proteins by Atg9Δ766-770 was not affected, and thus was not the causal factor for the autophagy deficiencies.

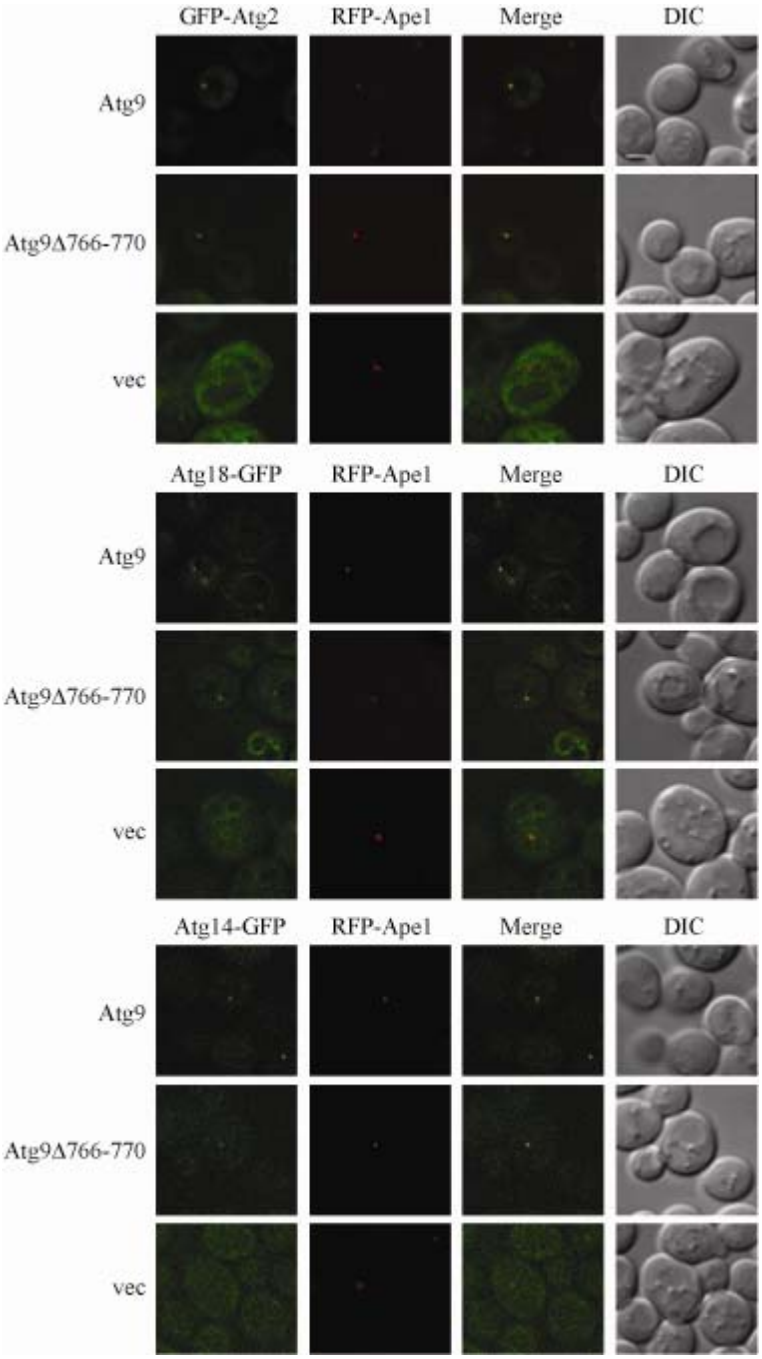

Figure A.4. Atg9Δ766-770 is not defective in the PAS recruitment of other Atg proteins. An *atg9*Δ strain expressing integrated RFP-Ape1 (CCH025) was cotransformed with a plasmid expressing either *CUP1* promoter-driven GFP-Atg2 or native *ATG18* promoter-driven Atg18-GFP and a 2-micron plasmid expressing wild-type Atg9, Atg9Δ766-770, or an empty vector. An *atg9*Δ strain expressing chromosomally tagged Atg14-GFP and RFP-Ape1 (CCH026) was transformed with the above 2-micron plasmid expressing wild-type Atg9, Atg9Δ766-770, or an empty vector. Cells were cultured in nutrient-rich medium to mid-log phase and imaged by fluorescence microscopy. DIC, differential interference contrast. Scale bar, 2 μm.

We then hypothesized that the self-interaction may be involved in the trafficking of Atg9. According to the "cycling" model of Atg9 transport, when the retrograde transport of Atg9 is impaired, Atg9 will accumulate at the PAS as one primary punctum (Reggiori, Tucker et al. 2004), but this accumulation was not observed with Atg9Δ766-770 in otherwise wild-type yeast cells; besides, Atg9Δ766-770 partially colocalized with mitochondria similar to wild-type Atg9 (unpublished data). Thus, Atg9 self-interaction is unlikely to be involved in the retrograde trafficking of Atg9 back to the peripheral (i.e., non-PAS) sites. Accordingly, to study whether self-interaction is involved in Atg9 anterograde transport, we used the TAKA (transport of Atg9 after knocking out *ATG1*) assay (Cheong, Yorimitsu et al. 2005). Atg1 is a key regulator that activates the retrieval of Atg9 from the PAS to the peripheral sites and deleting *ATG1* restricts Atg9 to the PAS. The TAKA assay examines the epistasis of a second mutation relative to *atg1*Δ with regard to Atg9 localization at the PAS. Using fluorescence microscopy, we imaged the localization of Atg9Δ766-770-GFP and wild-type Atg9-GFP in *atg1*Δ cells in nutrient-rich and starvation conditions.

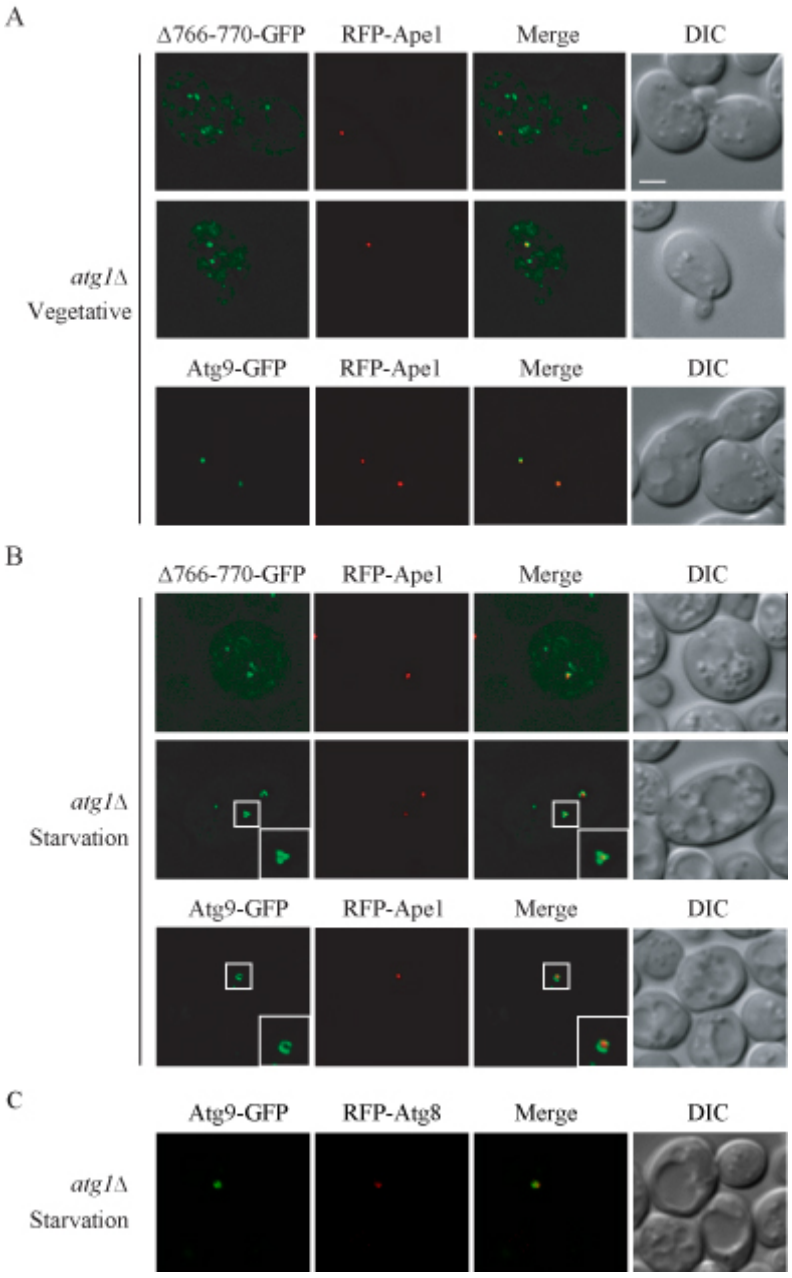

Figure A.5. Atg9Δ766-770 is defective in PAS targeting and phagophore formation. (A) Atg9Δ766-770 has a partial defect in anterograde transport from peripheral sites to the PAS during growth. The *atg1*Δ *atg9*Δ strain (CCH001) was cotransformed with a RFP-Ape1 plasmid and a plasmid expressing wild-type Atg9-GFP or Atg9Δ766-770-GFP driven by the *CUP1* promoter. Cells were cultured in nutrient rich medium to mid-log phase and imaged by fluorescence microcopy. (B) Atg9Δ766-770 forms an abnormal fragmented phagophore. The cells in (A) were cultured to mid-log phase and subject to nitrogen starvation for 3 h before imaging by fluorescence microscopy. Lower-right panels are enlarged images of the boxed regions. (C) The phagophore is co-labeled with Atg9 and Atg8. The *atg1*Δ *atg9*Δ strain (CCH001) was cotransformed with plasmids expressing Atg9-GFP and RFP-Atg8. Cells were cultured to mid-log phase and subject to nitrogen starvation for 2 h before imaging by fluorescence microscopy. DIC, differential interference contrast. Scale bar, 2 μm.

As shown in Fig. A.5A, in contrast to wild-type Atg9, which was restricted to the PAS (marked with RFP-Ape1) in 87% (52/60) of the cells, the Atg9Δ766-770 mutant distributed to multiple punctate or dispersed structures, in addition to the PAS location in 70% (52/74) of the cells. Such localization was observed regardless of nutrient supply (Fig. A.5B). During nitrogen starvation, in 53% (23/43) of the *atg1*Δ cells, Atg9Δ766-770 localized to multiple puncta, compared with only 11% (12/107) of the cells displaying peripheral localization with wild-type Atg9. Thus, these results demonstrated that loss of Atg9 self-interaction partially blocked the anterograde trafficking of Atg9 to the PAS during selective and bulk autophagy. Self-interacting and forming a complex could concentrate Atg9 molecules as clusters at the peripheral compartments, which may be important for efficient trafficking of Atg9 from these sites for subsequent delivery to the PAS.

Upon nutrient deprivation, formation of continuous cup-shaped or ring-like structures by wild-type Atg9-GFP was visualized around the cargo prApe1 at the PAS and co-labeled with Atg8 by fluorescence microscopy (Fig. A.5B and C), suggesting that they were functional rather than dead-end structures, based on previous studies showing that in *atg1* temperature-sensitive cells autophagosomes started to emerge from the Atg8-labeled PAS in 10 min and subsequently entered the vacuole after shift from nonpermissive to permissive temperature (Suzuki, Kirisako et al. 2001). These structures were approximately 500 nm in diameter, which fits within the size range of completed autophagosomes in yeast (400-900 nm; Takeshige et al., 1992). Together, these data suggested that the expanding phagophore (or precursor membranes of phagophore) is an Atg9-containing intermediate. Additionally, the Atg9-containing structures were seen

with various sizes and curvatures (Fig. A.S3), which may represent different expansion stages of the phagophore. Although, caution must be taken with this observation, as cup-shaped phagophores are not readily visualized in wild-type cells, probably due to the transient existence of phagophores and fast dissociation of Atg9 upon autophagosome completion. It is also possible that these structures may appear exaggerated under the fluorescence microscope by accumulation of fluorescent Atg9 proteins due to *ATG1* deletion.

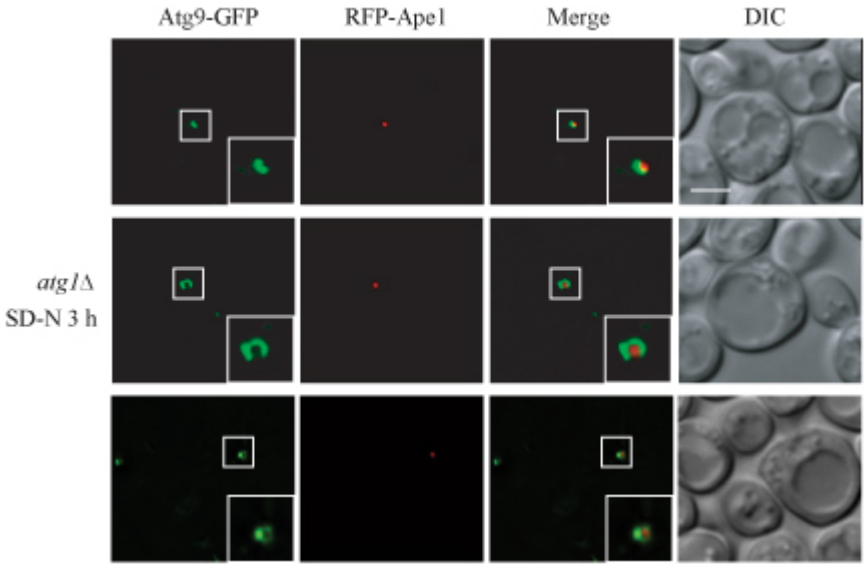

Figure A.S3. Atg9-containing phagophores at different expansion stages. The *atg1*Δ *atg9*Δ strain (CCH001) was cotransformed with a RFP-Ape1 plasmid and a plasmid expressing *CUP1* promoter-driven wild-type Atg9-GFP. Cells were cultured in nutrient-rich medium to mid-log phase, and subject to nitrogen starvation for 3 h before imaging by fluorescence microscopy. Lower-right panels are enlarged images of the boxed regions. DIC, differential interference contrast. Scale bar, 2 μm.

Interestingly, the phagophore structure was fragmented and/or failed to elongate normally when Atg9Δ766-770-GFP replaced the wild-type Atg9-GFP (Fig. A.5B). To further characterize the Atg9-containing structures at the PAS at a higher resolution, we applied immunoelectron microscopy (IEM). Atg9-GFP or Atg9Δ766-770-GFP was

expressed in an *atg1*Δ *atg9*Δ strain and the Atg9 protein detected with anti-GFP antibody. As previously reported (Baba, Osumi et al. 1997), the Cvt complex formed by prApe1 and its receptor Atg19 was localized as a spherical electron-dense particle usually near the vacuole. Consistent with our result by fluorescence microscopy, wild-type Atg9 gold particles (arrows) were concentrated on the surface of membranous structures (arrowheads) surrounding the Cvt complex, whereas the Atg9Δ766-770 mutant that lost self-interaction appeared less clustered at the PAS (Fig. A.6A and B). In sections prepared by freeze substitution but not immunostained, the membrane structures were more readily detected. In this case, it appeared that there were more membranes, potentially corresponding to the phagophore, surrounding the Cvt complex in wild-type cells relative to the Atg9Δ766-770 mutant. This result suggests that Atg9 self-interaction may be required to foster expansion of, or maintain the integrity of, the phagophore at the PAS.

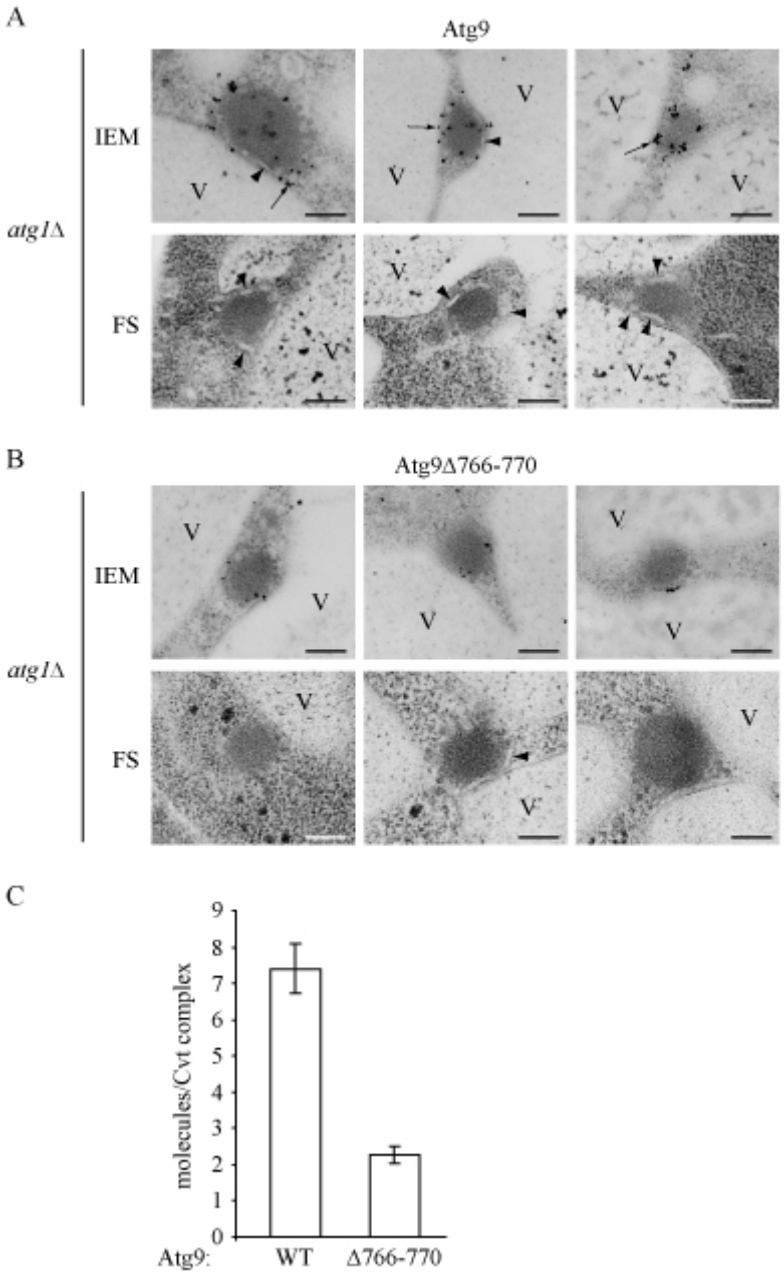

Figure A.6. Atg9 localizes to the phagophore structure surrounding the Cvt complex. (A and B) The *atg1*Δ *atg9*Δ strain was transformed with a plasmid expressing *CUP1* promoter-driven Atg9-GFP (A) or Atg9Δ766-770-GFP (B). Cells were grown to mid-log phase, shifted to SD-N for 3 h, and prepared for electron microscopy using freeze substitution (FS) and stained with anti-GFP antibody followed by immunogold as indicated (IEM). Representative images are shown. Arrows mark Atg9 and membranous structures enwrapping the Cvt complex are indicated by arrowheads. V, vacuole. (C) The number of Atg9 or Atg9Δ766-770 molecules around Cvt complexes was quantified based on IEM images shown in (A) and (B). n=100; $P < 0.0001$. Error bars indicate s.e.m. and statistical significance was analyzed by Student's two-tailed *t* test. Scale bar, 200 nm.

To quantitatively analyze this difference, we further counted the average number of wild-type or mutant Atg9 molecules around the Cvt complex. As shown in Fig. A.6C, the molecule number of Atg9Δ766-770 per Cvt complex was markedly reduced compared with wild-type Atg9, suggesting that Atg9 self-association is essential for efficient delivery to the PAS. Base on these data and our previous Atg9 "cycling" model, we propose that an Atg9 complex is dependent upon its self-interaction, and that the complex formation may facilitate not only the flow of membrane to the PAS but also the fusion of small membrane fragments into a continuous larger phagophore to form an autophagosome.

The ability to multimerize is required for Atg9 function at the PAS

Since Atg9Δ766-770 partially affected the anterograde trafficking of Atg9 to the PAS, it is possible that the abnormal phagophore structure we observed with Atg9Δ766-770 is due to insufficient supply of this protein to the PAS. To test this possibility, we relied on the overexpression of Atg11, which increases the anterograde transport of Atg9 to the PAS (He, Song et al. 2006). We imaged the GFP-tagged Atg9 and CFP-tagged Atg11 pairs with a YFP/CFP filter set by fluorescence microscopy, and, as reported previously (Kaksonen, Sun et al. 2003), no detectable bleed-through of the GFP signal from the CFP filter was seen. Since Atg9Δ766-770 did not affect its interaction with Atg11 (Fig. A.2F), we were able to overcome the inefficient anterograde transport of Atg9Δ766-770 to the PAS by overexpressing Atg11 in both *atg1*Δ and wild-type cells (Fig. A.7A and unpublished data), such that in nutrient-rich conditions the subcellular localization of Atg9Δ766-770 (68%; 36/53 cells) basically was indistinguishable from

wild-type Atg9 (84%; 48/57 cells). The transport restoration was also observed in starvation conditions (Fig. A.7A; 73% of Atg9Δ766-770 cells (36/49) and 84% of wild-type Atg9 cells (46/55)). This phenotype indicates that the deletion of residues 766-770 did not absolutely block the ability of Atg9 to transit to the PAS and rules out accumulation in the endoplasmic reticulum due to protein misfolding as the cause of the functional defect. The increase in PAS localization of Atg9Δ766-770, however, did not result in the maturation of prApe1, indicating that this type of selective autophagy was still defective (Fig. A.7B). The Pho8Δ60 activity assay also showed that bulk autophagy was not rescued by enhancing the anterograde flow of the mutant Atg9 (Fig. A.7C). In either case, the overexpression of Atg11 did not interfere with the function of wild-type Atg9, indicating that this level of Atg11 did not cause a dominant negative phenotype. Therefore, these results clearly suggested that a normal multimeric state or the ability to multimerize is essential for Atg9 function after it reaches the PAS, which is a critical step during phagophore formation.

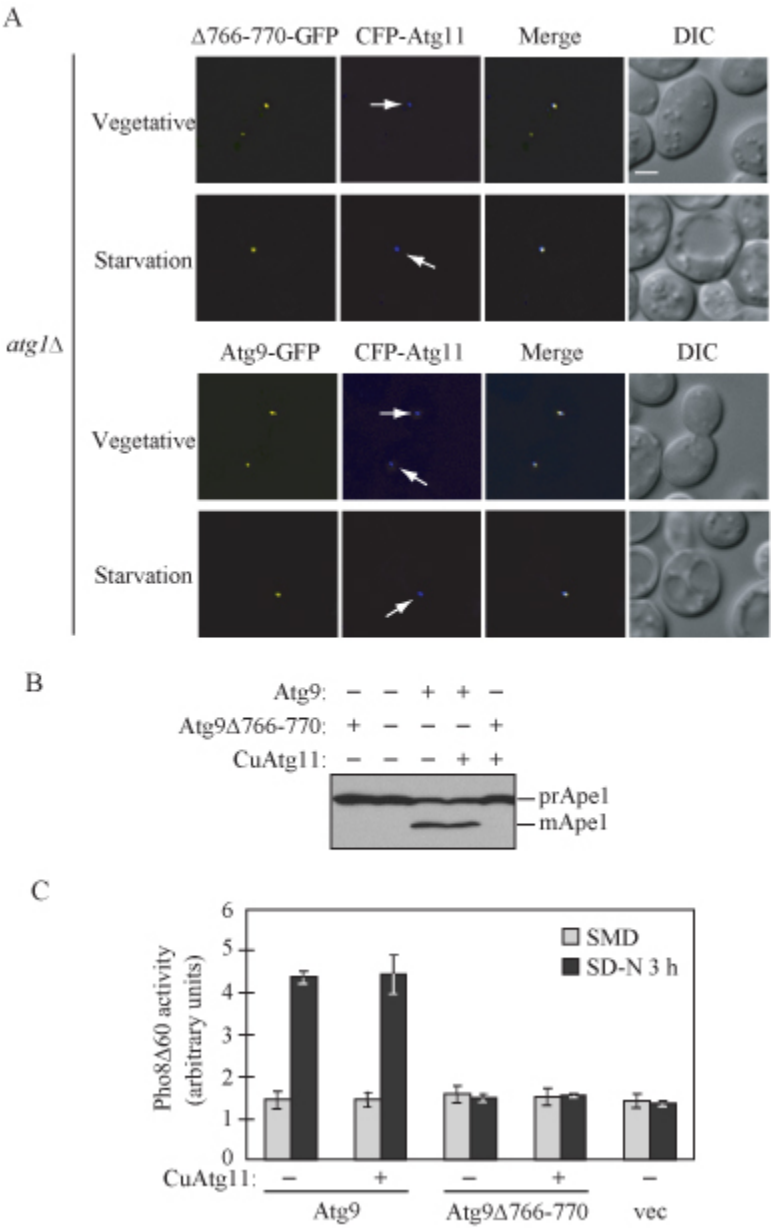

Figure A.7. Atg9 functions in an oligomeric state at the PAS. (A) Overexpression of Atg11 rescues Atg9Δ766-770 transport to the PAS in both nutrient-rich and starvation conditions. The *atg1*Δ *atg9*Δ strain (CCH001) was cotransformed with centromeric plasmids containing *CUP1* promoter-driven CFP-Atg11 and wild-type Atg9-GFP, or Atg9Δ766-770-GFP. Cells were cultured in nutrient-rich medium to mid-log phase and imaged by fluorescence microscopy (Vegetative), or shifted to starvation medium for 3 h before microscopy imaging (Starvation). DIC, differential interference contrast. Scale bar, 2 μm. (B) Atg11 overexpression does not rescue the Cvt pathway in cells expressing Atg9Δ766-770. The *atg9*Δ strain (JKY007) expressing plasmid-borne wild-type Atg9 or Atg9Δ766-770, with or without *CUP1* promoter-driven Atg11, were grown to mid-log phase, and protein extracts were analyzed by Western blotting using anti-Ape1 antiserum. (C) Atg11 overexpression does not rescue Atg9Δ766-770 function in bulk autophagy. The *atg9*Δ strain (CCH002) expressing plasmid-borne *CUP1* promoter-driven wild-type Atg9 or Atg9Δ766-770, or an empty vector (vec), with or without *CUP1* promoter-driven Atg11, were grown in SMD to mid-log phase and shifted to SD-N for 3 h. The Pho8Δ60 activity was measured according to Materials and methods. Error bars indicate the standard deviation of three independent experiments.

To further investigate the nature of the Atg9 complex, we performed a native gel analysis using the MKO strain expressing wild-type Atg9 or the mutant. We discovered that Atg9Δ766-770 migrated faster than wild-type Atg9 in native conditions (Fig. A.8A). As a control, we examined the dodecamer complex assembled by prApe1 (Kim, Scott et al. 1997) and found that it remained intact, suggesting that Atg9Δ766-770 was not able to form complexes as large (or as stable) as those seen with the wild-type protein. Consistent with the previous results showing that overexpression of Atg11 did not rescue the functional defect of the Atg9Δ766-770 mutant (Fig. A.7B), overexpression of Atg11 did not rescue the defect in complex formation of Atg9Δ766-770 in native conditions (Fig. A.8B). We further analyzed the Atg9 complex size in the wild-type background, by expressing wild-type or mutant Atg9 in the *atg9*Δ strain. As shown in Fig. A.8C, both wild-type and mutant Atg9 displayed similar migration patterns as in the MKO cells, suggesting that the known Atg9 interaction partners among Atg proteins may be dynamically associated with Atg9, rather than stably present in the core Atg9 complex. In addition, consistent with Fig. A.1 and A.S2, we also detected that the Atg9 complex remained intact upon rapamycin treatment (Fig. A.8C).

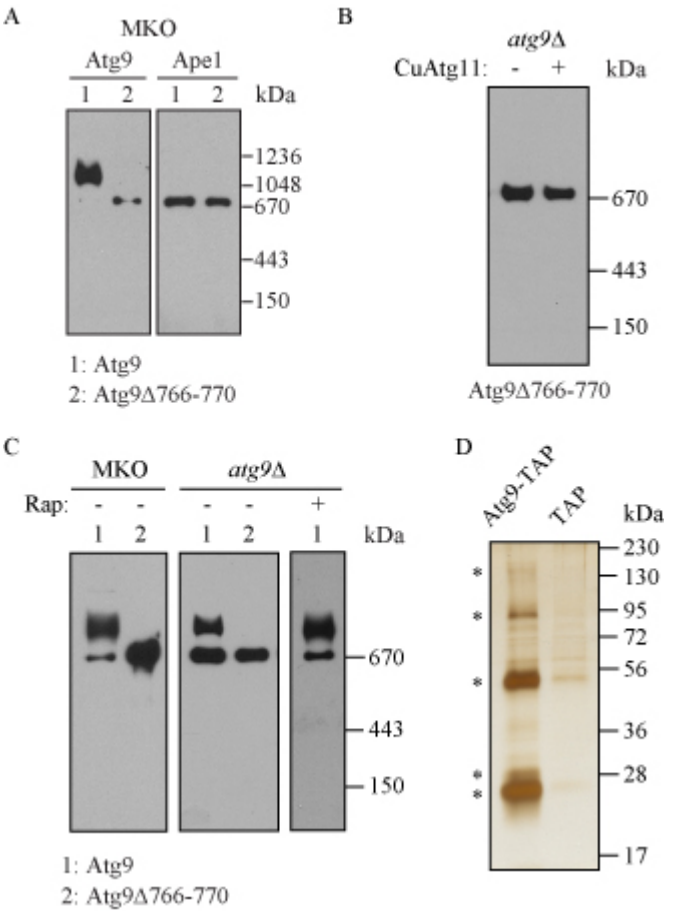

Figure A.8. Biochemical characterization of the Atg9-containing complex. (A) Atg9Δ766-770 forms smaller complexes than wild-type Atg9 in the MKO strain. The MKO strain (YCY123) was transformed with a 2-micron plasmid expressing wild-type Atg9 or Atg9Δ766-770. Cell lysates were prepared under native conditions as described in Materials and methods and analyzed on native gels in (A), (B) and (C). (B) Atg11 overexpression does not rescue the defect in complex formation resulting from Atg9 loss of self-interaction. The *atg9*Δ strain was cotransformed with plasmids expressing *CUP1* promoter-driven HA-Atg11 and Atg9Δ766-770 as indicated. (C) Atg9 forms stable complexes in the wild-type strain during starvation. The MKO (YCY123) or *atg9*Δ (JKY007) strain was transformed with a 2-micron plasmid expressing wild-type Atg9 or Atg9Δ766-770. Cells were grown in SMD to mid-log phase, and treated with rapamycin for additional 1.5 h if indicated. Native gels are detected with antiserum to Atg9 or Ape1 in (A), and with Atg9 antiserum in (B) and (C). (D) The Atg9 complex contains five different proteins. Two strains expressing the chromosomally tagged Atg9-TAP (CCH019) or an integrated TAP tag alone driven by the *ATG9* promoter (CCH027) were used in tandem affinity purification as described in Materials and Methods. The eluates were analyzed on 10% SDS-PAGE gels and detected by silver staining. Proteins coprecipitated with Atg9 are marked by asterisks.

We noticed that Atg9Δ766-770 did not migrate as a monomer (~150 kDa on native gels, unpublished data), but ran at a position that might correspond to a tetramer.

This might reflect the fact that the mutant only partially impaired Atg9 complex formation as suggested by a compromised, but not complete loss of, interaction seen by the yeast two-hybrid assay (Fig. A.2F), but it is also possible that the Atg9 complex contains unknown protein components as potential regulators of Atg9 function. To distinguish between these two possibilities, we performed the native purification of the Atg9 complex by the tandem affinity purification (TAP) method. We generated a strain expressing the chromosomally tagged Atg9-TAP fusion and another strain expressing the TAP tag alone integrated immediately after the *ATG9* promoter as control. The TAP tag was cleaved from Atg9-TAP following the first immunoprecipitation by IgG sepharose, and the Atg9 complex was isolated by a second immunoprecipitation with calmodulin affinity resin. The proteins precipitated by Atg9 were analyzed on SDS-PAGE gels and detected by silver strain. Besides Atg9 (at the size of ~130 kDa), four major protein bands were detected at approximately 94 kDa, 54 kDa, 28 kDa and 25 kDa, compared with control (Fig. A.8D), suggesting that the Atg9 complex is actually composed of multiple proteins, although we cannot rule out at present that these represent degradation products. It will be helpful to further study the identity and function of these components in the Atg9 complex during phagophore formation and expansion.

Discussion

Atg9 is the only known integral membrane protein that is required in the formation of sequestering vesicles during all types of autophagy, including the Cvt pathway, pexophagy, mitophagy (Kanki and Klionsky 2008) and bulk autophagy, and it may play a key role in lipid delivery to the PAS. In addition to the PAS, Atg9 is localized at cytoplasmic punctate structures, which undergo dynamic movement revealed by time-lapse microscopy (Reggiori, Shintani et al. 2005). Our data indicate that the clustered organization of Atg9 may be mediated by the ability to self-interact. We also found that self-interaction is important for efficient anterograde transport of Atg9 to the PAS (Fig. A.5). It is possible that Atg9 multimerization as clusters may function in promoting membrane "budding", although the mechanism that triggers Atg9 movement from the peripheral compartments is not clear.

Our microscopy analyses revealed for the first time that Atg9 is localized on the membrane structures enwrapping the Cvt complex at the PAS, and hence Atg9 may be used as a marker for monitoring phagophore expansion, although the PAS in *atg1*Δ may represent a fairly static membrane structure, compared with the authentic growing phagophore in wild-type cells. Also, we do note that we cannot unequivocally identify the apparent membrane fragments as belonging to the phagophore because we did not carry out dual immunolabeling with anti-Atg8, which is known to localize to the PAS in the *atg1*Δ strain. We speculate that the precise regulation of Atg9 self-interaction may facilitate tethering and fusion of small membranes at the PAS. Notably, no yeast SNAREs have yet been localized to the PAS (Reggiori, Wang et al. 2004), implying that

membrane fusion at, and closure of, the phagophore may adopt a mechanism different from the conventional SNARE-mediated manner, although it is possible that SNAREs are present at too low a level to detect by fluorescence microscopy. Recent studies suggest that lipidated Atg8–PE mediates membrane hemifusion of liposomes *in vitro* (Nakatogawa, Ichimura et al. 2007). Yet, how Atg8 leads to membrane hemifusion *in vivo* and how hemifusion of lipid bilayers contributes to phagophore expansion is not clear. A recent analysis of Atg8 function suggests that Atg8 may largely determine the autophagosome size, but not the biogenesis of the initial phagophore or its completion (Xie, Nair et al. 2008). As suggested in this study, it is possible that Atg9 plays a critical role in initiating the phagophore. Furthermore, Atg9 along with Atg8–PE, and other Atg proteins, actively participate in the fusion process that expands the phagophore into the autophagosome. However, as noted above, it is not yet known whether Atg8–PE is present on the Atg9-containing membrane segments that are involved in autophagosome biogenesis.

It should be noted that the cup-shaped phagophore is formed in cells lacking Atg1 (Fig. A.5B, A.6A, A.6B and A.S3). Thus the Atg1 kinase, originally proposed to function in phagophore initiation, appears to be dispensable for this process. In addition, both Atg2 and Atg18 are absent from the PAS in *atg1*Δ cells (Suzuki, Kubota et al. 2007). Therefore, the cup-shaped phagophore we observed around prApe1 seems to form independently of Atg1, Atg2 and Atg18. Given the previous reports showing that the absence of any of these three proteins causes accumulation of Atg9 at the PAS (Reggiori, Tucker et al. 2004), it would be reasonable to hypothesize that Atg1, Atg2 and Atg18 function at the vesicle completion step and promote dissociation of Atg9 after vesicle

sealing, and lacking any of them will arrest the phagophore as an intermediate structure. Notably, Atg1 also seems to function at a late stage and not required for induction of micropexophagy in the methylotrophic yeast *Pichia pastoris* (Mukaiyama, Oku et al. 2002). Thus, the protein machinery responsible for autophagy induction, and the exact role of Atg1, remain to be further elucidated.

The multiple knockout (MKO) strain allowed us to investigate the formation of the Atg9 complex bypassing the complexity caused by multiple Atg9 binding partners among Atg proteins. Using Atg9 as a phagophore marker, the MKO strain will provide advantages for studying proteins required in distinct steps during autophagosome formation including nucleation, expansion and completion of the sequestering vesicle. We found that additional proteins may be stably present in the Atg9 complex (Fig. A.8D), and it is possible that they function as regulatory units. It will be interesting to further characterize these members of the Atg9 complex for a better understanding of membrane dynamics during de novo autophagosome biogenesis.

Materials and methods

Yeast strains and media

The *S. cerevisiae* strains used in this study are listed in Table A.1. For disruption of *ATG9*, the entire coding region was replaced by the *Kluyveromyces lactis LEU2* gene using PCR primers containing ~45 bases of identity to the regions flanking the open reading frame. For PCR-based integration of the GFP or TAP tag, pFA6a-GFP(S65T)-TRP1, or pBS1479 and pBS1539, was used as the template, respectively (Longtine, McKenzie et al. 1998; Puig, Caspary et al. 2001). For integration of the Atg9-3GFP fusion, the integrative plasmid pATG9-3GFP(306) was linearized by digestion with StuI and integrated into the *URA3* gene locus. For integration of the Atg9-3DsRed fusion, the DNA fragment containing the *ATG9* gene and native promoter was released from pATG9-3GFP(306) and cloned into pTPIARP2-3DsRed(305) using XhoI and BamHI; the resulting integrative plasmid pAtg9-3DsRed(305) was linearized by digestion with AflII and integrated into the *LEU2* gene locus.

Yeast cells were grown in rich medium (YPD; 1% yeast extract, 2% peptone, 2% glucose) or synthetic minimal medium (SMD; 0.67% yeast nitrogen base, 2% glucose, amino acids, and vitamins as needed). Starvation experiments were conducted in synthetic medium lacking nitrogen (SD-N; 0.17% yeast nitrogen base without amino acids, 2% glucose).

Plasmids

Plasmids expressing HA-Atg13 (pHAAtg13(315); (Cheong, Nair et al. 2008), RFP-Ape1 (pRFPApe1(414); (Stromhaug, Reggiori et al. 2004), GFP-Atg8 (pGFP-AUT7(414); (Abeliovich, Zhang et al. 2003), Atg9 (pAPG9(416); essentially constructed the same as pAPG9(414); (Noda, Kim et al. 2000), Atg9-GFP (pAPG9GFP(416) and pCuAPG9GFP(416); (Noda, Kim et al. 2000), Atg9-PA (pAtg9PA(314); (He, Song et al. 2006), HA-Atg11 (pCuHA-CVT9(414); (Kim, Kamada et al. 2001), CFP-Atg11 (pCuHACFPCVT9(414); (Kim, Huang et al. 2002), GFP-Atg2 (pCuGFPAPG2(414); (Wang, Kim et al. 2001) and Atg18-GFP (pCVT18GFP(414); (Guan, Stromhaug et al. 2001) have been described previously. Yeast two-hybrid plasmids expressing Atg11 (pAD-Atg11), Atg18 (pAD-Atg18), Atg23 (pAD-Atg23), Atg27 (pAD-Atg27), Atg9 (pAD-Atg9 and pBD-Atg9), the Atg9 N terminus (pAD-Atg9N) or the C terminus (pAD-Atg9C) have been described previously (He, Song et al. 2006).

The plasmids pAtg9Δ787-997(416) and pAtg9Δ870-997(416) were generated by amplifying the Atg9Δ787-997 and Atg9Δ870-997 fragments from pAPG9(416) and cloning them into the two AatII sites in pAPG9(416). To generate the plasmid expressing Atg9Δ766-997-GFP driven by the *TPI1* promoter (pS1S2(416)), the N-terminus of *ATG9* (928 bp) was amplified and cloned in the vector pPEP416 (Reggiori, Black et al. 2000) digested with EcoRI/SacII. The 3' primer introduced an XbaI site and a SacII site preceded by a stop codon. The resulting pS1(416) plasmid was then cut with XbaI/SacII, and the central part of *ATG9* (1404 bp) was amplified and inserted using the same enzymes. For internal deletions of Atg9 (Atg9Δ766-785-GFP, Atg9Δ766-770-GFP, Atg9Δ771-775-GFP, Atg9Δ776-780-GFP and Atg9Δ781-785-GFP), the truncated open reading frames were amplified by PCR and cloned into NotI and BamHI sites of

pAPG9GFP(416). For generation of non-tagged pAtg9Δ766-785(416), pAtg9Δ766-770(416), pAtg9Δ781-785(416), or pCuAtg9Δ766-770-GFP(416), and pAtg9Δ766-770-3HA(426), the fragment containing the indicated deletion was released from pAtg9Δ766-785-GFP(416), pAtg9Δ766-770-GFP(416), or pAtg9Δ781-785-GFP(416) by AgeI and SphI digestion and introduced into pAPG9(416), pCuAPG9GFP(416), or pAtg9-3HA(426), respectively. Point mutations in Atg9 amino acids 766-770 were introduced by site-directed mutagenesis. To construct the two-hybrid plasmid pBD-Atg9Δ766-770, the Atg9Δ766-770 fragment was amplified from pAtg9Δ766-770GFP(416) and cloned into pGBDU-C1 using BamHI and SalI sites.

Protein A affinity isolation

Cells were grown to OD_{600} = 0.8 in SMD; for rapamycin treatment, cells were cultured with 0.2 μg/ml rapamycin at 30°C for an additional 2 h. 50 ml of cells were harvested and resuspended in lysis buffer (20 mM Tris-HCl pH 7.5, 150 mM KCl, 5 mM $MgCl_2$, 1% Triton X-100, 1 mM PMSF and protease inhibitor cocktail). The detergent extracts were incubated with IgG-sepharose beads overnight at 4°C. The beads were washed with lysis buffer 6 times and eluted in SDS-PAGE sample buffer by incubating at 37°C for 30 min. The eluates were resolved by SDS-PAGE and immunoblotted with anti-Atg9 antiserum, or anti-HA or anti-PA antibody.

Fluorescence microscopy

Fluorescence signals were visualized on an Olympus IX71 fluorescence microscope (Olympus, Mellville, NY). The images were captured by a Photometrics

CoolSNAP HQ camera (Roper Scientific, Inc., Tucson, AZ) and deconvolved using DeltaVision software (Applied Precision, Issaquah, WA). When necessary, a mild fixation procedure was applied as previously described to visualize Atg9 without affecting various fluorescent proteins (He, Song et al. 2006).

Native gel analysis

3-12% Bis-Tris Gels (Invitrogen, Carlsbad, CA) were used for blue native gel electrophoresis. Spheroplasts were generated from 25 ml of cells at mid-log phase as described previously (Tomashek, Sonnenburg et al. 1996), and cell lysates were prepared according to the Invitrogen NativePAGE Novex Bis-Tris Gel System manual.

Tandem affinity purification

400 ml cells were cultured to OD_{600} = 0.8 in YPD. Spheroplasts were prepared and TAP purification done as previously reported (Tomashek, Sonnenburg et al. 1996; Puig, Caspary et al. 2001). The eluates were resolved by SDS-PAGE, and silver staining of proteins in polyacrylamide gels was preformed using the SilverSNAP Stain Kit II (Thermo Scientific, Rockford, IL).

Electron microscopy

Immunoelectron microscopy (IEM) was performed according to the procedures described previously (Baba, Osumi et al. 1997) with the following modifications: The blocking solution contained 0.05% Tween 20 or 0.5% cold fish gelatin (Sigma-Aldrich,

St. Louis, MO), and the secondary antibody was conjugated to Ultra Small gold particles (Aurion, Wageningen, The Netherlands) and visualized with silver enhancement.

Additional assays

The GFP-Atg8 processing assay and the Pho8Δ60 activity assay were carried out as previously described (Abeliovich, Zhang et al. 2003; Shintani and Klionsky 2004).

References

Abeliovich, H., C. Zhang, et al. (2003). "Chemical genetic analysis of Apg1 reveals a non-kinase role in the induction of autophagy." Mol Biol Cell **14**(2): 477-90.

Baba, M., M. Osumi, et al. (1997). "Two distinct pathways for targeting proteins from the cytoplasm to the vacuole/lysosome." J Cell Biol **139**(7): 1687-95.

Cheong, H., U. Nair, et al. (2008). "The Atg1 kinase complex is involved in the regulation of protein recruitment to initiate sequestering vesicle formation for nonspecific autophagy in *Saccharomyces cerevisiae*." Mol Biol Cell **19**(2): 668-81.

Cheong, H., T. Yorimitsu, et al. (2005). "Atg17 regulates the magnitude of the autophagic response." Mol Biol Cell **16**(7): 3438-53.

Guan, J., P. E. Stromhaug, et al. (2001). "Cvt18/Gsa12 is required for cytoplasm-to-vacuole transport, pexophagy, and autophagy in *Saccharomyces cerevisiae* and *Pichia pastoris*." Mol Biol Cell **12**(12): 3821-38.

He, C., H. Song, et al. (2006). "Recruitment of Atg9 to the preautophagosomal structure by Atg11 is essential for selective autophagy in budding yeast." J Cell Biol **175**(6): 925-35.

Huang, W.-P., S. V. Scott, et al. (2000). "The itinerary of a vesicle component, Aut7p/Cvt5p, terminates in the yeast vacuole via the autophagy/Cvt pathways." J Biol Chem **275**(8): 5845-51.

James, P., J. Halladay, et al. (1996). "Genomic libraries and a host strain designed for highly efficient two-hybrid selection in yeast." Genetics **144**(4): 1425-36.

Kaksonen, M., Y. Sun, et al. (2003). "A pathway for association of receptors, adaptors, and actin during endocytic internalization." Cell **115**(4): 475-87.

Kanki, T. and D. J. Klionsky (2008). "Mitophagy in yeast occurs through a selective mechanism." J Biol Chem **283**(47): 32386-93.

Kim, J., W.-P. Huang, et al. (2002). "Convergence of multiple autophagy and cytoplasm to vacuole targeting components to a perivacuolar membrane compartment prior to *de novo* vesicle formation." J Biol Chem **277**(1): 763-73.

Kim, J., Y. Kamada, et al. (2001). "Cvt9/Gsa9 functions in sequestering selective cytosolic cargo destined for the vacuole." J Cell Biol **153**(2): 381-96.

Kim, J., S. V. Scott, et al. (1997). "Transport of a large oligomeric protein by the cytoplasm to vacuole protein targeting pathway." J Cell Biol **137**(3): 609-18.

Kirisako, T., M. Baba, et al. (1999). "Formation process of autophagosome is traced with Apg8/Aut7p in yeast." J Cell Biol **147**(2): 435-46.

Legakis, J. E., W.-L. Yen, et al. (2007). "A cycling protein complex required for selective autophagy." Autophagy **3**(5): 422-32.

Levine, B. and D. J. Klionsky (2004). "Development by self-digestion: molecular mechanisms and biological functions of autophagy." Dev Cell **6**(4): 463-77.

Longtine, M. S., A. McKenzie III, et al. (1998). "Additional modules for versatile and economical PCR-based gene deletion and modification in *Saccharomyces cerevisiae*." Yeast **14**(10): 953-61.

Mukaiyama, H., M. Oku, et al. (2002). "Paz2 and 13 other PAZ gene products regulate vacuolar engulfment of peroxisomes during micropexophagy." Genes Cells **7**(1): 75-90.
Nakatogawa, H., Y. Ichimura, et al. (2007). "Atg8, a ubiquitin-like protein required for autophagosome formation, mediates membrane tethering and hemifusion." Cell **130**(1): 165-78.
Noda, T., J. Kim, et al. (2000). "Apg9p/Cvt7p is an integral membrane protein required for transport vesicle formation in the Cvt and autophagy pathways." J Cell Biol **148**(3): 465-80.
Noda, T., A. Matsuura, et al. (1995). "Novel system for monitoring autophagy in the yeast *Saccharomyces cerevisiae*." Biochem Biophys Res Commun **210**(1): 126-32.
Puig, O., F. Caspary, et al. (2001). "The tandem affinity purification (TAP) method: a general procedure of protein complex purification." Methods **24**(3): 218-29.
Reggiori, F., M. W. Black, et al. (2000). "Polar transmembrane domains target proteins to the interior of the yeast vacuole." Mol Biol Cell **11**(11): 3737-49.
Reggiori, F., T. Shintani, et al. (2005). "Atg9 cycles between mitochondria and the pre-autophagosomal structure in yeasts." Autophagy **1**(2): 101-9.
Reggiori, F., K. A. Tucker, et al. (2004). "The Atg1-Atg13 complex regulates Atg9 and Atg23 retrieval transport from the pre-autophagosomal structure." Dev Cell **6**(1): 79-90.
Reggiori, F., C.-W. Wang, et al. (2004). "Early stages of the secretory pathway, but not endosomes, are required for Cvt vesicle and autophagosome assembly in *Saccharomyces cerevisiae*." Mol Biol Cell **15**(5): 2189-204.
Robinson, J. S., D. J. Klionsky, et al. (1988). "Protein sorting in *Saccharomyces cerevisiae*: isolation of mutants defective in the delivery and processing of multiple vacuolar hydrolases." Mol Cell Biol **8**(11): 4936-48.
Shintani, T. and D. J. Klionsky (2004). "Autophagy in health and disease: a double-edged sword." Science **306**(5698): 990-5.
Shintani, T. and D. J. Klionsky (2004). "Cargo proteins facilitate the formation of transport vesicles in the cytoplasm to vacuole targeting pathway." J Biol Chem **279**(29): 29889-94.
Stromhaug, P. E., F. Reggiori, et al. (2004). "Atg21 is a phosphoinositide binding protein required for efficient lipidation and localization of Atg8 during uptake of aminopeptidase I by selective autophagy." Mol Biol Cell **15**(8): 3553-66.
Suzuki, K., T. Kirisako, et al. (2001). "The pre-autophagosomal structure organized by concerted functions of *APG* genes is essential for autophagosome formation." EMBO J **20**(21): 5971-81.
Suzuki, K., Y. Kubota, et al. (2007). "Hierarchy of Atg proteins in pre-autophagosomal structure organization." Genes Cells **12**(2): 209-18.
Tomashek, J. J., J. L. Sonnenburg, et al. (1996). "Resolution of subunit interactions and cytoplasmic subcomplexes of the yeast vacuolar proton-translocating ATPase." J Biol Chem **271**(17): 10397-404.
Wang, C.-W., J. Kim, et al. (2001). "Apg2 is a novel protein required for the cytoplasm to vacuole targeting, autophagy, and pexophagy pathways." J Biol Chem **276**(32): 30442-51.

Xie, Z. and D. J. Klionsky (2007). "Autophagosome formation: core machinery and adaptations." Nat Cell Biol **9**(10): 1102-9.
Xie, Z., U. Nair, et al. (2008). "Atg8 controls phagophore expansion during autophagosome formation." Mol Biol Cell **19**(8): 3290-8.
Yen, W.-L., J. E. Legakis, et al. (2007). "Atg27 is required for autophagy-dependent cycling of Atg9." Mol Biol Cell **18**(2): 581-93.
Yorimitsu, T., U. Nair, et al. (2006). "Endoplasmic reticulum stress triggers autophagy." J Biol Chem **281**(40): 30299-304.
Young, A. R.J., E. Y.W. Chan, et al. (2006). "Starvation and ULK1-dependent cycling of mammalian Atg9 between the TGN and endosomes." J Cell Sci **119**(18): 3888-900.